UNIVERSITY OF CALIFORNIA,

IRVINE

# Immunomodulation of the CD200 axis protects Microglia from Alzheimer's Disease-induced Damage

DISSERTATION

submitted in partial satisfaction of the requirements for the degree of

DOCTOR OF PHILOSOPHY

In Biomedical Engineering

By

Thuy-Khanh Tran-Dao

Dissertation Committee:
Professor Wendy F. Liu
Professor Elliot Botvinick
Professor Gregory Brewer

2026

## DEDICATION

This work is dedicated to my family and fiancé, without whose support my success would not have been possible. I would also like to thank my dogs Mocha and Mochi, and my cats Miso and Nala for their emotional support.

**Acknowledgements**

I would like to thank all the collaborators and mentors who were involved in this incredible journey. Besides my three dedicated mentors Professor Wendy Liu, Professor Gregory Brewer, and Professor Elliot Botvinick, I would also like to acknowledge Miles Yang Nguyen for his help with analyzing mitochondrial dynamics and Jerry Wu for his help with the study of EV production in CD200-treated microglia – I do believe the future of this project is in good hands. I am indebted to my undergraduate student researchers Leilany Lim, Amal Tabban, Athena Niu, Jessica Mebe, Melissa Nunes, Wendy Pham, Matthew Morales, Deana Horta, Golzar Sahid, Arnav Sharma, and Marilyn Nguyen. I have grown under the additional tutelage of Dr. Li Xing and Dr. Dequina Nicholas. Lastly, I would like to acknowledge Li-Mor David and my fellow graduate students in the Liu lab: Daniela Enriquez Ochoa, YuChun Wang, and Daanish Kulkarni for their invaluable advice and solidarity.

**Table of Contents**

VITA ..... **Error! Bookmark not defined.**
Acknowledgements ..... iii
Table of Contents ..... iv
List of Figures ..... vii
Chapter 1: Regulation of Neuroinflammation and Debris Clearance in the Alzheimer's Brain .... ix
Abstract ..... 1
1.1 Introduction ..... 1
1.1a Alzheimer's Epidemiology ..... 1
1.1b. Age as a Disease Factor ..... 3
1.2 Alzheimer Disease Hallmarks ..... 4
1.2a Neuroinflammation ..... 4
1.2b Neuroinflammation and Debris Accumulation: Chicken or the egg? ..... 7
1.3 Debris Accumulation ..... 9
1.3a Glia-Mediated Debris Clearance ..... 9
1.3b Types of pathogenic debris seen in AD ..... 10
1.3c Debris Clearance Mechanisms ..... 12
1.3d LANDO/LAP bridge phagocytosis and autophagy ..... 13
1.4. Cell Metabolism ..... 15
1.4a Autophagic Regulation of cell metabolism ..... 15
1.4b Microglial Energetics ..... 16
1.4c Lactate: More than a Byproduct ..... 18
1.5 Current AD treatments ..... 18
1.6 Conclusion ..... 20
References ..... 21
Chapter 2: CD200 prevents microglial dysfunction by modulating inflammation, LC3-mediated phagocytosis, and mitochondrial morphology in an Alzheimer's model *in vitro* ..... 32
Abstract ..... 32
2.1 Introduction ..... 32
2.2 Materials and methods ..... 34
CD200 protein production ..... 34
BV2 microglia cell culture ..... 35
THP1 cell culture and stimulation ..... 36

iPSC-derived human microglia cell culture and stimulation ..... 36
Fibrillar Amyloid-beta preparation ..... 36
Flow cytometry sample preparation ..... 36
Microscopy sample preparation ..... 37
RNA extraction and qPCR sample preparation ..... 38
ELISA sample preparation ..... 38
Mitochondria analysis ..... 39
Metabolic assays ..... 39
2.3 Results ..... 40
CD200 dampens inflammation in BV2 mouse microglia ..... 40
CD200 treatment influences BV2 microglial morphology ..... 43
CD200 treatment enhanced Aβ42 uptake in mouse and human microglia ..... 43
CD200 treatment enhanced colocalization of Aβ42 and lysosomes ..... 45
CD200 dampened inflammation in human cell lines ..... 55
2.4 Discussion ..... 56
Supplemental ..... 63
References ..... 67
Chapter 3: CD200 effect on mitochondria transfer in mouse microglia ..... 78
Abstract ..... 78
3.1 Introduction ..... 78
3.2 Materials and Methods ..... 79
Fibrillar Amyloid-beta preparation ..... 79
General BV2 cell culture ..... 80
BV2 cell culture for EV analysis ..... 80
BV2 cell culture for mitochondrial transfer analysis ..... 80
BV2 cell culture for cell projection analysis ..... 81
EV isolation ..... 81
3.3 Results ..... 81
CD200 treatment enhances cell projections and EV-like structures ..... 81
CD200 treatment enhances mitochondrial transfer ..... 82
CD200 treatment enhances CD200R+ mitoEV production ..... 84
CD200 treatment increases mitochondria-dense cell projections ..... 85
3.4 Discussion ..... 86

Chapter 4: Summary of Findings ..... 88
4.1 Summary of Findings ..... 88
4.2 Future steps ..... 88
Appendix ..... 92
Abbreviations ..... 92
CD200 Production Protocol ..... 92
Seahorse Protocol ..... 99
Mitochondria Transfer Protocol ..... 102

## List of Figures

Figure 1.1: Neuroinflammation in the AD brain ..... **Error! Bookmark not defined.**

Figure 1.2: Debris clearance mechanisms prevent toxic aggregates ..... **Error! Bookmark not defined.**

Figure 1.3: Canonical autophagy and LAP share many similarities ..... **Error! Bookmark not defined.**

Figure 1.4: Components of Cellular Respiration ..... **Error! Bookmark not defined.**

Figure 2.1: CD200 dampens inflammation in BV2 mouse microglia ..... **Error! Bookmark not defined.**

Figure 2.3: CD200 treatment enhanced *f*Aβ42 colocalization to lysosomes **Error! Bookmark not defined.**

Figure 2.4: CD200 treatment protected mitochondria from fAβ42-induced damage ..... **Error! Bookmark not defined.**

Figure 2.5: CD200 treatment impacts oxygen consumption and glycolytic dependence ..... **Error! Bookmark not defined.**

Figure 2.5: CD200 treatment effect on inflammation and uptake in human cell lines ..... **Error! Bookmark not defined.**

Figure S1: CD200 production protocol ..... **Error! Bookmark not defined.**

Figure S2: Trem2 expression is measured by flow cytometry. ..... **Error! Bookmark not defined.**

Figure S3: Additional Mito Stress Assay Quantifications. ..... **Error! Bookmark not defined.**

Figure 3.1: CD200 treatment affected cell projections and vesicular structures **Error! Bookmark not defined.**

Figure 3.2: Mitochondrial transfer in BV2 Microglia ..... **Error! Bookmark not defined.**

Figure 3.3: Possible MitoEV production in CD200-treated Microglia ..... **Error! Bookmark not defined.**

Figure 3.4: Microglia feature mitochondria-dense projections ..... **Error! Bookmark not defined.**

## List of Tables

Table 1.1: Alzheimer's Disease General Information ..... 2
Table 1.2: Current AD treatments ..... 19
Table A1: Materials required for CD200 protein production ..... 65
Table A2: Materials required for BV2, iMGL, and THP1 cell culture ..... 65
Table A3: Primers, antibodies, and ELISA kits ..... 66
Table 4.1: Summary of finding ..... 88

# VITA

**Thuy-Khanh Tran-Dao**

## EDUCATION

University of California, Irvine
Ph.D., Biomedical Engineering, 2026

University of California, Santa Cruz
B.S., Biomolecular Engineering, 2019

## FIELD OF STUDY

CD200-mediated immunomodulation in Alzheimer's disease models

## PUBLICATIONS

Hicks M, **Tran-Dao T-K**, Mulroney L, Bernick DL. 2021. *De-novo Assembly of Limnospira fusiformis Using Ultra-Long Reads. Front Microbiol 12:657995. Doi: 10.3389/fmicb.2021.657995*

**Tran-Dao TK**, Brewer GJ, Liu WF. *Regulation of Neuroinflammation and Debris Clearance in the Alzheimer's Brain.* **Manuscript in preparation.**

**Tran-Dao TK**, Nguyen MY, Wu J, Pham W, Sahidi G, Sharma A, Nguyen M, Xing L, Wang YC, David LM, Botvinick E, Brewer GJ, Liu WF. *CD200 prevents microglial dysfunction by modulating inflammation, cell surveillance, and mitochondrial morphology in an Alzheimer's model in vitro.* **Manuscript in preparation.**

## HONORS & AWARDS

2025 BMES Cellular & Molecular Bioengineering Poster Award
Third Place Poster Award – Engineering + Society Conference (2025)

## SELECTED ORAL PRESENTATIONS

**Tran-Dao TK**. *CD200 prevents microglial dysfunction by modulating inflammation, cell surveillance, and mitochondrial morphology in an Alzheimer's model in vitro.* Biomedical Engineering Seminar. University of California, Irvine. 2026.

**Tran-Dao TK**, Sharma A, Nguyen M, Saidi G, Pham W, Morales M, Horta D, Nunes M, Tabban A, Lim L, Dai S, Wu J, Ochoa-Enriquez D, Kulkarni D, David LM, Nicholas D, Digman M, Syed A, Liu WF. *CD200 enhances uptake and degradation of Aβ by modulating mitochondria and lysosomes of microglia.* Cell and Molecular Immunoengineering, Biomedical Engineering Society Conference. San Diego. 2025.

MacKay J, Obasi M, **Tran-Dao TK**, Liu WF, Digman M. *Exploring Amyloid-Beta induced TNT Formation in an Alzheimer's Model in vitro.* Undergraduate Student Initiative for Biomedical Research Symposium. University of California, Irvine. 2025.

**POSTER PRESENTATIONS**

**Tran-Dao TK**, David LM, Kulkarni D, Morales M, Pham W, Horta D, Niu A, Nunes M, Tabban A, Lim L, Liu WF. *Soluble CD200 modulation of microglia as a neuroprotective strategy against Alzheimer's Disease*. BMES Cellular and Molecular Bioengineering Conference. Carlsbad. 2025. **Award: BMES Cellular & Molecular Bioengineering Poster Award.**

**Tran-Dao TK**, David LM, Kulkarni D, Morales M, Pham W, Horta D, Niu A, Nunes M, Tabban A, Lim L, Liu WF. *Soluble CD200 enhances plaque uptake by modulating mitochondrial dynamics*. Engineering + Society Conference: Transforming Society Through Disruptive Technology. UC Irvine. 2025. **Award: Third Place Poster Award.**

Morales M, **Tran-Dao TK**, Liu WF. Soluble CD200 protein regulates microglial Immune Response. Undergraduate Research Opportunity Symposium. UC Irvine. 2025.

Morales M, Pham W, Horta D, **Tran-Dao TK**, Liu WF. Searching for a HeRO: Stabilizing Thermally Degradable CD200 for Therapeutic Experiments. Undergraduate Research Opportunity Symposium. UC Irvine. 2025.

## Chapter 1: Regulation of Neuroinflammation and Debris Clearance in the Alzheimer's Brain


### Abstract

Alzheimer's Disease (AD) is the most prevalent form of dementia and is largely correlated to aging. Neuroinflammation and debris accumulation are discussed as hallmarks directly impacted by immune cells present in the central nervous system (CNS). Glial and myeloid cells have been shown to use debris clearance pathways similar to those seen in autophagy, the normal cellular process of proteostasis for turnover of damaged proteins and organelles. We compare canonical autophagy with LC3-associated phagocytosis (LAP) and discuss their implications on microglial metabolism. Finally, we propose targeting microglia by engaging cell-specific signaling axes to address AD hallmarks.


### 1.1 Introduction

#### 1.1a Alzheimer's Epidemiology

Around 7.2 million Americans aged 62 or older are suffering from Alzheimer's Disease as of 2025 (Hebert et al., 2013; Rajan et al., 2021). Alzheimer's Disease (AD) is the 6th leading cause of death in the United States as reported by the CDC in 2022, and the most prevalent form of dementia. In Wales and the UK, AD is reported to be the leading cause of death in women, surpassing even heart disease (Moutinho, 2025). While a small percentage of AD is hereditary or otherwise related to known genetic mutations, a far larger number of cases are considered sporadic and largely correlated to aging (Bagyinszky et al., 2014; Jack et al., 2024). The biological process begins with the hallmark appearance of AD neuropathologic changes (ADNPC), amyloid-beta (Aβ) plaques and phosphorylated tau (pTau) protein tangles. The current prognosis involves 3-15 years of irreversible symptom advancement caused by neurodegeneration. While non-specifically age-related, AD is positively correlated with some genetic markers and life events that contribute to chronic neuroinflammation (**Table 1.1**). The Alzheimer's Association expounds a biological AD diagnosis that is established when a patient

exhibits core biomarkers that include neuroinflammation, amyloid-beta (Aβ) pathology, or tauopathy, alongside co-pathologies such as alpha-synuclein (α-syn) or vascular brain injury (Jack et al., 2024). The European Union prefers a symptom-based diagnosis with fine distinctions of types of dementia (Frisoni et al., 2024). This review summarizes key hallmarks of AD in the context of the immune system of the central nervous system (CNS). Age and neuroinflammation are discussed as an independent risk factor for AD followed by the discussion of debris accumulation in the brain – the traditional target for current AD therapies. We compare anti-inflammation and immunomodulation studies and propose anti-inflammatory therapeutics that target microglia to prevent AD hallmarks.

**Table 1.1: Alzheimer's Disease General Information**

| | |
|---|---|
| **Symptoms** | Sleep Disturbances and wandering<br>Agitation and mood changes<br>Memory loss<br>Impaired judgement<br>Impaired movement and physical capabilities (Parkinson's Disease coupling) |
| **Biological Hallmarks** | Neuroinflammation<br>Impaired debris clearance (Aβ and pTau buildup)<br>Metabolic decline of mitochondrial bioenergetics, glucose uptake, oxyradical damage, cholinergic loss, Synapse and brain volume loss |
| **Other forms of dementia with frequent overlap** | Lewy Bodies and α-syn copathology<br>Limbic-predominant age-related TDP-43 encephalopathy (LATE)<br>Parkinson disease |

| | |
|---|---|
| | Frontal temporal dementia<br>Vascular dementia<br>Chemobrain<br>Hippocampal sclerosis<br>Vitamin B12 deficiency |
| **Sporadic** | Age<br>Traumatic Brain Injury (TBI)<br>Chronic Traumatic Encephalitis (CTE)<br>Viral infection / Viral encephalitis<br>Circadian disruptions<br>Other factors |
| **Genetic** | Mutation(s) in APP, ApoE4 haplotype, Trem2, PSEN1, PSEN2, or SORL1 |

### 1.1b. Age as a Disease Factor

There is evidence for age-related inflammation in the CNS through increased TNF-receptor expression in aged neurons that have been associated with increased Aβ toxicity compared to young neurons (Patel and Brewer, 2008). An age-related increase in Aβ was additionally observed in the brains of 3xTg-AD model mice. This increase was associated with changes in redox state and metabolism that resulted in declines in energy levels for autophagic clearance of Aβ (Dong et al., 2019; Pontrello et al., 2022; Martínez et al., 2023; Santana et al., 2025).

## 1.2 Alzheimer Disease Hallmarks

### 1.2a Neuroinflammation

Neuroinflammation is a natural process used by the brain's immune system to mediate pathogenic infection and removal of cellular byproducts (Müller and Di Benedetto, 2025; Müller et al., 2025). However, aging and events like traumatic brain injury or viral brain infection can lead to a chronic inflammatory environment in the CNS (**Figure 1.1**). Neuroinflammation is predominantly mediated by activated microglia and often accompanies debris hallmarks - leading many researchers to target the debris itself (Lippa et al., 1998; Bharadwaj et al., 2009; Chakrabarty et al., 2010; Ishiura et al., 2013; Chen et al., 2017; Guénette et al., 2017; Brewer et al., 2020; Choi et al., 2020; Bogale et al., 2021; d'Errico et al., 2022; Jäntti et al., 2022; Shim et al., 2022; Dutta et al., 2023; Alkhalifa et al., 2025)(Levine et al., 2023; Müller and Di Benedetto, 2025; Müller et al., 2025). When faced with injurious stimuli immune cells, like microglia, undergo phenotypic changes that enable specified functions associated with inflammatory signaling and debris engulfment (Povala et al., 2025). While canonically meant for neuroprotection, overactivated microglia can become desensitized and lose important regulatory functions.

Endogenous factors like disease associated molecular patterns (DAMPs), phosphorylated Tau (pTau) tangles, Aβ-plaques, and alpha-synuclein (α-syn) aggregates are believed to trigger neuroinflammation in the AD brain (Müller and Di Benedetto, 2025). However, some studies suggest neuroinflammation occurs much earlier than debris accumulation. While debris accumulation likely plays a role in propagating neuroinflammation, it should be noted that neuroinflammation often precedes the clinical onset of various neurodegenerative diseases, including Alzheimer's disease, by years or frequently even decades (Kiraly et al., 2023). Diseases and injury like viral encephalitis or traumatic brain injury (TBI) are both examples of life events that can lead to neuroinflammation (Zhao et al., 2020; Levine et al., 2023; Zhang et al., 2023).

Following Covid-19, the effect of neuroinflammation caused by viral infections on neurodegenerative diseases has gained increased attention (Lee et al., 2024; Singh et al., 2024).

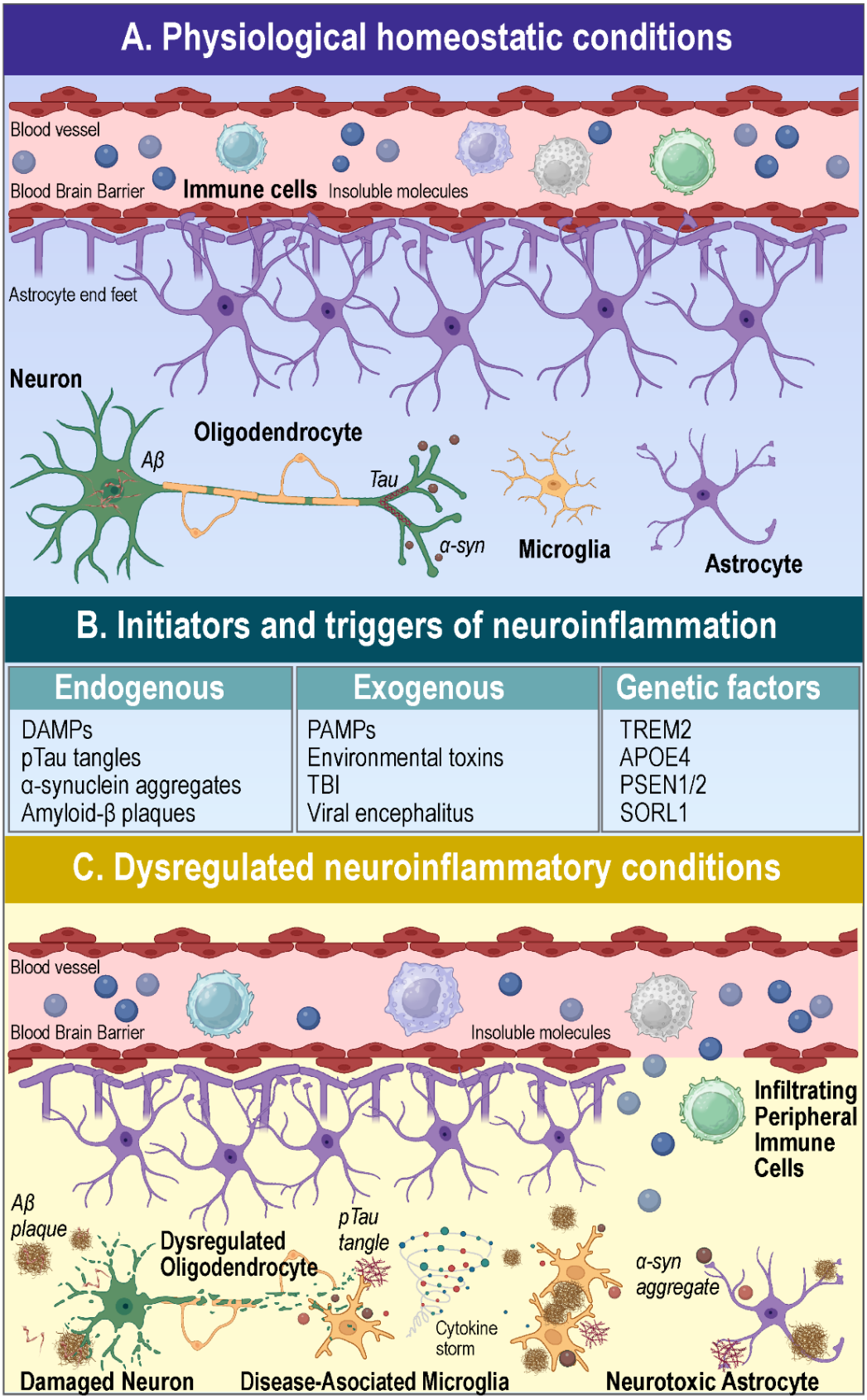

**Figure 1.1: Neuroinflammation in the AD brain**
(A) Under homeostatic conditions, astrocytes and endothelial cells make up the blood brain barrier (BBB) which separates circulating immune cells and insoluble molecules from neurons and glial cells found in the CNS. (B) Varying factors that contribute to neuroinflammatory dysregulation. (C) Dysregulated neuroinflammatory conditions include neuronal damage, disease-associated microglia (DAMs), neurotoxic astrocytes, and oligodendrocytes with impaired myelination function. Adapted from Muller et al., 2025 (Müller et al., 2025). Created with Bio**R**ender (Science Suite Inc., 2026).

Levine et al. analyzed genotype data available through a nationwide Finnish biobank (FinnGen) and associated viral exposures with increased risk of neurodegenerative disease (Levine et al., 2023). The strongest association was found between viral encephalitis and AD. Their findings suggest neuroinflammation alone, as introduced throughout a patient's lifetime exposure to infectious diseases, can impact AD prognosis. Indeed, patients undergoing long term anti-inflammatory treatments for conditions like rheumatoid arthritis (RA) tend to have lower AD prevalence, suggesting combating inflammation in the body can have a beneficial effect on preventing AD (Policicchio et al., 2017). A study conducted over the course of twelve years showed evidence of reduced AD risk associated with use of NSAIDs and anti-hypertensive medications as well as a varied diet consisting of recommended nutrient groups, and greater intake of dietary and supplemental use of antioxidant vitamins E and C (Tschanz et al., 2005, 2013). These findings suggest mediating inflammation in the body can prevent AD-associated cognitive decline. The appearance of inflammation before other disease hallmarks presents the scientific community with a chicken-or-egg scenario. Nevertheless, whether debris clearance or neuroinflammation acts as the original trigger of AD, the complicated relationship between the two contributes to disease progression.

### 1.2b Neuroinflammation and Debris Accumulation: Chicken or the egg?

Due to the interplay between inflammatory mediation and debris recognition and clearance, whether neuroinflammation is to blame for impaired debris clearance or vice versa is still under debate (Millet et al., 2024). In AD, chronic neuroinflammation is suspected to impair mechanisms that normally protect the delicate biochemical balance in the CNS. The extracellular space is normally “kept clean” through the cerebral glymphatic system and roaming immune cells (**Figure 1.2a**) (Ransohoff and Brown, 2012; Kölliker-Frers et al., 2021; Wang et al., 2023). Recent literature no longer considers the CNS as an entirely immune-privileged organ due to the involvement of the glial-dependent lymphatic (glymphatic) system – a “pseudo-lymphatic” system that flushes out debris during sleep by removing soluble proteins and metabolites from the central nervous system while perivascular tunnels formed by astrocytes supply the brain with glucose, lipids and neuromodulators (Iliff et al., 2012; Negi and Das, 2018; Reddy and van der Werf, 2020). Unlike waste clearance in peripheral tissues which is predominantly handled by the lymphatic system draining interstitial fluid (ISF) and solutes toward the lymph nodes, the glymphatic system uses cerebrospinal fluid (CSF) and interstitial fluid (ISF) to drain pathogens, waste and infiltrating immune cells from the brain to meningeal lymphatic vessels (MLV) in the dura mater of the brain and spinal cord (Voumvourakis et al., 2026). Glymphatic clearance has been shown to predominantly occur during sleep or anesthesia – presenting a problem in patients who experience disrupted sleep either through disease or circadian disruptions from lifestyle choices, genetic and epigenetic predisposition, or environmental misalignment (Ren et al., 2025).

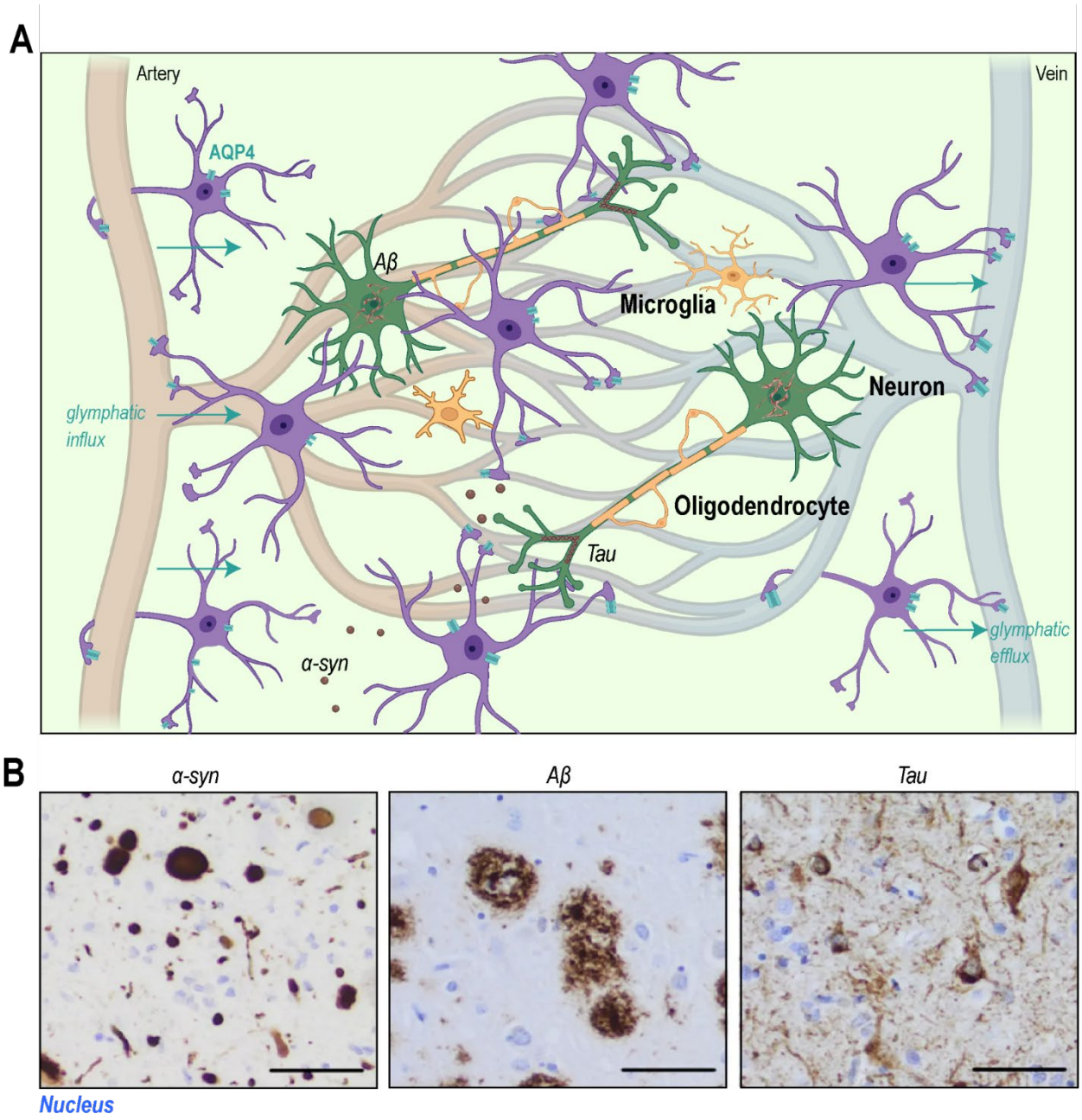


**Figure 1.2: Debris clearance mechanisms prevent toxic aggregates**

(A) Debris clearance in the CNS predominantly occurs during sleep through the glymphatic pathway. (B) Immunohistochemical staining of alpha-synuclein, amyloid-beta, and pTau. Adapted from (Zampar et al., 2024) (41,45). Scale bar = 50μm. Figures adapted from (Ransohoff and Brown, 2012; Wang et al., 2023; Zampar et al., 2024).

### 1.3 Debris Accumulation

#### 1.3a Glia-Mediated Debris Clearance

Astroglia (astrocytes) and microglia are roaming immune cells that use chemical and mechanical cues to detect injurious stimuli and break down debris. Astrocytes regulate neurotransmitter balance, ion exchange, and metabolic support as well as immune signaling (Potokar and Jorgačevski, 2025). When these mechanisms are impaired either through overload or energy deprivation in AD, debris buildup and neuroinflammation work in tandem to further exacerbate the disease (Santana et al., 2025). While microglia are crucial to synaptic pruning during development, they are also required in the adult brain to mediate clearance of debris like apoptotic cells or other cellular byproducts (Mattson et al., 1998; Fraser et al., 2010; Brioschi et al., 2020; Cornell et al., 2021). To avoid improper clearance by nearby microglia, adult neurons rely on “Don’t eat me” signals to inhibit phagocytic activity (Elward and Gasque, 2003; Lehrman et al., 2018; Elberg et al., 2019).

Phagocytic exhaustion can occur however, when immune cells are chronically activated. This chronic activation leads to desensitization towards substrates that would normally be recognized, and subsequent uptake impairment (Millet et al., 2024). Microglial synaptic pruning for example, has been identified as a major contributor to synapse loss in AD, with positron emission tomography (PET) scans of patients with early AD confirming a significant association between lower synaptic density and decreased cognitive performance (Mecca et al., 2022; Wang et al., 2023). To combat impaired function in exhausted microglia, Elmore et al depleted microglia using a CSF1R inhibitor (PLX5622) *in vivo* for 14 days, followed by a recovery period that triggered new microglia proliferation. This was associated with reversed cognitive, synaptic, and neuronal deficits (Elmore et al., 2018).

### 1.3b Types of pathogenic debris seen in AD

*Alpha-synuclein* proteins (α-Syn) are naturally produced by neurons and glial cells to mediate synaptic vesicle trafficking, mitochondrial and endoplasmic reticulum (ER) homeostasis, lysosome and phagosome function, and cytoskeleton organization (Bogale et al., 2021; Mavroeidi and Xilouri, 2021). The pathological form of α-Syn assembles in prion-like polymeric structures by inducing the conformational conversion of native α-Syn (**Figure 1.2b**) (Zampar et al., 2024). α-Syn deposition in Lewy bodies defines the Lewy body variant of AD and has been shown to colocalize with pTau and Aβ (Shim et al., 2022; Forloni, 2023). In one study, 63% of subjects with familial AD (FAD) contained α-Syn positive Lewy bodies (Forloni, 2023). A study conducted in 2025 detected α-syn co-pathology in 60% of AD cases, more frequently, although not significantly, in women (Lippa et al., 1998). Povala et al. investigated the co-pathology of Aβ and pTau and inflammation by assessing PET scans to observe the binding of the inflammatory microglial marker, TSPO (translocator protein) (Povala et al., 2025). They found two neuroinflammatory waves. The first was associated with brain Aβ deposition, and the second with widespread pTau tangle pathology. Interventional causation studies are needed to disentangle these associations as either 1) increased production of Aβ and pTau induce inflammation, or 2) waves of inflammation evoke increased production of Aβ and pTau, or 3) two-hits from increased inflammation and increased production of Aβ and pTau lead to microglia-mediated clearance and deposition of Aβ and pTau in plaques.

*pTau tangles* emerge when tau proteins, originally responsible for microtubule stabilization, become hyperphosphorylated and aggregate with one another instead of binding to their canonical targets. These aggregates, called pTau tangles, disrupt the neuron's transport system and synaptic communication with other neurons (Medeiros et al., 2010; Rohn, 2015). Intracellular pTau can be released from neurons by exocytosis through the secretion of free protein, extracellular vesicles, or neuronal death pathways (Pérez et al., 2019; Chen and Yu,

2023). pTau aggregates have been shown to induce glial inflammation through the TLR2 inflammation pathway which induces the release of pro-inflammatory molecules such as TNFα and MCP1 (Kielian et al., 2005; Dutta et al., 2023).

*Amyloid-beta plaques* originate from amyloid precursor proteins (APP) which are single-pass transmembrane kinesin-I membrane receptors that mediate the axonal transport of beta-secretase and presenilin-1, and synaptic adhesion (Kamal et al., 2001; Bharadwaj et al., 2009). Pathogenic amyloid-beta (Aβ40 and Aβ42) emerges when APP is cleaved by β or γ-secretase instead of α-secretase (Chow et al., 2010; Ishiura et al., 2013; Brewer et al., 2020). Preferential cleaving by the two former enzymes create “sticky” fragments that result in intraneuronal aggregates that are deposited in dense aggregates that make up a major component of extracellular plaque found in AD brains (Bharadwaj et al., 2009; Brewer et al., 2020). Aβ aggregates have been shown to induce sensitized TLR4 signaling in rats in which the TLR4 signaling cascade induced production of inflammatory cytokines TNFα and IL1-β (Hughes et al., 2020). A study by Capilla-López et al in 2025 investigated the effects of both pTau and Aβ *in vivo* and associated different cognitive effects depending on which protein aggregate was present (Capilla-López et al., 2025). Hippocampal pTau was associated with memory deficits while intracellular Aβ in the basolateral amygdala were linked to anxiety and fear. While Aβ, pTau, and α-syn are capable of causing damage individually, interactions *in vivo* have been shown to promote the aggregation and accumulation of each other to accelerate cognitive dysfunction (Clinton et al., 2010). Apoptosis associated speck-like protein containing a caspase recruitment domain (ASC) is an adaptor protein required for inflammasome activation of caspase-1 (Stutz et al., 2013; Ballotto et al., 2026). After inflammasome activation, ASC assembles into a large protein complex called an ASC speck designated for release by activated microglia. ASC specks bind rapidly to Aβ and increase the formation of Aβ oligomers and aggregates, thus acting as an inflammation-driven cross-seed for Aβ pathology, possibly supporting the two-hit process (Venegas et al., 2017).

### 1.3c Debris Clearance Mechanisms

*Phagocytosis* is the engulfment of debris, apoptotic synapses or pathogens by immune cells, like microglia and astrocytes, followed by lysosomal degradation. In response to injury, microglia can employ either inflammatory or non-inflammatory phagocytosis (efferocytosis) to remove debris while astrocytes mainly focus on reforming the blood brain barrier (BBB) to prevent further damage (Neumann et al., 2009; Vainchtein and Molofsky, 2020). When microglia come into contact with a phagocytic target through one of its many receptors (TLR, SRA1, SRB1), clathrin pulls the cell membrane into a pocket to engulf the substrate and dynamin pinches the membrane closed to form a phagosomal vesicle tagged for lysosomal degradation (Solé-Domènech et al., 2016).

*Autophagy* was first identified as a self-degradative process used by cells undergoing nutrient stress (Takeshige et al., 1992; Glick et al., 2010). Recent literature has situated autophagy as an integral cellular process responsible for regulating lipid homeostasis, neuroinflammation, and pTau pathology (Xu et al., 2021). An inflammation model using lipopolysaccharide (LPS) and N9 microglial cells showed a suppressive effect of inflammation on autophagic flux (Ye et al., 2020). Additionally, neuronal autophagy deficits were implicated in neurodegenerative disease in a mouse model (Hara et al., 2006). *Selective autophagy* is a specialized form of autophagy involved in the autophagic degradation of specific substrates (Jülg et al., 2021). Microglia have been shown to clear neuron-released α-syn via selective autophagy through TLR4-induced upregulation of p62, also known as sequestosome 1 (SQSTM1) (Choi et al., 2020; Potokar and Jorgačevski, 2025). Notably, increased SQSTM1 expression has been observed in the presence of pTau (Kuusisto et al., 2001).

SQSTM1 binding has been linked directly to microtubule associated protein 1 light chain 3 (LC3) recruitment to autophagosomes in a Huntington's Disease model and to LC3-facilitated degradation of ubiquitinated protein aggregates by autophagy in HeLa cells (Bjørkøy et al., 2005;

Pankiv et al., 2007). Inhibition of autophagy in microglia and macrophages has been shown to exacerbate innate immune responses and worsen brain injury outcomes (Hegdekar et al., 2023). Human (HeLa) cells grown under starvation conditions have also been shown to activate autophagy through the AMPK pathway (Li et al., 2013).

*LC3-associated phagocytosis (LAP)* and *LC3-associated endocytosis (LANDO)* are phagocytosis pathways used by both astrocytes and microglia that involve autophagy related proteins (ATG) (Takeshige et al., 1992; Zhou et al., 2022; Chen et al., 2023; Peña-Martinez et al.). Various ATG proteins play a part in eventually securing an LC3 tag on the single-membrane endosome surface to enable lysosomal fusion (Kumar and Mills, 2023). The involvement of these proteins enables the fusion of endosomes and phagosomes to lysosomes by enabling the HOPs Complex to bind to SNARE proteins present on both the vesicle and lysosome surface (Jiang et al., 2014). An *in vitro* study by Chen et al. further suggests the involvement of the p38-DAPK signaling axis via Beclin-1 in the regulation of LAP in mouse microglia (Chen et al., 2023).

### 1.3d LANDO/LAP bridge phagocytosis and autophagy

While Canonical autophagy and LAP are clearance pathways used for different purposes, many of the mechanisms used to assemble and tag vesicles are remarkably similar (**Figure 1.3**). In autophagy, protein and organelle turnover drives the cell to digest organelles by forming a double membrane lipid bilayer called a phagophore around the target cargo (Takeshige et al., 1992; Reggiori and Mauthe, 2016). LAP and LANDO however, use single-membrane phagosomes and endosomes to encapsulate cargo.

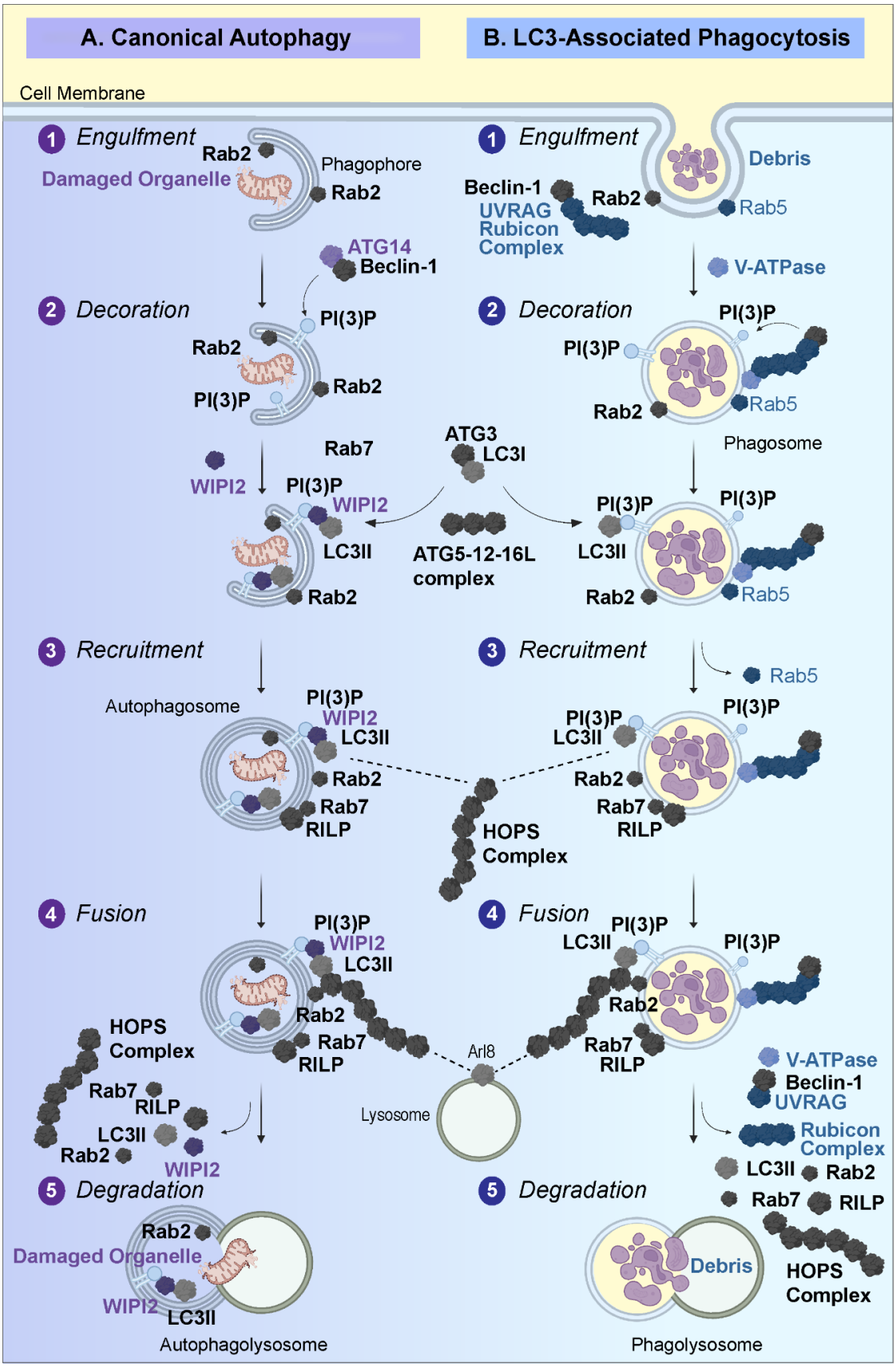
A. Canonical Autophagy
B. LC3-Associated Phagocytosis
Cell Membrane
1 Engulfment
Rab2
Damaged Organelle
Phagophore
Rab2
ATG14
Beclin-1
2 Decoration
PI(3)P
Rab2
PI(3)P
Rab2
Rab7
WIPI2
PI(3)P
WIPI2
LC3II
Rab2
ATG3
LC3I
ATG5-12-16L complex
3 Recruitment
Autophagosome
PI(3)P
WIPI2
LC3II
Rab2
Rab7
RILP
4 Fusion
PI(3)P
WIPI2
LC3II
Rab2
Rab7
RILP
HOPS Complex
Rab7
RILP
LC3II
Rab2
WIPI2
5 Degradation
Rab2
Damaged Organelle
WIPI2
LC3II
Autophagolysosome
1 Engulfment
Debris
Beclin-1
UVRAG
Rubicon
Complex
Rab2
Rab5
V-ATPase
2 Decoration
PI(3)P
PI(3)P
Rab2
Rab5
Phagosome
PI(3)P
LC3II
Rab2
PI(3)P
Rab5
3 Recruitment
Rab5
PI(3)P
PI(3)P
LC3II
Rab2
Rab7
RILP
HOPS Complex
4 Fusion
PI(3)P
LC3II
PI(3)P
Rab2
Rab7
RILP
Arl8
Lysosome
V-ATPase
Beclin-1
UVRAG
Rubicon Complex
LC3II
Rab2
Rab7
RILP
5 Degradation
Debris
HOPS Complex
Phagolysosome

**Figure 1.3: Canonical autophagy and LAP share many similarities**
Canonical autophagy enables cellular turnover of damaged organelles while LC3-associated phagocytosis (LAP) involves "decorating" phagosomes with autophagy marker LC3, causing it to sometimes be referred to as "non-canonical" autophagy.

While resource deprivation induces the binding of Beclin-1 to ATG14, LAP involves the binding of Beclin-1 to UVRAG and Rubicon in response to a short respiratory burst by NOX2 when it consumes NADPH to produce the damaging oxyradical $O2^{-}$(Wong et al., 2018). Despite mediation through different Beclin-containing complexes, both pathways result in the addition of a "lipid flag" on the vesicle membrane recognizable by LC3. Freshly translated LC3 proteins are processed by ATG4 to become the soluble LC3I for use in the cytosol. ATG3 and the ATG5-12-16L complex then facilitate LC3I binding to the vesicle surface to become its bound form, LC3II (Itakura and Mizushima, 2010). The vesicular protein Rab7 binds to Rab-interacting lysosomal proteins (RILP) to enable migration of these phagosomes towards lysosomes and enable LC3II and Ras2 anchoring of the HOPS complex (Wu et al., 2005; Lin et al., 2014). The other end of the HOPS complex binds to Arl8 proteins present on the lysosomal membrane (Khatter et al., 2015). Finally, the HOPS complex binds to SNARE proteins present on both vesicle and lysosome surface to force the vesicle and lysosome together to form an autophagolysosome in canonical autophagy, or phagolysosome in LAP/LANDO (Jiang et al., 2014). Thus, despite early steps being carried out by different proteins, both canonical autophagy and LAP pathways result in lysosomal degradation and can be described as the engulfment of cargo, decoration of vesicles, recruitment of HOPS, fusion to lysosome, and degradation of cargo.

## 1.4. Cell Metabolism

### 1.4a Autophagic Regulation of cell metabolism

Mitochondria are maternally inherited organelles that play critical roles in oxidative stress, energy and intermediate metabolism, calcium homeostasis, and cell survival (Rambold

and Lippincott-Schwartz, 2011; McAvoy and Kawamata, 2019; Li et al., 2022). Mitochondrial quality control is maintained through a type of selective autophagy called mitophagy that allows the cell to target dysfunctional mitochondria to maintain regular cell homeostasis. Genes known to regulate mitophagy are autophagy related gene 32 (ATG32), Beclin-1, and PINK1, among many others (Kanki et al., 2009; Geisler et al., 2010; Xu et al., 2021; Quiles et al., 2023).

Healthy mitochondria use cytoplasmic nutrients to produce ATP in the inner mitochondrial membrane (IMM) where the electron transport chain (ETC) facilitates a proton gradient in the intermembrane space (**Figure 4**). As mitochondrial cristae enable increased surface area that can be populated by the ETC, mitochondrial network formation is often a sign of healthy mitochondria, particularly in immune cells as it further supports energy demands by allowing more space for ATP production (Li et al., 2020).

### 1.4b Microglial Energetics

Microglia need pyruvate from glucose, lipids, and proteins to power regular cell function through oxidative phosphorylation (OxPhos) (Huang et al., 2024). Resting microglia employ motile processes that continuously undergo cycles of formation and withdrawal, making them remarkably motile despite limited movement of the cell somata itself (Nimmerjahn et al., 2005). Activated microglia however, require short bursts of energy supplied through increased glucose absorption, anaerobic glycolysis, and oxidative pentose phosphate pathway (PPP) activation (Gimeno-Bayón et al., 2014). Despite a reliance on alternatives to OxPhos for energy production, fluorescent lifetime imaging microscopy (FLIM) measurements of NADH/NADPH autofluorescence indicate that LPS stimulation actually reduces free NADH/NADPH signal in microglia (Sagar et al., 2020). This phenomenon could be explained by enhanced cell surveillance

in “resting” microglia through LC3-mediated endocytosis of the surrounding microenvironment (Stolz et al., 2016).

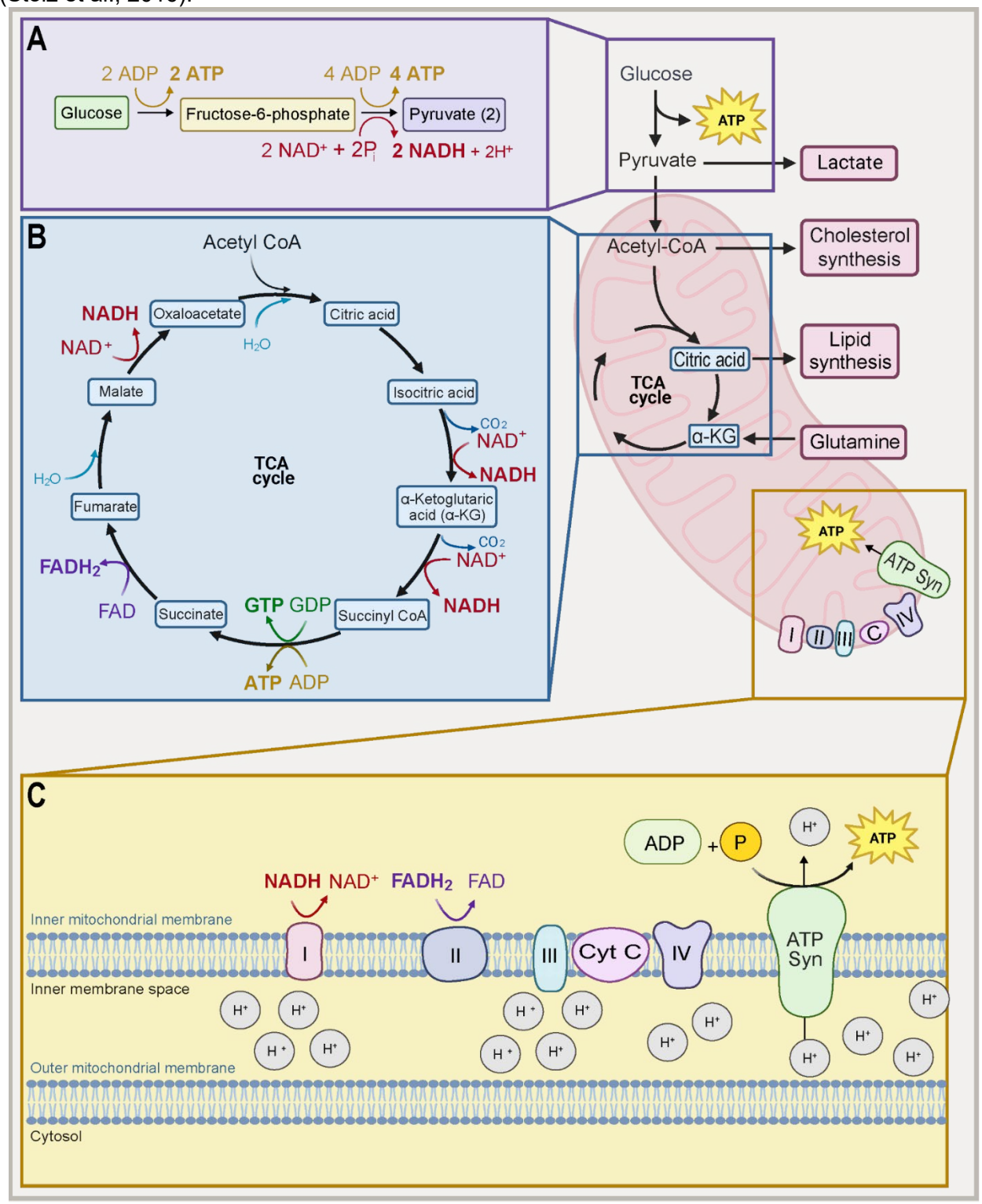

**Figure 1.4: Components of Cellular Respiration**

(A) Glucose is broken down into pyruvate in glycolysis and transported into mitochondria to be converted into Acetyl-CoA. (B) Acetyl-CoA conversion to citric acid kickstarts the TCA cycle, resulting in the production of NADH, FADH2, GTP, and ATP. (C) NADH and FADH2 are used by mitochondrial complex I and II to generate a proton gradient that powers ATP synthase. Adapted from (Nolfi-Donegan et al., 2020; Guerbette et al., 2022).

### 1.4c Lactate: More than a Byproduct

Lactate is a crucial metabolite that also plays a role in cellular function (Monsorno et al., 2022). Lactate dehydrogenase (LDH) comprises two subunits, LDHA and LDHB, with LDHB being significantly expressed in microglia in the adult hippocampus (Zhang et al., 2014; Mattei et al., 2020; Huang et al., 2024). The LDHA subunit converts pyruvate into lactate under anaerobic conditions and in the process, also regenerates NAD+. LDHA knockdown has been shown to suppress LPS-induced expression of TNF-α, IL-6, iNOS, COX-2, and IL-1β (Cheng et al., 2021). The LDHB subunit on the other hand, converts lactate into pyruvate for NADH use in mitochondria. In the process, cytosolic NAD+ accepts a proton to become NADH (Jain et al., 2026). Together, these studies suggest that homeostatic microglia can maintain mitochondrial function through proteins like LDH while also producing high levels of free NADH/NADPH.

## 1.5 Current AD treatments

Current AD treatments predominantly focus on ameliorating cognitive symptoms by using cholinesterase inhibitors or by targeting Aβ directly using anti-Aβ antibodies (**Table 1.2**) (Čolović et al., 2013; Wu and Fuh, 2025). The latter has been a controversial therapeutic target however, as even non-diseased brains have been shown to contain Aβ (Dickson et al., 1992). The treatment landscape is also shifting towards treating neuroinflammation as a strategy against AD as studies increasingly point to immune cells as key propagators of the disease. However, general anti-inflammatories have so far been ineffective. Randomized trials performed across six US clinics concluded naproxen and celecoxib, two types of NSAIDs, were ineffective in preventing disease onset in patients with family history of AD. Similarly, a phase 2 trial of

subcutaneous Etanercept, an anti-TNFα blocker, failed to improve the cognition of mild AD patients.

**Table 1.2: Current AD treatments**

| Drug | Brand Name | Target | Mechanistic target | FDA status | Reference |
|---|---|---|---|---|---|
| Donepezil | Aricept | Cognitive decline Memory loss | Cholinesterase inhibitor | Approved (1996) | (Rogers et al., 1998) NCT02822573 |
| Galantamine | Reminylm, Razadyne, Razadyne ER | Cognitive decline Memory loss | Cholinesterase inhibitor | Approved (2001) | NCT00679627 |
| Rivastigmine | Exelon, Exelon Patch | Cognitive decline Memory loss | Cholinesterase inhibitor | Approved (2000) | (Farlow et al., 2013) NCT00988117 |
| Benzgalantamine | Zunveyl | Cognitive decline Memory loss | Cholinesterase inhibitor | Approved via 505(b)(2) (2024) | NDA 218549 |
| Tacrine | Cognex | Cognitive decline Memory loss | Cholinesterase inhibitor | Discontinued in US (2012) | (Ford et al., 1993) NCT00104442 |
| Namenda | Memantine | Cognitive decline Memory loss | Glutamate receptor | Approved (2003) | NCT00857649 |
| Lecanemab | Leqembi | Debris clearance | Aβ42 | Approved (2023) | (Alkhalifa et al., 2025) NCT03887455 |
| Donanemab | Kisunla, Lomalzi | Debris Clearance | Aβ42 | Approved (2024) | (Herrmann et al., 2013) NCT04437511 |

| | | | | | |
|---|---|---|---|---|---|
| Mastinib | Masican | Inflammation, Mast Cells | Tyrosine Kinase inhibitor | Phase 2b / 3 Trial complete (2023) | (Dubois et al., 2023)<br><br>NCT05564169 |
| NE3107 | Bezisterim | Inflammation, Blood Insulin abnormalities | ERK1/2 | Phase 2b / 3 Trial complete (2020) | NCT04669028 |

A phase 2 clinical trial of Neflamapimod, an anti-inflammatory therapeutic targeting the p38α pathway, concluded that while Neflamapimod was able to decrease CSF biomarkers of synaptic dysfunction it did not improve episodic memory in patients with mild AD (Prins et al., 2021). These results suggest a more cell-specific approach may be required to effectively target hallmarks propagated by immune cells.

Masitinib, a selective oral tyrosine kinase inhibitor, was used to target mast cells as a way of combating neuroinflammation in AD in a Phase 2 clinical trial (Piette et al., 2011). Treatment was associated with slower cognitive decline in AD, with an acceptable tolerance profile. Masitinib selectively inhibits tyrosine kinase by targeting c-Kit (also known as CD117), platelet-derived growth factor receptors (PDGFR), and, to a lesser extent, Lyn, Fyn, and the FAK pathway, without inhibiting kinases of known toxicities (Naeim, 2008; Dubreuil et al., 2009). A Phase 2 trial investigating NE3107 – an oral, anti-inflammatory and insulin-sensitizing molecule – found an association between NE3107 treatment and clinician-rated improvements in cerebral blood flow and functional connectivity within the brain, making it a successful therapeutic that can address multiple disease hallmarks (Yoon et al., 2023; Haroon et al., 2024).

**1.6 Conclusion**

Microglia connect two major AD hallmarks by directly influencing neuroinflammation and Aβ clearance. This makes microglia a promising cellular target for the prevention of AD hallmarks. Targeting microglial signaling pathways to leverage the CNS immune system to prevent chronic inflammation phenotypes and impaired functions could be a promising

therapeutic target. Existing literature supports the use of signaling axes like CD200:CD200R or SIRPα:CD47, which have been linked to dampened inflammation and enhanced phagocytosis in microglia (Barclay et al., 2002; Walker et al., 2009; Kim et al., 2014; Varnum et al., 2015; Chen et al., 2017; Lehrman et al., 2018; Elberg et al., 2019; Jalil et al., 2022). Varnum et al. assessed the phagocytic capability of CD200-treated microglia *in vitro* and *in vivo* and saw an increase in microglial uptake of Aβ (Varnum et al., 2015). As such, targeting microglial inflammation and debris clearance through the CD200 signaling axis may be a valuable strategy in preventing Alzheimer's Disease hallmarks.

**References**


Alkhalifa AE, Al Mokhlf A, Ali H, Al-Ghraiybah NF, Syropoulou V. 2025. Anti-Amyloid Monoclonal Antibodies for Alzheimer's Disease: Evidence, ARIA Risk, and Precision Patient Selection. J Pers Med 15:437.

Bagyinszky E, Youn YC, An SSA, Kim S. 2014. The genetics of Alzheimer's disease. Clin Interv Aging 9:535–551.

Ballotto L, Baratta T, Winterberg H, Dusanter C, Sambin S, Corvol JC, Iovino L, Bubacco L, Corti O, Greggio E, Novello S. 2026. Nuclear ASC speck formation in microglia is associated with inflammasome priming and is exacerbated in LRRK2-G2019S Parkinson's disease. Neurobiol Dis 218:107237.

Bharadwaj PR, Dubey AK, Masters CL, Martins RN, Macreadie IG. 2009. Aβ aggregation and possible implications in Alzheimer's disease pathogenesis. J Cell Mol Med 13:412–421.

Bjørkøy G, Lamark T, Brech A, Outzen H, Perander M, Overvatn A, Stenmark H, Johansen T. 2005. p62/SQSTM1 forms protein aggregates degraded by autophagy and has a protective effect on huntingtin-induced cell death. J Cell Biol 171:603–614.

Bogale TA, Faustini G, Longhena F, Mitola S, Pizzi M, Bellucci A. 2021. Alpha-Synuclein in the Regulation of Brain Endothelial and Perivascular Cells: Gaps and Future Perspectives. Front Immunol 12:611761.

Brewer GJ, Herrera RA, Philipp S, Sosna J, Reyes-Ruiz JM, Glabe CG. 2020. Age-Related Intraneuronal Aggregation of Amyloid-β in Endosomes, Mitochondria, Autophagosomes, and Lysosomes. J Alzheimers Dis JAD 73:229–246.

Brioschi S, d'Errico P, Amann LS, Janova H, Wojcik SM, Meyer-Luehmann M, Rajendran L, Wieghofer P, Paolicelli RC, Biber K. 2020. Detection of Synaptic Proteins in Microglia by Flow Cytometry. Front Mol Neurosci 13:149.

Capilla-López MD, Deprada A, Andrade-Talavera Y, Martínez-Gallego I, Coatl-Cuaya H, Sotillo P, Rodríguez-Alvarez J, Rodríguez-Moreno A, Parra-Damas A, Saura CA. 2025. Synaptic vulnerability to amyloid-β and tau pathologies differentially disrupts emotional and memory neural circuits. Mol Psychiatry 30:2966–2979.

Chakrabarty P, Jansen-West K, Beccard A, Ceballos-Diaz C, Levites Y, Verbeeck C, Zubair AC, Dickson D, Golde TE, Das P. 2010. Massive gliosis induced by interleukin-6 suppresses Aβ deposition in vivo: evidence against inflammation as a driving force for amyloid deposition. FASEB J 24:548–559.

Chen G, Xu T, Yan Y, Zhou Y, Jiang Y, Melcher K, Xu HE. 2017. Amyloid beta: structure, biology and structure-based therapeutic development. Acta Pharmacol Sin 38:1205–1235.

Chen X-X, Tao T, Liu X-Z, Wu W, Wang J-W, Yue T-T, Li X-J, Zhou Y, Gao S, Sheng B, Peng Z, Xu H-J, Ding P-F, Wu L-Y, Zhang D-D, Lu Y, Hang C-H, Li W. 2023. P38-DAPK1 axis regulated LC3-associated phagocytosis (LAP) of microglia in an in vitro subarachnoid hemorrhage model. Cell Commun Signal CCS 21:175.

Chen Y, Yu Y. 2023. Tau and neuroinflammation in Alzheimer's disease: interplay mechanisms and clinical translation. J Neuroinflammation 20:165.

Cheng J, Zhang R, Xu Z, Ke Y, Sun R, Yang H, Zhang X, Zhen X, Zheng L-T. 2021. Early glycolytic reprogramming controls microglial inflammatory activation. J Neuroinflammation 18:129.

Choi I, Zhang Y, Seegobin SP, Pruvost M, Wang Q, Purtell K, Zhang B, Yue Z. 2020. Microglia clear neuron-released α-synuclein via selective autophagy and prevent neurodegeneration. Nat Commun 11:1386.

Chow VW, Mattson MP, Wong PC, Gleichmann M. 2010. An Overview of APP Processing Enzymes and Products. Neuromolecular Med 12:1–12.

Clinton LK, Blurton-Jones M, Myczek K, Trojanowski JQ, LaFerla FM. 2010. Synergistic Interactions between Aβ, Tau, and α-Synuclein: Acceleration of Neuropathology and Cognitive Decline. J Neurosci 30:7281–7289.

Čolović MB, Krstić DZ, Lazarević-Pašti TD, Bondžić AM, Vasić VM. 2013. Acetylcholinesterase Inhibitors: Pharmacology and Toxicology. Curr Neuropharmacol 11:315–335.

Cornell J, Salinas S, Huang H-Y, Zhou M. 2021. Microglia regulation of synaptic plasticity and learning and memory. Neural Regen Res 17:705–716.

Dickson DW, Crystal HA, Mattiace LA, Masur DM, Blau AD, Davies P, Yen S-H, Aronson MK. 1992. Identification of normal and pathological aging in prospectively studied nondemented elderly humans. Neurobiol Aging 13:179–189.

Dong Y, Digman MA, Brewer GJ. 2019. Age- and AD-related redox state of NADH in subcellular compartments by fluorescence lifetime imaging microscopy. GeroScience 41:51–67.

Dubois B, López-Arrieta J, Lipschitz S, Doskas T, Spiru L, Moroz S, Venger O, Vermersch P, Moussy A, Mansfield CD, Hermine O, Tsolaki M, AB09004 Study Group Investigators. 2023. Masitinib for mild-to-moderate Alzheimer's disease: results from a randomized, placebo-controlled, phase 3, clinical trial. Alzheimers Res Ther 15:39.

Dubreuil P, Letard S, Ciufolini M, Gros L, Humbert M, Castéran N, Borge L, Hajem B, Lermet A, Sippl W, Voisset E, Arock M, Auclair C, Leventhal PS, Mansfield CD, Moussy A, Hermine O. 2009. Masitinib (AB1010), a potent and selective tyrosine kinase inhibitor targeting KIT. PloS One 4:e7258.

Dutta D, Jana M, Paidi RK, Majumder M, Raha S, Dasarathy S, Pahan K. 2023. Tau fibrils induce glial inflammation and neuropathology via TLR2 in Alzheimer's disease–related mouse models. J Clin Invest 133:e161987.

d'Errico P, Ziegler-Waldkirch S, Aires V, Hoffmann P, Mezö C, Erny D, Monasor LS, Liebscher S, Ravi VM, Joseph K, Schnell O, Kierdorf K, Staszewski O, Tahirovic S, Prinz M, Meyer-Luehmann M. 2022. Microglia contribute to the propagation of Aβ into unaffected brain tissue. Nat Neurosci 25:20–25.

Elberg G, Liraz-Zaltsman S, Reichert F, Matozaki T, Tal M, Rotshenker S. 2019. Deletion of SIRPα (signal regulatory protein-α) promotes phagocytic clearance of myelin debris in Wallerian degeneration, axon regeneration, and recovery from nerve injury. J Neuroinflammation 16.

Elmore MRP, Hohsfield LA, Kramár EA, Soreq L, Lee RJ, Pham ST, Najafi AR, Spangenberg EE, Wood MA, West BL, Green KN. 2018. Replacement of microglia in the aged brain reverses cognitive, synaptic, and neuronal deficits in mice. Available from: https://onlinelibrary.wiley.com/doi/10.1111/acel.12832

Elward K, Gasque P. 2003. "Eat me" and "don't eat me" signals govern the innate immune response and tissue repair in the CNS: emphasis on the critical role of the complement system. Mol Immunol 40:85–94.

Farlow MR, Grossberg GT, Sadowsky CH, Meng X, Somogyi M. 2013. A 24-Week, Randomized, Controlled Trial of Rivastigmine Patch 13.3 mg/24 h Versus 4.6 mg/24 h in Severe Alzheimer's Dementia. CNS Neurosci Ther 19:745–752.

Ford JM, Truman CA, Wilcock GK, Roberts CJ. 1993. Serum concentrations of tacrine hydrochloride predict its adverse effects in Alzheimer's disease. Clin Pharmacol Ther 53:691–695.

Forloni G. 2023. Alpha Synuclein: Neurodegeneration and Inflammation. Int J Mol Sci 24:5914.

Fraser DA, Pisalyaput K, Tenner AJ. 2010. C1q enhances microglial clearance of apoptotic neurons and neuronal blebs, and modulates subsequent inflammatory cytokine production. J Neurochem 112:733–743.

Frisoni GB, Festari C, Massa F, Cotta Ramusino M, Orini S, Aarsland D, Agosta F, Babiloni C, Borroni B, Cappa SF, Frederiksen KS, Froelich L, Garibotto V, Haliassos A, Jessen F, Kamondi A, Kessels RP, Morbelli SD, O'Brien JT, Otto M, Perret-Liaudet A, Pizzini FB, Vandenbulcke M, Vanninen R, Verhey F, Vernooij MW, Yousry T, Boada Rovira M, Dubois B, Georges J, Hansson O, Ritchie CW, Scheltens P, van der Flier WM, Nobili F. 2024. European intersocietal recommendations for the biomarker-based diagnosis of neurocognitive disorders. Lancet Neurol 23:302–312.

Geisler S, Holmström KM, Treis A, Skujat D, Weber SS, Fiesel FC, Kahle PJ, Springer W. 2010. The PINK1/Parkin-mediated mitophagy is compromised by PD-associated mutations. Autophagy 6:871–878.

Gimeno-Bayón J, López-López A, Rodríguez MJ, Mahy N. 2014. Glucose pathways adaptation supports acquisition of activated microglia phenotype. J Neurosci Res 92:723–731.

Glick D, Barth S, Macleod KF. 2010. Autophagy: cellular and molecular mechanisms. J Pathol 221:3–12.

Guénette S, Strecker P, Kins S. 2017. APP Protein Family Signaling at the Synapse: Insights from Intracellular APP-Binding Proteins. Front Mol Neurosci 10:87.

Guerbette T, Boudry G, Lan A. 2022. Mitochondrial function in intestinal epithelium homeostasis and modulation in diet-induced obesity. Mol Metab 63:101546.

Hara T, Nakamura K, Matsui M, Yamamoto A, Nakahara Y, Suzuki-Migishima R, Yokoyama M, Mishima K, Saito I, Okano H, Mizushima N. 2006. Suppression of basal autophagy in neural cells causes neurodegenerative disease in mice. Nature 441:885–889.

Haroon J, Jordan K, Mahdavi K, Rindner E, Becerra S, Surya JR, Zielinski M, Venkatraman V, Goodenowe D, Hofmeister K, Zhang J, Ahlem C, Reading C, Palumbo J, Pourat B, Kuhn T, Jordan S. 2024. A phase 2, open-label study of anti-inflammatory NE3107 in patients with dementias. Medicine (Baltimore) 103:e39027.

Hebert LE, Weuve J, Scherr PA, Evans DA. 2013. Alzheimer disease in the United States (2010–2050) estimated using the 2010 census. Neurology 80:1778–1783.

Herrmann N, Gauthier S, Boneva N, Lemming OM, 10158 Investigators. 2013. A randomized, double-blind, placebo-controlled trial of memantine in a behaviorally enriched sample of patients with moderate-to-severe Alzheimer's disease. Int Psychogeriatr 25:919–927.

Hegdekar N, Sarkar C, Bustos S, Ritzel RM, Hanscom M, Ravishankar P, Philkana D, Wu J, Loane DJ, Lipinski MM. 2023. Inhibition of autophagy in microglia and macrophages exacerbates innate immune responses and worsens brain injury outcomes. Autophagy 19:2026–2044.

Huang Q, Wang Y, Chen S, Liang F. 2024. Glycometabolic Reprogramming of Microglia in Neurodegenerative Diseases: Insights from Neuroinflammation. Aging Dis 15:1155–1175.

Hughes C, Choi ML, Yi J-H, Kim S-C, Drews A, George-Hyslop PSt, Bryant C, Gandhi S, Cho K, Klenerman D. 2020. Beta amyloid aggregates induce sensitised TLR4 signalling causing long-term potentiation deficit and rat neuronal cell death. Commun Biol 3:79.

Iliff JJ, Wang M, Liao Y, Plogg BA, Peng W, Gundersen GA, Benveniste H, Vates GE, Deane R, Goldman SA, Nagelhus EA, Nedergaard M. 2012. A Paravascular Pathway Facilitates CSF Flow Through the Brain Parenchyma and the Clearance of Interstitial Solutes, Including Amyloid β. Sci Transl Med 4:147ra111-147ra111.

Ishiura S, Asai M, Hattori C, Hotoda N, Szabo B, Sasagawa N, Tanuma S. 2013. APP α-Secretase, a Novel Target for Alzheimer Drug Therapy. In: Madame Curie Bioscience Database [Internet]. Landes Bioscience. Available from: https://www.ncbi.nlm.nih.gov/books/NBK6595/

Itakura E, Mizushima N. 2010. Characterization of autophagosome formation site by a hierarchical analysis of mammalian Atg proteins. Autophagy 6:764–776.

Jack CR, Andrews JS, Beach TG, Buracchio T, Dunn B, Graf A, Hansson O, Ho C, Jagust W, McDade E, Molinuevo JL, Okonkwo OC, Pani L, Rafii MS, Scheltens P, Siemers E, Snyder HM, Sperling R, Teunissen CE, Carrillo MC. 2024. Revised criteria for diagnosis and staging of Alzheimer's disease: Alzheimer's Association Workgroup. Available from: https://alz-journals.onlinelibrary.wiley.com/doi/10.1002/alz.13859

Jain C, Kuzmychova H, Grewal A, Chawla U, Mukherjee R, Banerji V, Anderson CM, Martell E, Sharif T. 2026. Extracellular lactate reprograms mitochondrial metabolism and NAD+/NADH redox balance in blood-brain barrier endothelial cells via an LDHB-MPC-NAD+ axis. Free Radic Biol Med 253:377–392.

Jäntti H, Sitnikova V, Ishchenko Y, Shakirzyanova A, Giudice L, Ugidos IF, Gómez-Budia M, Korvenlaita N, Ohtonen S, Belaya I, Fazaludeen F, Mikhailov N, Gotkiewicz M, Ketola K, Lehtonen Š, Koistinaho J, Kanninen KM, Hernández D, Pébay A, Giugno R, Korhonen P, Giniatullin R, Malm T. 2022. Microglial amyloid beta clearance is driven by PIEZO1 channels. J Neuroinflammation 19:147.

Jiang P, Nishimura T, Sakamaki Y, Itakura E, Hatta T, Natsume T, Mizushima N. 2014. The HOPS complex mediates autophagosome-lysosome fusion through interaction with syntaxin 17. Mol Biol Cell 25:1327–1337.

Jülg J, Strohm L, Behrends C. 2021. Canonical and Noncanonical Autophagy Pathways in Microglia. Mol Cell Biol 41:e00389-20.

Kamal A, Almenar-Queralt A, LeBlanc JF, Roberts EA, Goldstein LS. 2001. Kinesin-mediated axonal transport of a membrane compartment containing beta-secretase and presenilin-1 requires APP. Nature 414:643–648.

Kanki T, Wang K, Cao Y, Baba M, Klionsky DJ. 2009. Atg32 Is a Mitochondrial Protein that Confers Selectivity during Mitophagy. Dev Cell 17:98–109.

Khatter D, Raina VB, Dwivedi D, Sindhwani A, Bahl S, Sharma M. 2015. The small GTPase Arl8b regulates assembly of the mammalian HOPS complex on lysosomes. J Cell Sci 128:1746–1761.

Kielian T, Esen N, Bearden ED. 2005. Toll-like receptor 2 (TLR2) is pivotal for recognition of S. aureus peptidoglycan but not intact bacteria by microglia. Glia 49:567–576.

Kiraly M, Foss JF, Giordano T. 2023. Neuroinflammation, Its Role in Alzheimer's Disease and Therapeutic Strategies. J Prev Alzheimers Dis 10:686–698.

Kölliker-Frers R, Udovin L, Otero-Losada M, Kobiec T, Herrera MI, Palacios J, Razzitte G, Capani F. 2021. Neuroinflammation: An Integrating Overview of Reactive-Neuroimmune Cell Interactions in Health and Disease. Mediators Inflamm 2021:9999146.

Kumar AV, Mills J. 2023. Non-canonical autophagy in aging and age-related diseases. Front Cell Dev Biol 11:1137870.

Kuusisto E, Salminen A, Alafuzoff I. 2001. Ubiquitin-binding protein p62 is present in neuronal and glial inclusions in human tauopathies and synucleinopathies. Neuroreport 12:2085–2090.

Lee JD, Solomon IH, Slack FJ, Mavrikaki M. 2024. Cognition-associated long noncoding RNAs are dysregulated upon severe COVID-19. Front Immunol [Internet] 15. Available from: https://www.frontiersin.org/journals/immunology/articles/10.3389/fimmu.2024.1290523/full

Lehrman EK, Wilton DK, Litvina EY, Welsh CA, Chang ST, Frouin A, Walker AJ, Heller MD, Umemori H, Chen C, Stevens B. 2018. CD47 Protects Synapses from Excess Microglia-Mediated Pruning during Development. Neuron 100:120-134.e6.

Levine KS, Leonard HL, Blauwendraat C, Iwaki H, Johnson N, Bandres-Ciga S, Ferrucci L, Faghri F, Singleton AB, Nalls MA. 2023. Virus exposure and neurodegenerative disease risk across national biobanks. Neuron 111:1086-1093.e2.

Li L, Chen Y, Gibson SB. 2013. Starvation-induced autophagy is regulated by mitochondrial reactive oxygen species leading to AMPK activation. Cell Signal 25:50–65.

Li Y, He Y, Miao K, Zheng Y, Deng C, Liu T-M. 2020. Imaging of macrophage mitochondria dynamics *in vivo* reveals cellular activation phenotype for diagnosis. Theranostics 10:2897–2917.

Li Y, Xia X, Wang Y, Zheng JC. 2022. Mitochondrial dysfunction in microglia: a novel perspective for pathogenesis of Alzheimer's disease. J Neuroinflammation 19:248.

Lin X, Yang T, Wang S, Wang Z, Yun Y, Sun L, Zhou Y, Xu X, Akazawa C, Hong W, Wang T. 2014. RILP interacts with HOPS complex via VPS41 subunit to regulate endocytic trafficking. Sci Rep 4:7282.

Lippa CF, Fujiwara H, Mann DM, Giasson B, Baba M, Schmidt ML, Nee LE, O'Connell B, Pollen DA, St George-Hyslop P, Ghetti B, Nochlin D, Bird TD, Cairns NJ, Lee VM, Iwatsubo T, Trojanowski JQ. 1998. Lewy bodies contain altered alpha-synuclein in

brains of many familial Alzheimer's disease patients with mutations in presenilin and amyloid precursor protein genes. Am J Pathol 153:1365–1370.

Martínez RAS, Pinky PD, Harlan BA, Brewer GJ. 2023. GTP energy dependence of endocytosis and autophagy in the aging brain and Alzheimer's disease. GeroScience 45:757–780.

Mattei D, Ivanov A, van Oostrum M, Pantelyushin S, Richetto J, Mueller F, Beffinger M, Schellhammer L, Vom Berg J, Wollscheid B, Beule D, Paolicelli RC, Meyer U. 2020. Enzymatic Dissociation Induces Transcriptional and Proteotype Bias in Brain Cell Populations. Int J Mol Sci 21:7944.

Mattson MP, Keller JN, Begley JG. 1998. Evidence for synaptic apoptosis. Exp Neurol 153:35–48.

Mavroeidi P, Xilouri M. 2021. Neurons and Glia Interplay in α-Synucleinopathies. Int J Mol Sci 22:4994.

McAvoy K, Kawamata H. 2019. Glial mitochondrial function and dysfunction in health and neurodegeneration. Mol Cell Neurosci 101:103417.

Mecca AP, O'Dell RS, Sharp ES, Banks ER, Bartlett HH, Zhao W, Lipior S, Diepenbrock NG, Chen M-K, Naganawa M, Toyonaga T, Nabulsi NB, Vander Wyk BC, Arnsten AFT, Huang Y, Carson RE, van Dyck CH. 2022. Synaptic density and cognitive performance in Alzheimer's disease: A PET imaging study with [11C]UCB-J. Alzheimers Dement 18:2527–2536.

Medeiros R, Baglietto-Vargas D, LaFerla FM. 2010. The Role of Tau in Alzheimer's Disease and Related Disorders. CNS Neurosci Ther 17:514–524.

Millet A, Ledo JH, Tavazoie SF. 2024. An exhausted-like microglial population accumulates in aged and *APOE4* genotype Alzheimer's brains. Immunity 57:153-170.e6.

Monsorno K, Buckinx A, Paolicelli RC. 2022. Microglial metabolic flexibility: emerging roles for lactate. Trends Endocrinol Metab 33:186–195.

Moutinho S. 2025. Women twice as likely to develop Alzheimer's disease as men — but scientists do not know why. Nat Med 31:704–707.

Müller L, Di Benedetto S. 2025. Neuroimmune crosstalk in chronic neuroinflammation: microglial interactions and immune modulation. Front Cell Neurosci [Internet] 19. Available from: https://www.frontiersin.org/journals/cellular-neuroscience/articles/10.3389/fncel.2025.1575022/full

Müller L, Di Benedetto S, Müller V. 2025. The dual nature of neuroinflammation in networked brain. Front Immunol [Internet] 16. Available from: https://www.frontiersin.org/journals/immunology/articles/10.3389/fimmu.2025.1659947/full

Naeim F. 2008. Chapter 2 - Principles of Immunophenotyping. In: Hematopathology. Oxford: Academic Press. p 27–55. Available from: https://www.sciencedirect.com/science/article/pii/B9780123706072000028

Negi N, Das BK. 2018. CNS: Not an immunoprivilaged site anymore but a virtual secondary lymphoid organ. Int Rev Immunol 37:57–68.

Neumann H, Kotter MR, Franklin RJM. 2009. Debris clearance by microglia: an essential link between degeneration and regeneration. Brain 132:288–295.

Nimmerjahn A, Kirchhoff F, Helmchen F. 2005. Resting Microglial Cells Are Highly Dynamic Surveillants of Brain Parenchyma in Vivo. Science 308:1314–1318.

Nolfi-Donegan D, Braganza A, Shiva S. 2020. Mitochondrial electron transport chain: Oxidative phosphorylation, oxidant production, and methods of measurement. Redox Biol 37:101674.

Pankiv S, Clausen TH, Lamark T, Brech A, Bruun J-A, Outzen H, Øvervatn A, Bjørkøy G, Johansen T. 2007. p62/SQSTM1 Binds Directly to Atg8/LC3 to Facilitate Degradation of Ubiquitinated Protein Aggregates by Autophagy*. J Biol Chem 282:24131–24145.

Patel JR, Brewer GJ. 2008. Age-related changes to tumor necrosis factor receptors affect neuron survival in the presence of beta-amyloid. J Neurosci Res 86:2303–2313.

Peña-Martinez C, Rickman AD, Heckmann BL. Beyond autophagy: LC3-associated phagocytosis and endocytosis. Sci Adv 8:eabn1702.

Pérez M, Avila J, Hernández F. 2019. Propagation of Tau via Extracellular Vesicles. Front Neurosci 13:698.

Piette F, Belmin J, Vincent H, Schmidt N, Pariel S, Verny M, Marquis C, Mely J, Hugonot-Diener L, Kinet J-P, Dubreuil P, Moussy A, Hermine O. 2011. Masitinib as an adjunct therapy for mild-to-moderate Alzheimer's disease: a randomised, placebo-controlled phase 2 trial. Alzheimers Res Ther 3:16.

Policicchio S, Ahmad AN, Powell JF, Proitsi P. 2017. Rheumatoid arthritis and risk for Alzheimer's disease: a systematic review and meta-analysis and a Mendelian Randomization study. Sci Rep 7:12861.

Pontrello CG, McWhirt JM, Glabe CG, Brewer GJ. 2022. Age-Related Oxidative Redox and Metabolic Changes Precede Intraneuronal Amyloid-β Accumulation and Plaque Deposition in a Transgenic Alzheimer's Disease Mouse Model. J Alzheimers Dis JAD 90:1501–1521.

Potokar M, Jorgačevski J. 2025. Targeting autophagy in astrocytes: a potential for neurodegenerative disease intervention. Front Cell Neurosci [Internet] 19. Available from: https://www.frontiersin.org/journals/cellular-neuroscience/articles/10.3389/fncel.2025.1584767/full

Povala G, Bellaver B, Bastiani MAD, Ferrari-Souza JP, Aguzzoli CS, Leffa DT, Ferreira PCL, Lussier FZ, Rocha A, Zalzale H, Soares C, Bauer-Negrini G, Therriault J,

Rahmouni N, Stevenson J, Servaes S, Tissot C, Zatt B, Karikari TK, Ikonomovic MD, Villemagne VL, Gauthier S, Zimmer ER, Tudorascu DL, Benedet AL, Rosa-Neto P, Pascoal TA. 2025. Amyloid beta and tau are associated with the dual effect of neuroinflammation on neurodegeneration. Alzheimers Dement J Alzheimers Assoc 21:e70746.

Prins ND, Harrison JE, Chu H-M, Blackburn K, Alam JJ, Scheltens P, Arnold, Coskinas, Gonzales, Joseph, Khan, McConnehey, Paricio, Taylor, Rowell Z, Groom, Summers, White, Thein, Bolouri, Schwartz, Vasquez, Asher, Ball, Munthali, Kabir, Langford, Komuravelli, Lynch, MacSweeney, Pearson, Faulkner, Miller, Underwood, Prins, Dautzenberg, Norden V, Pazdera, Bar, Dvacka, Valis, Votypkova, Areovimata, Justesen, Schmidt, for the REVERSE-SD Study Investigators. 2021. A phase 2 double-blind placebo-controlled 24-week treatment clinical study of the p38 alpha kinase inhibitor neflamapimod in mild Alzheimer's disease. Alzheimers Res Ther 13:106.

Quiles JM, Najor RH, Gonzalez E, Jeung M, Liang W, Burbach SM, Zumaya EA, Diao RY, Lampert MA, Gustafsson ÅB. 2023. Deciphering Functional Roles and Interplay Between Beclin1 and Beclin2 in Autophagosome Formation and Mitophagy. Sci Signal 16:eabo4457.

Rajan KB, Weuve J, Barnes LL, McAninch EA, Wilson RS, Evans DA. 2021. Population estimate of people with clinical Alzheimer's disease and mild cognitive impairment in the United States (2020–2060). Alzheimers Dement 17:1966–1975.

Rambold AS, Lippincott-Schwartz J. 2011. Mechanisms of mitochondria and autophagy crosstalk. Cell Cycle 10:4032–4038.

Ransohoff RM, Brown MA. 2012. Innate immunity in the central nervous system. J Clin Invest 122:1164–1171.

Reddy OC, van der Werf YD. 2020. The Sleeping Brain: Harnessing the Power of the Glymphatic System through Lifestyle Choices. Brain Sci 10:868.

Reggiori F, Mauthe M. 2016. At the Center of Autophagy: Autophagosomes. Encycl Cell Biol:243–247.

Ren Q, Gu M, Fan X. 2025. Circadian clock genes and insomnia: molecular mechanisms and therapeutic implications. Ann Med 57:2576643.

Rogers SL, Farlow MR, Doody RS, Mohs R, Friedhoff LT. 1998. A 24-week, double-blind, placebo-controlled trial of donepezil in patients with Alzheimer's disease. Donepezil Study Group. Neurology 50:136–145.

Rohn TT. 2015. Caspase Cleaved Tau in Alzheimer's Disease: A Therapeutic Target Realized. Int J Neurol Neurother [Internet] 2. Available from: https://clinmedjournals.org/articles/ijnn/ijnn-2-014.php?jid=ijnn

Sagar MAK, Ouellette JN, Cheng KP, Williams JC, Watters JJ, Eliceiri KW. 2020. Microglia activation visualization via fluorescence lifetime imaging microscopy of intrinsically fluorescent metabolic cofactors. Neurophotonics 7:035003.

Santana R, McWhirt J, Brewer G. 2025. Treatment of age-related decreases in GTP levels restores endocytosis and autophagy. GeroScience 48.

Shim KH, Kang MJ, Youn YC, An SSA, Kim S. 2022. Alpha-synuclein: a pathological factor with Aβ and tau and biomarker in Alzheimer's disease. Alzheimers Res Ther 14:201.

Singh A, Adam A, Aditi, Peng B-H, Yu X, Zou J, Kulkarni VV, Kan P, Jiang W, Shi P-Y, Samir P, Cisneros I, Wang T. 2024. A murine model of post-acute neurological sequelae following SARS-CoV-2 variant infection. Front Immunol [Internet] 15. Available from: https://www.frontiersin.org/journals/immunology/articles/10.3389/fimmu.2024.1384516/full

Solé-Domènech S, Cruz DL, Capetillo-Zarate E, Maxfield FR. 2016. The Endocytic Pathway in Microglia During Health, Aging and Alzheimer's Disease. Ageing Res Rev 32:89–103.

Stolz A, Putyrski M, Kutle I, Huber J, Wang C, Major V, Sidhu SS, Youle RJ, Rogov VV, Dötsch V, Ernst A, Dikic I. 2016. Fluorescence-based ATG8 sensors monitor localization and function of LC3/GABARAP proteins. EMBO J 36:14.

Stutz A, Horvath GL, Monks BG, Latz E. 2013. ASC Speck Formation as a Readout for Inflammasome Activation. In: De Nardo CM, Latz E, editors. The Inflammasome: Methods and Protocols. Totowa, NJ: Humana Press. p 91–101. Available from: https://doi.org/10.1007/978-1-62703-523-1_8

Takeshige K, Baba M, Tsuboi S, Noda T, Ohsumi Y. 1992. Autophagy in yeast demonstrated with proteinase-deficient mutants and conditions for its induction. J Cell Biol 119:301–311.

Tschanz JT, Norton MC, Zandi PP, Lyketsos CG. 2013. The Cache County Study on Memory in Aging: Factors Affecting Risk of Alzheimer's disease and its Progression after Onset. Int Rev Psychiatry Abingdon Engl 25:673–685.

Tschanz JT, Treiber K, Norton MC, Welsh-Bohmer KA, Toone L, Zandi PP, Szekely CA, Lyketsos C, Breitner JCS. 2005. A Population Study of Alzheimer's Disease: Findings From the Cache County Study on Memory, Health, and Aging. Care Manag J 6:107–114.

Vainchtein ID, Molofsky AV. 2020. Astrocytes and microglia: in sickness and in health. Trends Neurosci 43:144–154.

Varnum MM, Kiyota T, Ingraham KL, Ikezu S, Ikezu T. 2015. The anti-inflammatory glycoprotein, CD200, restores neurogenesis and enhances amyloid phagocytosis in a mouse model of Alzheimer's disease. Neurobiol Aging 36:2995–3007.

Venegas C, Kumar S, Franklin BS, Dierkes T, Brinkschulte R, Tejera D, Vieira-Saecker A, Schwartz S, Santarelli F, Kummer MP, Griep A, Gelpi E, Beilharz M, Riedel D, Golenbock DT, Geyer M, Walter J, Latz E, Heneka MT. 2017. Microglia-derived ASC specks cross-seed amyloid-β in Alzheimer's disease. Nature 552:355–361.

Voumvourakis K, Thomaidis NS, Tsiodras S. 2026. Mapping the Brain's Glymphatic System. Biomedicines 14:409.

Wang Y-J, Sun Y-R, Pei Y-H, Ma H-W, Mu Y-K, Qin L-H, Yan J-H. 2023. The lymphatic drainage systems in the brain: a novel target for ischemic stroke? Neural Regen Res 18:485.

Wong S-W, Sil P, Martinez J. 2018. Rubicon: LC3-associated phagocytosis and beyond. FEBS J 285:1379–1388.

Wu C-K, Fuh J-L. 2025. A 2025 update on treatment strategies for the Alzheimer's disease spectrum. J Chin Med Assoc JCMA 88:495–502.

Wu M, Wang T, Loh E, Hong W, Song H. 2005. Structural basis for recruitment of RILP by small GTPase Rab7. EMBO J 24:1491–1501.

Xu Y, Propson NE, Du S, Xiong W, Zheng H. 2021. Autophagy deficiency modulates microglial lipid homeostasis and aggravates tau pathology and spreading. Proc Natl Acad Sci 118:e2023418118.

Ye X, Zhu M, Che X, Wang H, Liang X-J, Wu C, Xue X, Yang J. 2020. Lipopolysaccharide induces neuroinflammation in microglia by activating the MTOR pathway and downregulating Vps34 to inhibit autophagosome formation. J Neuroinflammation 17:18.

Yoon JH, Hwang J, Son SU, Choi J, You S-W, Park H, Cha S-Y, Maeng S. 2023. How Can Insulin Resistance Cause Alzheimer's Disease? Int J Mol Sci 24:3506.

Zampar S, Di Gregorio SE, Grimmer G, Watts JC, Ingelsson M. 2024. "Prion-like" seeding and propagation of oligomeric protein assemblies in neurodegenerative disorders. Front Neurosci [Internet] 18. Available from: https://www.frontiersin.org/journals/neuroscience/articles/10.3389/fnins.2024.1436262/full

Zhang W, Xiao D, Mao Q, Xia H. 2023. Role of neuroinflammation in neurodegeneration development. Signal Transduct Target Ther 8:267.

Zhang Y, Chen K, Sloan SA, Bennett ML, Scholze AR, O'Keeffe S, Phatnani HP, Guarnieri P, Caneda C, Ruderisch N, Deng S, Liddelow SA, Zhang C, Daneman R, Maniatis T, Barres BA, Wu JQ. 2014. An RNA-sequencing transcriptome and splicing database of glia, neurons, and vascular cells of the cerebral cortex. J Neurosci Off J Soc Neurosci 34:11929–11947.

Zhao S, Heng X, Ya-ping W, Di L, Wen-qian W, Ling-song M, Chu Z, Xu Y. 2020. CD200-CD200R1 signaling pathway regulates neuroinflammation after stroke. Brain Behav 10:e01882.

Zhou T, Li Y, Li X, Zeng F, Rao Y, He Y, Wang Y, Liu M, Li D, Xu Z, Zhou X, Du S, Niu F, Peng J, Mei X, Ji S-J, Shu Y, Lu W, Guo F, Wu T, Yuan T-F, Mao Y, Peng B. 2022. Microglial debris is cleared by astrocytes via C4b-facilitated phagocytosis and degraded via RUBICON-dependent noncanonical autophagy in mice. Nat Commun 13:6233.

## Chapter 2: CD200 prevents microglial dysfunction by modulating inflammation, LC3-mediated phagocytosis, and mitochondrial morphology in an Alzheimer's model *in vitro*


### Abstract

Alzheimer's Disease (AD) is the most prevalent form of dementia and a leading cause of death. Disease hallmarks include chronic neuroinflammation and impaired clearance of toxic protein aggregates. We use exogenous CD200 to polarize microglia towards a state that measurably dampens inflammation and enhances uptake of amyloid-beta fibrils (*f*Aβ42). Electron microscopy revealed the presence of single membrane vesicles in CD200-treated microglia associated with elevated LC3 expression. Together these data suggest CD200 enhances LC3-associated endocytosis (LANDO) which mediates cell surveillance and enables LC3-associated phagocytosis of *f*Aβ42. Finally, we assess the effects of CD200 treatment on mitochondrial health. CD200 treatment protected microglia from Aβ-induced mitochondrial damage despite increased levels of free NADH/NADPH. Together, our data suggests CD200 treatment dampens inflammation, enhances LANDO-mediated cell surveillance and LAP-mediated clearance of Aβ, and protects mitochondria from Aβ-induced damage.


### 2.1 Introduction

Alzheimer's disease (AD) is the most prevalent form of dementia and as of 2025, affects around 7.2 million Americans aged 62 or older. While most prominently caused by age, AD is also positively correlated with life events like injury and infectious diseases that contribute to a state of chronic neuroinflammation that ultimately leads to 3 to 15 years of irreversible symptomatic decline (Patel and Brewer, 2008; Graham and Sharp, 2019; Zhou et al., 2021; Levine et al., 2023; Ayerra et al., 2025). AD is defined by the Alzheimer's Association as a biological process that begins with the appearance of AD neuropathologic change (ADNPC) and is diagnosed when a patient exhibits core biomarkers that include both neuroinflammation and accumulation of hallmark debris such as amyloid-beta (Aβ) (Jack et al., 2024). Conflicting descriptions present a classic chicken-or-egg scenario between neuroinflammation and debris accumulation.

Nevertheless, their combined effects are known to progress AD in a measurable positive feedback loop.

Glial cells, such as astrocytes and microglia, are responsible for mediating inflammatory signaling in the CNS (Chen et al., 2019; Vainchtein and Molofsky, 2020; Müller and Di Benedetto, 2025). Microglial repopulation has shown a promising effect on reversing behavioral impairment in mice (Barca et al., 2021). Microglia are highly dynamic immune cells that are constantly surveying their surroundings even when at “rest” (Safaiyan et al., 2026). While crucial to synaptic pruning during development, they are also required by the adult brain for clearance of debris like apoptotic cells or other cellular byproducts (Mattson et al., 1998; Fraser et al., 2010; Brioschi et al., 2020; Cornell et al., 2021). Phagocytic exhaustion can occur however, when microglia are chronically activated and become desensitized to certain substrates – leading to the subsequent impairment of their ability to recognize and clear debris (Elmore et al., 2018; Millet et al., 2024). In AD, complement-mediated synaptic pruning through microglial phagocytosis has been identified as a major contributor to synapse loss (Schafer et al., 2012; Soteros and Sia, 2022; Wen et al., 2024). Positron emission tomography (PET) scans of patients with early AD confirmed a significant association between lower synaptic density and decreased cognitive performance (Mecca et al., 2022). Due to their involvement in both neuroinflammation and debris clearance, we suspect targeting microglia will be a useful strategy against early Alzheimer’s Disease.

Neurons rely on “Don’t eat me” signals to inhibit improper phagocytic activity by nearby microglia (Lehrman et al., 2018; Elberg et al., 2019). CD200 is a membrane protein expressed on neurons and astrocytes that acts as a ligand for its cognate receptor CD200R, present on microglia (Barclay et al., 2002; Walker et al., 2009). CD200 facilitates immunomodulatory signaling through engagement with CD200R1 over other CD200R isoforms CD200R2 and CD200R3 (Gorczynski et al., 2001; Hatherley et al., 2013). CD200R1 is an inhibitory receptor for CD200 (OX-2 in humans) and is found predominantly on myeloid cells. The CD200:CD200R signaling axis has been shown to inhibit inflammatory signaling in various tissue types, and

decreased expression of both ligand and receptor have been observed in post-mortem AD brain samples (Horie et al., 2013; Haghmorad et al., 2025). Studies conducted in Alzheimer's Disease models *in vitro* and *in vivo* models linked CD200 signaling to enhanced uptake of Aβ (Varnum et al., 2015). It can thus be speculated that the restoration of CD200 could play a role in preventing Alzheimer's pathology through modulation of inflammatory cell signaling and enhanced Aβ uptake (Walker et al., 2009).

This work establishes the recombinant, soluble extracellular domain of CD200 developed by Kim et al. as a viable immunomodulator of microglia *in vitro* (Kim et al., 2014). We report the effects of CD200 on dampening IL-6, IL-1β and MCP1 secretion in BV2 microglia. We further investigate how CD200 mediates cell surveillance and uptake of fibrillar amyloid-beta (1-42) (*f*Aβ42) in BV2 microglia and human induced-pluripotent stem cell-derived microglia (iMGL). Additionally, we show that CD200 enhances LC3-associated endocytosis (LANDO) and LC3-associated phagocytosis (LAP) using a combination of immunocytology, electron microscopy, and analysis of LC3 expression at both gene and protein levels. Finally, we report the effects of CD200 treatment on protecting mitochondrial health – particularly when under Aβ-challenge.

## 2.2 Materials and methods

### CD200 protein production

To produce recombinant CD200, we cultured transgenic Chinese hamster ovary (CHO) cells engineered to secrete the extracellular domain of the CD200 ligand in ESF protein expression media supplemented with 1% FBS and 1% PenStrep (Kim et al., 2014) (**Figure S1, Table A1**). Spent cell media was filtered using a 0.22 μm PES membrane vacuum filter and centrifuged to remove cells and cell debris. Filtered supernatant was then condensed using a Millipore LabScale Tangential Flow filtration (TFF) system to reduce the liquid volume by 90% while retaining the CD200 protein in solution. Amicon (10k) protein concentrator columns were used to further condense protein volume (4000 xg, 10 minutes at 4°C as needed). Protein

condensate was purified using a nickel column for his-tag purification (Cytivia, #28-4013-53), desalted using a Zeba column (Fisher Scientific, PI89882), then sterile filtered using a 0.22 µm spin filter (16,000 xg, 5min, 4°C) (Fisher Scientific, #UFC30GV0S) (**Table A1**). Protein concentration was measured using a Pierce µBCA protein assay kit (Fisher Scientific, #23225). On average, 1L of cell media yielded approximately 500µL of 6mg/mL CD200, or the solubilized equivalent of 3 mg of CD200 protein per protein production cycle.

**BV2 microglia cell culture**

Unless otherwise stated, BV2 microglia *(generously donated by the Tenner lab)* were seeded at $0.5x10^5$ cells per well 24-well at a final density of $2.63x10^4$ cells/cm$^2$. Cells were cultured in DMEM supplemented with 10% fbs and 1% Penstrep. High density experiments were seeded at $1.0x10^6$ per well, or $5.26x10^4$ cells/cm$^2$, for 72 hours with and without CD200 (10 µg/mL) on glass coverslips for morphological analysis (**Table A2**). Inflammation studies were performed on BV2 microglia that had been cultured for 2 hours with 10 µg/mL CD200 alone, followed by 0.1 µg/mL LPS co-stimulation for an additional 24 hours and assessed for IL6, IL1-β, and MCP1 secretion by ELISA (**Table A3**). To assess Trem2 protein expression, BV2 microglia were seeded at $0.1x10^5$ cells per well in a 96-well plate and treated with 10 µg/mL CD200 alone for 48 hours, followed by 48 hours of fibrillar Aβ42 co-stimulation. CD200 effect on Aβ42 uptake was assessed by culturing cells for 48 hours with 10µg/mL CD200 for 48 hours followed by 24 hours of co-stimulation with fluorescently labelled Aβ42-Alexa-Fluor-555 (Anaspec, #AS-60480-01). Aβ42 signal was detected using an Agilent Novocyte Flow cytometer with a PE-Texas Red detector and visualized in fixed cells labeled with Hoechst 33342 and Phalloidin-Alexa-Fluor-488 using confocal microscopy.

**THP1 cell culture and stimulation**

THP1 human monocytes were cultured in cRPMI media (10% FBS, 1% PenStrep, 0.1% β-Mercaptoethanol) and 25nM PMA overnight to activate their macrophage-like phenotypes, followed by 24 hours of PMA-free culture media to recover (**Table A2**). To assess the effect of CD200 on inflammation, cells were treated with 62.5 µg/mL human CD200 for 4 hours then co-stimulated with 1.0ng/mL LPS and 25 ng/mL hIFN-γ for 24 hours. To assess fibrillar Aβ42 uptake, cells were treated with 62.5 µg/mL CD200 for 72 hours followed by 24 hours of co-stimulation with 2 µg/mL fibrillar-Aβ42 fluorescently labeled with Alexa-Fluor-555.

**iPSC-derived human microglia cell culture and stimulation**

Hematopoietic stem cells (HPCs) were obtained from the Blurton-Jones lab and differentiated into iPSC-derived microglia (iMGL) using the StemCell microglia differentiation kit (STEMCELL 05310). iMGLs were cultured with 62.5 µg/mL human soluble CD200 for 72 hours followed by 24 additional hours of co-stimulation with 2 µg/mL fibrillar Aβ42.

**Fibrillar Amyloid-beta preparation**

Fibrillar Amyloid-beta was prepared from unlabeled Aβ42 and Aβ42-555 monomers, respectively (AnaSpec, #AS-20276, #AS-60480-01). Lyophilized Aβ42 powder was resuspended in sterile milliQ water to a concentration of 4mg/mL and kept at -80°C until one week prior to use. Resuspended Aβ42 was thawed on ice and diluted to 2mg/mL in 1% $NH_4OH$. Aβ42 monomers were incubated at 37°C for 7 days in the dark to allow aggregate formation (*f*Aβ42 and *f*Aβ42-555).

**Flow cytometry sample preparation**

To assess Trem2 expression in BV2 microglia, cells were seeded at 1000 cells per 96 well cultured with 10 µg/mL CD200 and challenged with 2 µg/mL *f*Aβ42. After 48 hours, cells were

lifted with 0.05% Trypsin (37°C, 3 min), transferred to a 96-well V-bottom plate, pelleted (500 xg, 5 min), and resuspended in TruStain FcX mouse blocking antibody for 10 minutes in the dark on ice (BioLegend, #156603). The blocking antibody was removed via pelleting and replaced with PE anti-TREM-2 antibody (BioLegend, #824805) antibody for 20 minutes on ice and in the dark. Cells were fixed, permeabilized for 30 minutes, then resuspended in 2% BSA for flow cytometry. To assess uptake in BV2 microglia and THP1 monocytes, cells were lifted with 0.05% Trypsin (37°C, 3 min) and resuspended in 1% BSA for flow cytometry.

**Microscopy sample preparation**

For morphological assessment, BV2 microglia were cultured with 10 μg/mL CD200 for 72 hours, fixed in 4% PFA and blocked with 2% BSA overnight at 4°C. Cells were stained with 1μM Phalloidin-Fluor-488 (ThermoFisher, #A12379) and 0.5μM Hoechst (Fisher Scientific, #R37605) for 15 minutes to enable visualization of F-actin and cell nuclei respectively. Coverslips were briefly washed twice with 1x PBS before mounting with Fluoromount onto a glass microscope slide. Images were obtained with an Olympus FV3000 microscope at 40x oil immersion. Uptake studies were performed using fluorescently labeled *f*Aβ42. Cells were similarly fixed, blocked, and stained for F-actin and Hoechst. To assess lysosomal activity and vesicle formation, microglia treated with CD200 for 48 hours were given fluorescently labeled fibrillar Aβ42 and stained with Lysotracker Green-DND for 20 minutes in serum free DMEM prior to live cell imaging using an Olympus confocal microscope at 40x oil (Thermofisher, #L7526). Quantification of *f*Aβ42 signal colocalized with Lysotracker Green-DND was performed using ImageJ by measuring PE-Texas-Red mean fluorescent intensity (MFI) at 555 nm to detect *f*Aβ42 signal within masks created from fluorescently labeled, punctate lysosomal structures labeled by Lysotracker Green DND-26 per cell. To obtain images of intracellular vesicles, live cells were imaged at 63x oil using an LSM-980 microscope in collaboration with the UCI Optical Biology Core (OBC). Similarly cultured cells were fixed overnight with a para-glutaraldehyde fixative at 4°C and imaged using transmission electron

microscopy (TEM) in collaboration with the Irvine Material Research Institute (IMRI) (Avantor, #15960-01).

**RNA extraction and qPCR sample preparation**

To assess mRNA expression of *IL6, IL1-β,* and *Mcp1* in BV2 microglia treated with CD200 and stimulated with LPS, cells were lysed in Trizol and molecular grade chloroform was used to initiate phase separation. The aqueous phase was collected, precipitated with equal volume of molecular grade isopropanol, and collected with DNA/RNA spin columns (300 xg, 1min, 4°C) (Zymo Research, #R1051). The column was washed with freshly prepared 70% molecular grade ethanol 3 times (300 xg, 1min), and blotted on lint-free tissue to eliminate residual ethanol prior to a final dry centrifugation at 21,300 xg for 2 minutes. RNA was eluted in RNAase-free water and converted to cDNA using a High-Capacity cDNA Reverse Transcription Kit (ThermoFisher, #4368814) and assessed using Azura GreenFast qPCR mix (Azura Genomics, #AZ-2320) and appropriate primers (**Table A3**).

**ELISA sample preparation**

Conditioned media was collected from BV2 microglia or THP1 macrophage-like cells treated with CD200 and stimulated with LPS. Samples were centrifuged (1000 xg, 10min, 4°C) and diluted in 1% BSA (Millipore Sigma 10735078001, Fisher Scientific 10010049) before protein secretion assessment using BioLegend Standard Max ELISA kits for each protein respectively (**Table A3**). BV2 microglia were assessed for IL6, IL1-β, and MCP-1 production using mouse ELISA kits while THP1 macrophage-like cells were assessed for TNFα secretion with human ELISA kits.

**Mitochondria analysis**

BV2 microglia were cultured with CD200 for 48 hours prior to *f*Aβ42 challenge. Cells were stained with 100nM of TMRM (Fisher Scientific, #I34361) in serum free media for 30 minutes prior to being imaged live at 40x oil using an Olympus confocal microscope. BV2 microglia seeded at $0.1x10^5$ cells per well in an 8-chamber well were given pKmito (Spirochrome, #SC055) for 1 hour in serum-free, phenol-red-free DMEM prior to visualization with a ELYRA Lattice SiM Microscope and 3D rendering with the IMARIS software.

**Metabolic assays**

To assess the effect of CD200 on BV2 microglia metabolism, we cultured BV2 with CD200 as previously described for 48 hours. Cells were lifted with 0.05% Trypsin, seeded into a 96-well Seahorse XF cell culture plate (Agilent, #103792-100) at $0.25x10^5$ cells per well, and incubated at 37°C for 3 hours to allow cells to adhere to the bottom of the well-plate. Cells were then exposed to *f*Aβ42 for 24 hours in cell culture media. Cells were briefly washed with XF DMEM pH 7.4 and incubated in XF DMEM pH 7.4 for one hour without $CO_2$. A Mito Stress test using 2μM Oligomycin to inhibit ATP synthase, 25nM BAM15 to enable maximum respiration, and 1μM Rotenone with 1μM Antimycin A to inhibit the electron transport chain (ETC). Oxygen consumption rate (OCR) was recorded using an Agilent Seahorse XF Analyzer and used to visualize the effects of CD200 on BV2 mitochondrial energetics. To assess whether CD200 treatment affects glycolysis, BV2 microglia were cultured with CD200 for 48 hours and co-stimulated with *f*Aβ42 for an additional 48 hours. 10mM 2DG was administered for 30 minutes followed by 1μM puromycin for an additional 40 minutes. 1 μM harringtonine was used as a positive control of protein synthesis collapse. Cells were briefly washed in 2% BSA, blocked with Mouse TruStain FX antibody for 10 minutes in the dark on ice, fixed and permeabilized, then stained with Alexa-Fluor-647-anti-puromycin antibody overnight (Millipore Sigma, #MABE343-

AF647). Cells were washed once then resuspended in 2% BSA prior to analysis via flow cytometry (Agilent Novocyte). APC fluorescence was used as an indicator of protein synthesis.

## 2.3 Results

### CD200 dampens inflammation in BV2 mouse microglia

Aβ42 has been shown to induce sensitized inflammatory signaling in mice through TLR4-mediated production of inflammatory cytokines TNFα and IL1-β (Hughes et al., 2020).The CD200:CD200R signaling axis causes an inhibitory signaling cascade that dampens Renin-Angiotensin system (Ras) proteins through Dok2 activation of RasGAP (Mihrshahi et al., 2009a; b; Hughes et al., 2020; Zhang et al., 2023; Ayerra et al., 2025). Chronic neuroinflammation is typically measured by identifying activated microglia, which are known to propagate inflammation by secreting cytokines such as IL6 and IL1-β (Burm et al., 2015; Kaneko et al., 2019; Shen et al., 2025, p 202). IL-6 is increased in both cerebrospinal fluid (CSF) and plasma of mild cognitive impairment (MCI) and AD patients compared to control individuals (Hernangómez et al., 2014; Lyra e Silva et al., 2021). Similarly, IL-1β increases in AD brains leads to microglial neurotoxicity (Parajuli et al., 2013; Remnitz et al., 2025). BV2 microglia that were treated with 10 μg/mL CD200 for two hours prior to 24 hours of LPS stimulation were assessed at a gene expression level using qRT-pcr and at the protein level using standard ELISA kits (**Figure 2.1a, b**). We observed significant downregulation of *Il6* and *Il1β* in CD200-treated microglia compared to untreated microglia stimulated with LPS, similar to trends seen in protein secretion. As expected, CD200 treatment alone had no effect on IL-1β or IL-6 expression.

Microgliosis, or microglial aggregation is used as a marker of enhanced microglial activation and is promoted through the secretion of chemokines like monocyte chemoattractant proteins (MCP1) (Hinojosa et al., 2011; Hansen et al., 2018). MCP-1 has been studied as a continuous variable associated with worsening episodic memory in France and Monaco (Sanchez-Sanchez et al., 2022). To assess the effect of CD200 on the production of MCP1, we

similarly treated BV2 cells with 10 μg/mL CD200 prior to 24 hours co-stimulation with 0.1 μg/mL LPS and observed a significant decrease in MCP-1 expression. We observed no significant change in *Mcp1* gene expression in CD200-treated microglia compared to the untreated control, independent of stimulation. Together these data suggest CD200 dampens IL6 and IL1-β at the RNA level while CD200-induced regulation of MCP1 occurs post-transcriptionally.

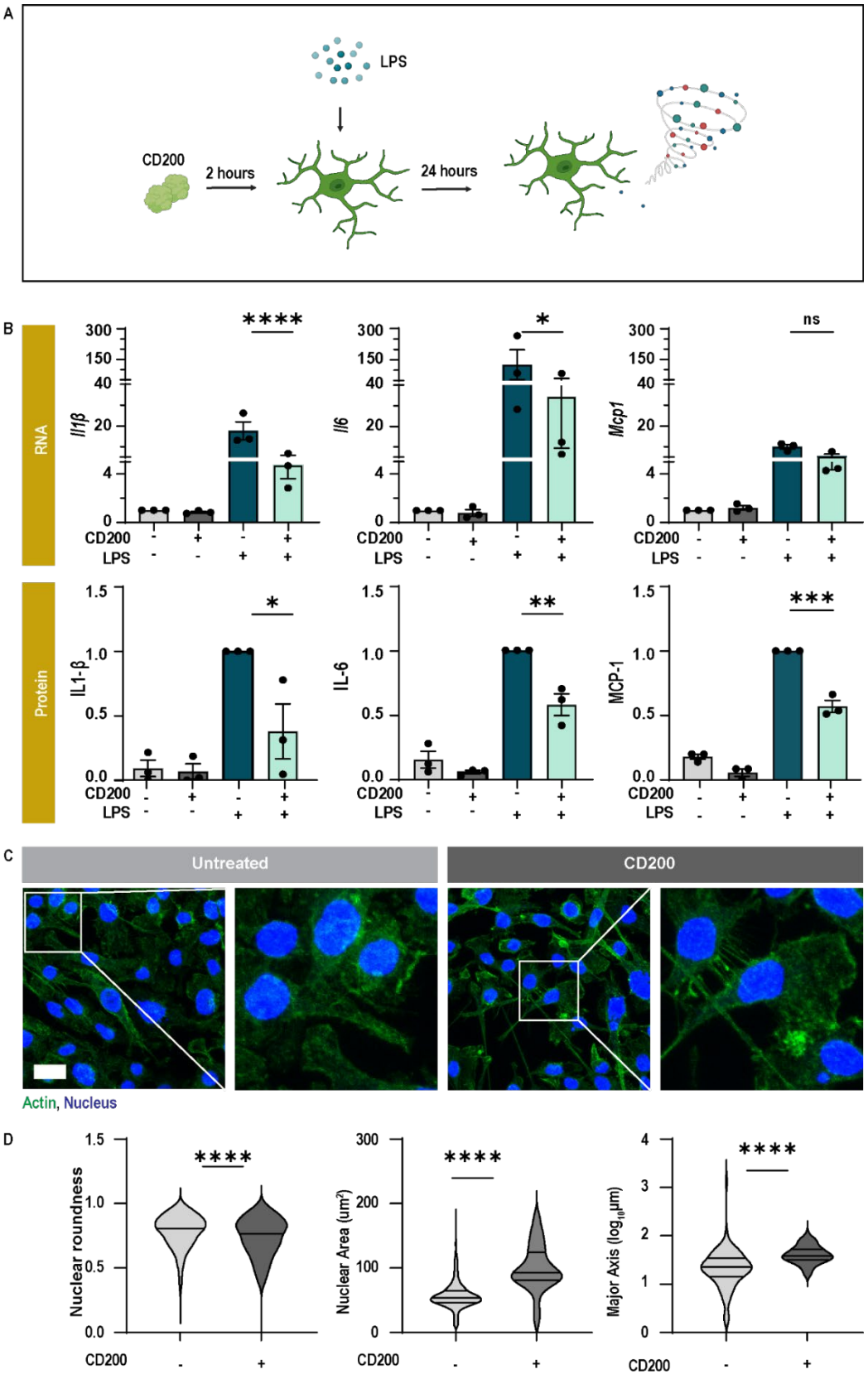
A
LPS
CD200
2 hours
24 hours
B
RNA
Il1β
Il6
Mcp1
****
*
ns
300
150
40
20
4
0
CD200
LPS
Protein
IL1-β
IL-6
MCP-1
1.5
1.0
0.5
0.0
**
***
C
Untreated
CD200
Actin, Nucleus
D
Nuclear roundness
Nuclear Area (um²)
Major Axis (log₁₀µm)
CD200

**Figure 2.1: CD200 dampens inflammation in BV2 mouse microglia**
(A) LPS was used to stimulate cytokine secretion in BV2 microglia pretreated with CD200. (B) Gene and protein expression of IL-1β, IL-6, and MCP-1 produced by CD200-treated BV2 microglia quantified with qRT-PCR and ELISA, respectively. RNA expression was normalized to untreated controls, and statistical analysis was performed on Cq values normalized to GAPDH. *<0.05, **<0.005, ***<0.001, ****<0.0001 Kruskal-Wallis test, n=3. Protein expression was normalized to LPS controls, *<0.05, **<0.01, *** <0.001 one-sample Wilcoxon signed-rank test, n=3. (C) BV2 microglia stained against f-actin and cell nuclei. Scale bar = 10 μm. (D) CD200-treated microglia exhibited significantly different morphological changes. Welch's *t*-test. ****<0.0001, n=3.

## CD200 treatment influences BV2 microglial morphology

Microglial nuclear shape is highly variable, with spherical, elliptical, irregularly shaped, and triangular nuclei (Morgan et al., 2014). While microglia are not typically known to fuse, multinucleated microglia still appear in AD due to impairments in cell division. Interestingly, these cells have been associated with enhanced phagocytosis of Aβ *in vivo* (Lee et al., 2024). While typically associated with amoeboid microglia, enlarged nuclei have also been linked to enhanced microglial surveillance during development (Zacher et al.). To observe the effect of CD200 treatment on microglial aggregation and nuclear morphology, we cultured BV2 microglia at high density with and without CD200 supplementation (**Figure 2.1c**). CD200-treated microglia contained larger nuclei with decreased circularity, accompanied by significantly farther-reaching cell projections (**Figure 2.1d**).

## CD200 treatment enhanced Aβ42 uptake in mouse and human microglia

Aβ plaques originate when amyloid precursor proteins (APP) are preferentially cleaved by β and γ-secretase instead of α-secretase (Chow et al., 2010; Hur, 2022). This process forms pathogenic "sticky" fragments that aggregate intraneuronally before being released and compacted into the dense plaques that comprise a major component of extracellular deposits found in AD brains (Kamal et al., 2001; Bharadwaj et al., 2009; Chow et al., 2010; Ishiura et al., 2013; Brewer et al., 2020; Hur, 2022). These fragments are predominantly 40-42 amino acids long, giving them the names Aβ40 and Aβ42.

Phagocytosis is a subset of endocytosis used by immune cells to engulf large particles like pathogens, synapses tagged for pruning, or cell debris. In response to injury, microglia can employ either inflammatory or non-inflammatory phagocytosis (efferocytosis) to remove debris (Neumann et al., 2009; Vainchtein and Molofsky, 2020). Chronic exposure to Aβ42 has been shown to decrease phagocytosis activity in microglia in an effect called phagocytic exhaustion (Elmore et al., 2018; Baik et al., 2019; Millet et al., 2024). Canonically, CD200 has been classified as a “don’t eat me” signal that is present on a variety of cells, including neurons. However, studies in macrophages have shown CD200 can enhance phagocytosis when introduced with a foreign particle (Chen et al., 2017).

To assess the effect of CD200 on Aβ42 uptake, we produced Aβ42 fibrils from fluorescently labelled Aβ42 (*f*Aβ42-555). BV2 microglia were pretreated with 10 µg/mL CD200 for 48 hours followed by co-stimulation with 2 µg/mL *f*Aβ42-555 for an additional 24 hours. Images taken of fixed BV2 microglia using confocal microscopy (40x oil, 5% $CO_2$, 22°C) revealed enhanced punctate *f*Aβ42 signals in CD200-treated cells (**Figure 2.2a**). Live microglia were additionally assessed using an LSD 980 confocal microscope at 63x oil immersion using phase contrast (not shown) to identify *f*Aβ42-555 within cell boundaries (**Figure 2.2b**). We quantified *f*Aβ42-555 uptake using flow cytometry to measure the median fluorescent intensity (MFI) in microglia treated with CD200 prior to *f*Aβ42-555 challenge and revealed a statistically nonsignificant increase in the number of cells positive for *f*Aβ42-555 signal (**Figure 2.2c,d**). Quantification of *f*Aβ42-555 in the positive population alone however, revealed enhanced *f*Aβ42-555 signal in microglia pretreated with CD200 (**Figure 2.2e**).

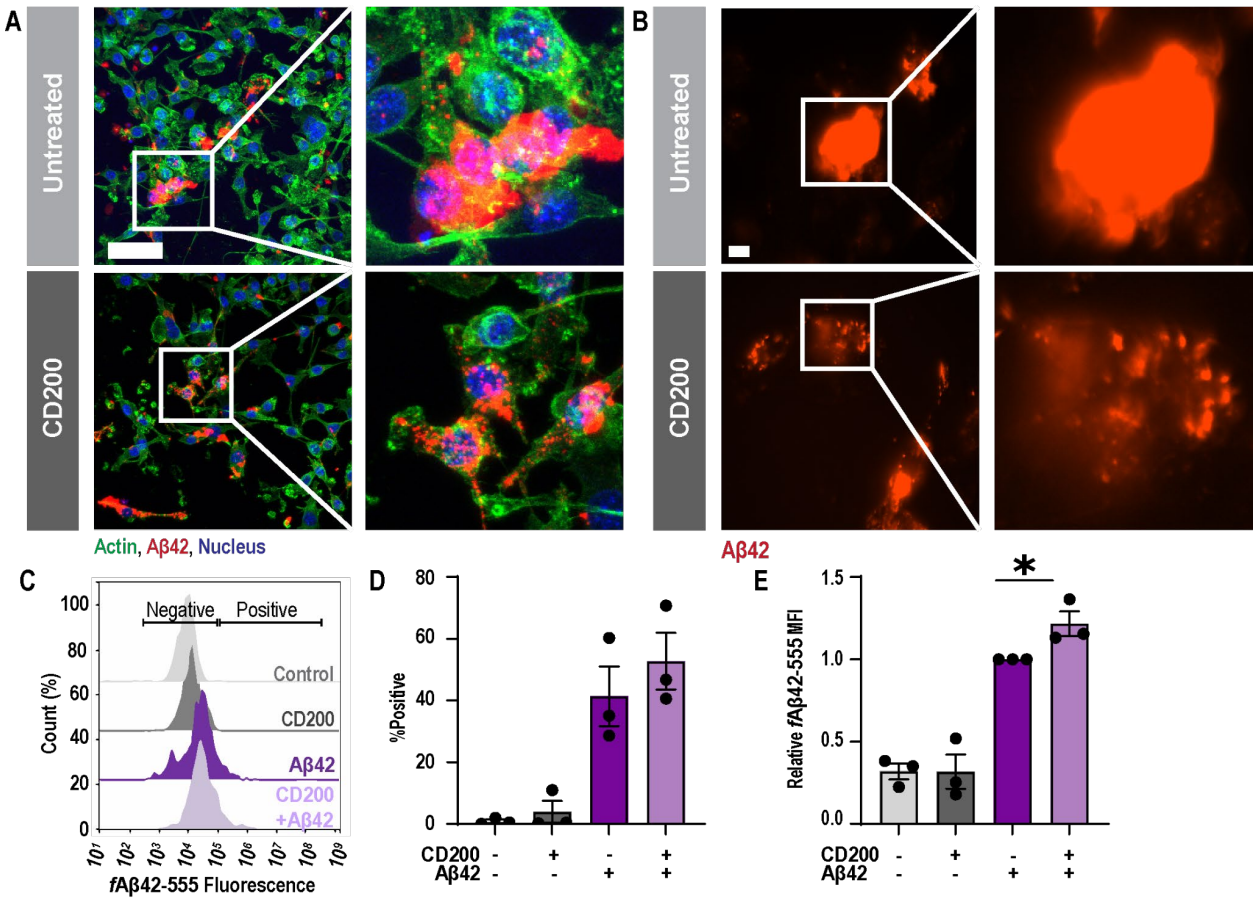


**Figure 2.2**: **CD200-treatment enhances *f*Aβ42 uptake in BV2 microglia** (A) Confocal microscopy images of CD200-treated BV2 microglia at 40x oil given fluorescently labeled Aβ42, fixed in 4% PFA and stained for f-actin and cell nuclei. Scale bar = 50μm. (B.) Confocal microscopy images of Aβ42 colocalized with live microglia at 63x oil. Scale bar = 5μm. (C) Histograms of untreated, CD200-treated, and Aβ42-challenged BV2 microglia (D) Percent cell population with positive Aβ42-Alexa-Fluor-555 signal. (E) Average Median fluorescence intensity (MFI) of *f*Aβ42 signal from cells cultured with CD200 before Aβ42 challenge. *<0.05, one sample *t*-test, n=3

### CD200 treatment enhanced colocalization of Aβ42 and lysosomes

Lysosomes are the endpoint organelle in *f*Aβ42 digestion. However, when lysosomes are unable to effectively clear amyloid-beta they act as a site of amyloid-beta accumulation that eventually leads to the rupturing of the lysosomal membrane (Marshall et al., 2020). We used phase contrast microscopy to identify increased vesicular structures in microglia treated with CD200 alone (**Figure 2.3a**). We then challenged microglia with *f*Aβ42-55 for 24 hours followed

by 20 minutes incubation with 100nM Lysotracker in serum free cell culture media to assess *f*Aβ42-55 colocalization with functional lysosomes. Quantification of lysotracker fluorescence revealed enhanced lysotracker signal in microglia treated with CD200 prior to *f*Aβ42 challenge compared to untreated controls (**Figure 2.3b**). To quantify colocalization of *f*Aβ42 with lysosomes, phase contrast images were used to produce a mask defined by the cell boundary in ImageJ. Within each cell, lysosomes labeled by lysotracker Green were used to create individual regions of interest (ROIs) within which the MFI of *f*Aβ42-555 was recorded (**Figure 2.3c, d**). Our findings suggest *f*Aβ42 is able to make it into lysosomes for final stage degradation and supports the hypothesis that CD200 not only promotes uptake, it also enhances digestion through Aβ42 and lysosome colocalization. We further quantify enhanced digestion of *f*Aβ42-555 by measuring the number of individual *f*Aβ42-555 particles within each cell and the area of each particle (**Figure 2.3e, f**). CD200-treated microglia trended towards containing a greater number of particles per cell, with the particles themselves being significantly smaller than those found in untreated microglia.

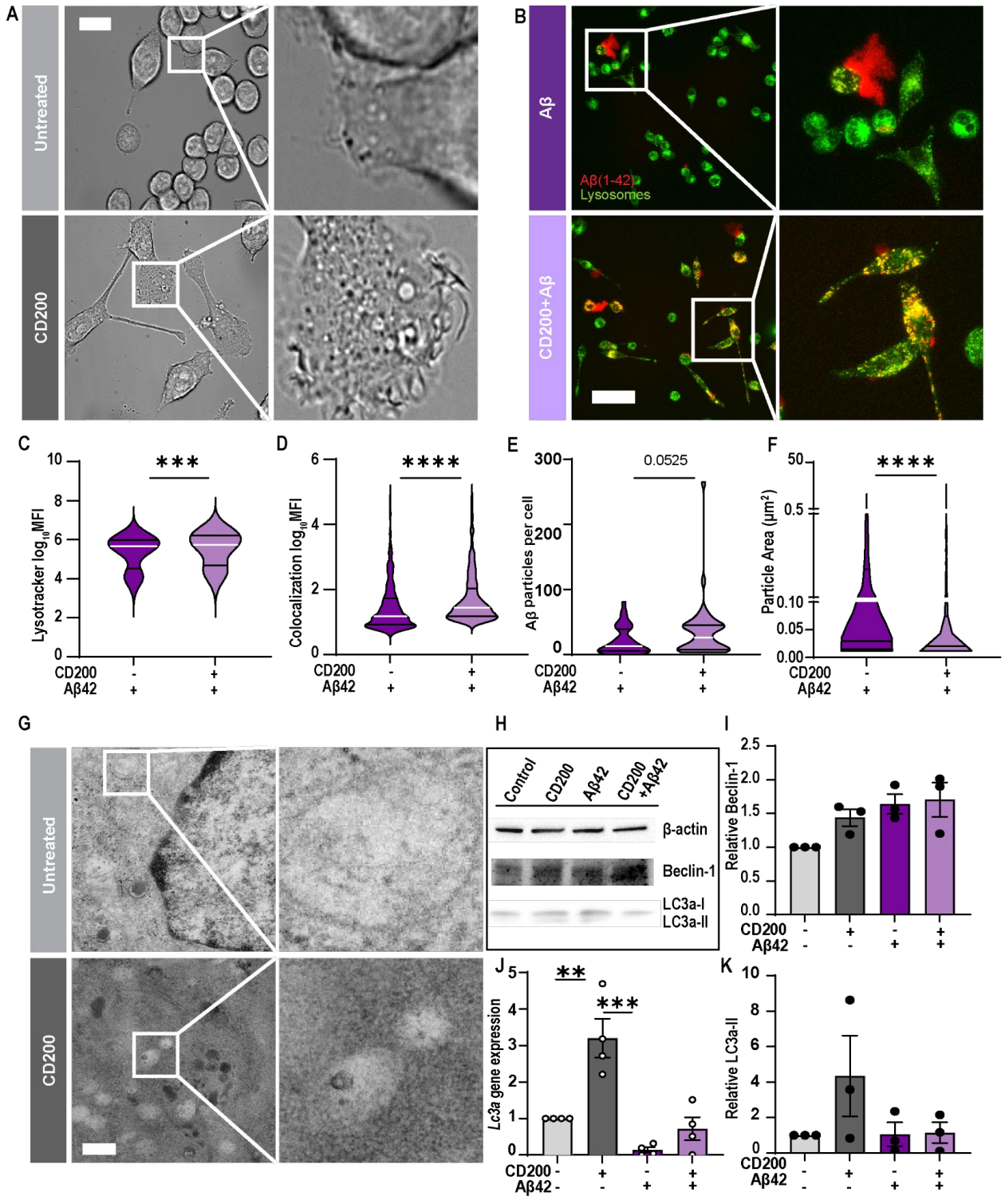
A
Untreated
CD200
B
Aβ
CD200+Aβ
Aβ(1-42)
Lysosomes
C
Lysotracker log10MFI
***
D
Colocalization log10MFI
****
E
Aβ particles per cell
0.0525
F
Particle Area (μm²)
****
CD200
Aβ42
G
Untreated
CD200
H
Control
CD200
Aβ42
CD200 +Aβ42
β-actin
Beclin-1
LC3a-I
LC3a-II
I
Relative Beclin-1
J
Lc3a gene expression
**
***
K
Relative LC3a-II

**Figure 2.3: CD200 treatment enhanced *f*Aβ42 colocalization to lysosomes**

(A) Phase Contrast images of fluorescent amyloid-beta located near or inside cells. Scale bar = 10 μm. (B) Lysotracker Green-DND was used to visualize lysosome colocalization with fluorescently labeled *f*Aβ42 in live BV2 microglia under 40x oil confocal microscopy. Scale bar = 20 μm. (C) Quantification of lysotracker intensity per cell indicates a significant difference in lysotracker intensity between treated and untreated microglia. n=120 cells, ***<0.001, Student's t-test. (D) Colocalization of *f*Aβ42 signal (red) within lysosomal compartments (green) were performed using ImageJ. n=120 cells, Student's t-test. ****<0.0001. (E) CD200-treated microglia were more likely to contain more individual fAβ42 particles per cell. Mann-Whitney test, n=120 cells, ****<0.0001. (F) fAβ42 particles colocalized with CD200-treated microglia were significantly smaller than those found in or adherent to untreated microglia. Mann-Whitney test, n=120 cells, ****<0.0001. (G) TEM images indicate single-membrane vesicle clusters surrounding lysosome-like structures in CD200-treated microglia. Scale bar = 100nm. (H) Western blots of LC3 and Beclin-1. (I) Quantifications of Beclin-1 show a non-significant increase in all treatment conditions. Kruskal-Wallis test, n=3, ns>0.05. (J) RNA expression of *mapk1lc3*, the gene encoding LC3, is significantly increased in CD200-treated microglia compared to untreated controls. RNA expression was normalized to untreated controls, and statistical analysis was performed on Cq values normalized to GAPDH. **<0.01, ***<0.001, Kruskal-Wallis test, n=3. (K) Quantifications of LC3-II show a nonsignificant increase in CD200-treated microglia. Kruskal-Wallis test, n=3, ns>0.05.

**CD200 treatment enhanced LAP-mediated Aβ clearance**

Glial cells use specialized clearance pathways like LC3-associated phagocytosis (LAP) and selective autophagy to process debris. Notably, LAP is known to facilitate fusion of single-membrane phagosomes to lysosomes using autophagy-related mechanisms (Bjørkøy et al., 2005, Pankiv et al., 2007, Kanki et al., 2009; Glick et al., 2010; Wong et al., 2018; Choi et al., 2020; Zhou et al., 2022; Pfeifer et al., 2023; Quiles et al., 2023). TEM imaging confirmed clusters of single-membrane vesicles near lysosome-like structures in BV2 microglia treated with CD200 alone for 72 hours while untreated controls contained sparsely distributed vesicles with double membranes congruent with canonical autophagy (**Figure 2.3g**). LC3 is an autophagy marker that has been detected in both canonical autophagy and LC3-associated phagocytosis (LAP) and LC3-associated endocytosis (LANDO) (Kabeya et al., 2000; Wong et al., 2018; Heckmann et al., 2020; Chen et al., 2023; Peña-Martinez et al.). To confirm whether these vesicles are correlated with LC3 expression, we probed for *Lc3* at an RNA level using qRT-PCR and observed a significant difference in *Lc3* gene expression in microglia treated with CD200 alone (**Table A3**). We then used western blot to quantify LC3-II, the bound form of LC3, and Beclin-1. While neither

were significantly different across experimental groups, Beclin-1 did trend upwards in all groups while LC3II trended upwards only in microglia treated with CD200 alone (**Figure 2.3j, k**). Due to a lack of negative autophagic control using an inhibitor like chloroquine, natural autophagic turnover is suspected to have impacted LC3-II and Beclin-1 levels.

**CD200 treatment protected mitochondria from fAβ42-induced damage**

Mitochondrial impairment is implicated in AD pathology (Bhatia et al., 2022; Pszczołowska et al., 2024). Mitophagy is a subset of autophagy used by cells to control mitochondria quality (Kanki et al., 2009; Quiles et al., 2023). Healthy mitochondria tend to form elongated networks that allow higher surface area and therefore more efficient ATP production within the mitochondrial membrane (Zahedi et al., 2018). Alternatively, swollen and punctate mitochondria may imply increased mitochondrial fragmentation. As LC3 is a known marker of autophagy, we suspected CD200-treated cells that upregulate this marker would also exhibit more robust mitochondria compared to untreated controls challenged with *f*Aβ42. We used Lattice SiM microscopy to image mitochondria labeled with pkMito Deep Red (Spirochrome, # SC055). Imaris software was then used to create 3D renderings of mitochondria to enable their classification as networked, punctate, or swollen (**Figure 2.4a**). Indeed, microglia challenged with *f*Aβ42 contained significantly less networked and swollen mitochondria compared to their CD200-treated counterparts (**Figure 2.4b**). Similarly, microglia challenged with *f*Aβ42 contained significantly less total mitochondrial volume compared to the unstimulated controls. Microglia treated with CD200 alone contained significantly less punctate mitochondria, suggesting a protective effect against mitochondrial fragmentation in general.

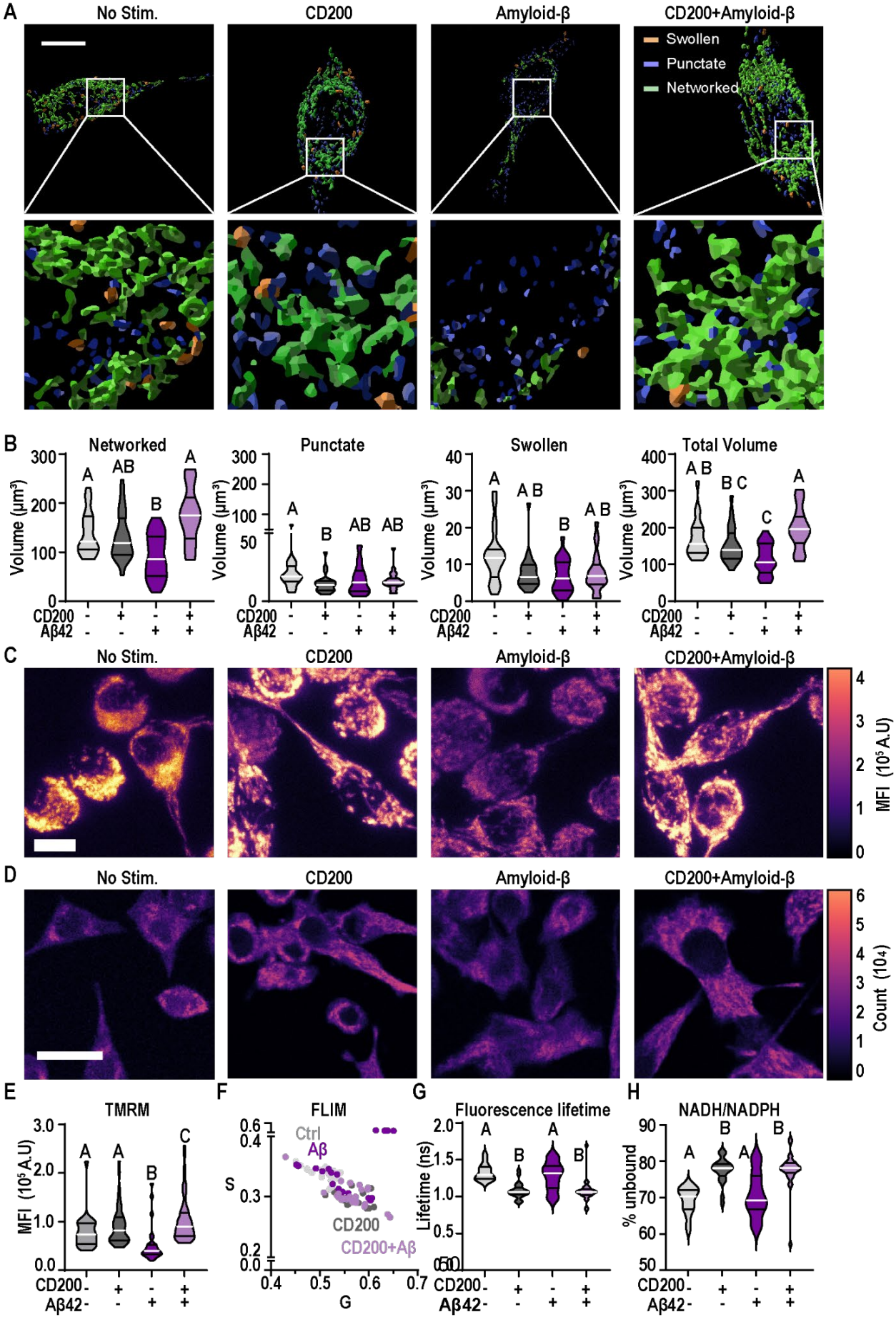
A
No Stim.
CD200
Amyloid-β
CD200+Amyloid-β
Swollen
Punctate
Networked
B
Networked
Punctate
Swollen
Total Volume
Volume (µm³)
CD200
Aβ42
C
No Stim.
CD200
Amyloid-β
CD200+Amyloid-β
MFI (10⁵ A.U)
D
No Stim.
CD200
Amyloid-β
CD200+Amyloid-β
Count (10⁴)
E
TMRM
MFI (10⁵ A.U)
F
FLIM
Ctrl
Aβ
CD200
CD200+Aβ
S
G
G
Fluorescence lifetime
Lifetime (ns)
H
NADH/NADPH
% unbound

**Figure 2.4: CD200 treatment protected mitochondria from fAβ42-induced damage**
(A) Lattice Sim images 3D rendered with IMARIS software. Scale bar = 10μm. FLIM analysis suggests CD200 treatment causes a (B) Mitochondrial volume per cell. Compact letter displays (CLD) denote statistical groupings; groups sharing the same letter are not significantly different. n=20 cells, $p<0.05$, Kruskal-Wallis test with Dunn's post-hoc test and Bonferroni correction. (C) Confocal microscopy images of BV3 microglia stained with TMRM. Scale bar = 10μm (D) Fluorescent lifetime imaging microscopy (FLIM) was used to capture bound versus free NADH/NADPH per cell (E) Quantification of TMRM-labeled mitochondria per cell was performed using the median fluorescent intensity (MFI) of TMRM signal per cell using ImageJ. $p<0.05$, n=60 cells, Kruskal-Wallis test with Dunn's post-hoc test and Bonferroni correction, CLD denote statistical groupings. (F) Phasor plot generated from G, S coordinates per cell using VistaVision software. (G) Fluorescence lifetime calculated from FLIM phasor plots per cell. n= 20 cells, $p<0.05$, Kruskal-Wallis test with Dunn's post-hoc test and Bonferroni correction, CLD denote statistical groupings. (H) Percent unbound NADH/NADPH calculated from fluorescence lifetime. n= 20 cells. CLD denotes statistical groupings. Groups sharing the same letter are not statistically significant, ns > 0.05, Kruskal-Wallis test with Dunn's post-hoc test and Bonferroni correction.

Tetramethylrhodamine methyl ester (TMRM) is a fluorescent probe that accumulates in the inner mitochondrial membrane (IMM) in proportion to mitochondrial membrane potential (MMP) (Saimi et al., 2025). TMRM has been shown to decrease in BV2 microglia challenged with Aβ (Scaduto and Grotyohann, 1999; Liu et al., 2026). To assess whether the effects in mitochondrial morphology correlated with mitochondrial activity, we labeled CD200-treated microglia with 1 μM TMRM dye for 20 minutes in serum-free cell culture media. Cells were briefly washed with 10% FBS-supplemented cell culture medium and imaged live with confocal microscopy (40x oil, 37°C, 5% $CO_2$) oil (**Figure 2.4c**). As suspected, cells challenged with *f*Aβ42 for 24 hours exhibited decreased TMRM fluorescence (**Figure 2.4e**). This effect was attenuated in microglia that had been treated with CD200 prior to *f*Aβ42 exposure. Interestingly, TMRM fluorescence was significantly greater in microglia given both CD200 and *f*Aβ42 despite no significant difference in the total mitochondrial volume. Fluorescent lifetime imaging microscopy uses NADH/NADPH autofluorescence to enable the quantification of bound to unbound NADH/NADPH. Notably, cytosolic NADPH conversion to NADP+ by NOX (NADPH oxidoreductase) to produce a short and localized superoxide burst is a crucial step in LAP (Grijmans et al., 2022). As such, we suspected CD200-treatment would enhance NADH/NADPH

availability in the cytosol – a trend that has also been observed in homeostatic microglia (Sagar et al., 2020). Microglia treated with CD200 shifted right on FLIM phasor plots compared to untreated controls (**Figure 2.4f**). Lifetime was calculated using **Equation 1** adapted from Spencer and Weber et al., 1969 (Spencer and Weber, 1969).

$$T_{\Phi} = \frac{1}{\omega} \times \frac{S}{G} \quad \textbf{(1)}$$

Events captured by FLIM trended towards shorter lifetimes (**Figure 2.4g**). When treated with CD200 alone, microglia experience the same decrease in median lifetime seen in cells given both CD200 and *f*Aβ42. We used the lifetime calculations produced by equation 1 to calculate the median percent of free NADH/NADPH using **Equation 2** adapted from Stringari et al., 2012, Bernier et al., 2020, and Sagar et al., 2020, Ai et al., 2022,)

$$Percent\ Free\ = \frac{3.4 - T_{\Phi}}{3.4 - 0.4} \times 100 \quad \textbf{(2)}$$

Microglia that were given CD200 contained higher percentages of free NADH/NADPH, independent of *f*Aβ42 challenge (**Figure 2.4h**). Microglia that had undergone *f*Aβ42 challenge alone did not experience a significant shift in lifetime when compared to the untreated control, suggesting the NADH/NADPH availability is not due to a response to pathogenic stimulation. These data suggest CD200 treatment alone increases cytosolic NADH/NADPH, enabling the cell to carry on LC3-mediated functions even when challenged with *f*Aβ42. The increase in NADH/NADPH could also indicate increased glycolysis to make more substrate available for oxidative phosphorylation.

While FLIM indicated an increase in free NADH/NADPH, TMRM staining did not show mitochondrial membrane depolarization in CD200-treated cells. Together, these data suggest the increase in NADH/NADPH is not correlated with mitochondrial damage. Microglia that had been exposed to CD200 prior to *f*Aβ42 exposure did not experience membrane potential depolarization. Indeed, quantification of the mean fluorescent intensity (MFI) as measured by ImageJ of these TMRM images revealed significant membrane hyperpolarization in CD200-treated microglia when

challenged with *f*Aβ42, possibly due to increased energetic demand in cells undergoing phagocytosis. Together these data suggest CD200 treatment protects microglia from *f*Aβ42-induced mitochondrial fragmentation and depolarization.

Mitochondrial membrane potential (MMP) is directly tied to the electron transport chain (ETC) used in mitochondrial respiration to generate ATP (Nicholls, 2004; Ali et al.). To assess the effect of CD200 treatment on mitochondrial respiration, we induced mitochondrial stress using oligomycin, BAM15, rotenone, and Antimycin A. Oxygen consumption was measured with an Agilent Seahorse XF analyzer and visualized with Wave and GraphPad Prism (**Figure 2.5a**) (Agilent Technologies; GraphPad Software).

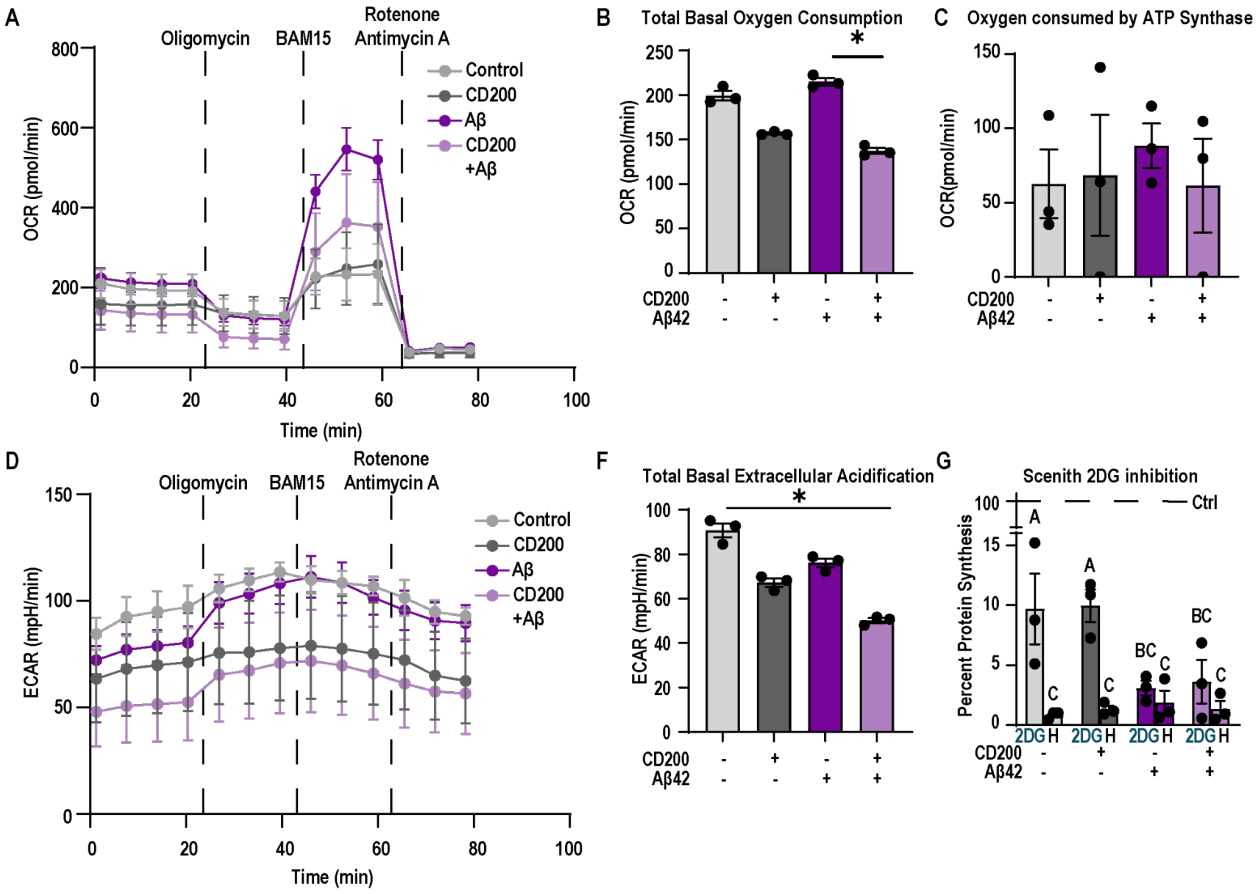

**Figure 2.5: CD200 treatment impacts oxygen consumption and glycolytic dependence**
(A) Oxygen Consumption Rate (OCR) of BV2 microglia given CD200 and *f*Aβ42 (B) Total Basal Oxygen Consumption rate quantified by measuring OCR before ATP synthase inhibition. n=3, Friedman test, ****<0.001. (C) Oxygen consumed by ATP Synthase did not differ significantly between conditions. n=3, Friedman test, ****<0.001. (D) Extracellular Acidification Rate (ECAR) of BV2 microglia calculated from seahorse assay. (F) Basal ECAR before ATP synthase inhibition. n=3, Friedman test, ****<0.001. (G) 2DG inhibition significantly dampened protein synthesis in microglia undergoing *f*Aβ42 challenge, independent of CD200 treatment. n=3, CLD denotes statistical groupings, 2-way ANOVA.

We observed significantly less oxygen consumption in cells given both CD200 and *f*Aβ42 compared to untreated microglia given *f*Aβ42 (**Figure 2.4b**). The increase seen in cells given *f*Aβ42 could be due to a compensatory mechanism as the cell attempts to generate more mitochondria or to a backlog of oxygen in a damaged ETC (Nolfi-Donegan et al., 2020). Lattice SiM findings indicate the former is unlikely however, as *f*Aβ42 challenge did not produce any significant increases in punctate or swollen mitochondria. TMRM staining supports a theory of increased proton leak in microglia challenged with *f*Aβ42, which would result in a temporary spike in oxygen consumption. This spike in oxygen consumption is not observed in microglia given both CD200 and *f*Aβ42, suggesting CD200 treatment is able to protect microglia from ETC damage. Oxygen consumed by ATP synthase is calculated by the Wave software using **Equation 3** (Agilent Technologies).

$$ATP\ Synthase\ Respiration\ =\ OCR_{Before\ Oligo.} - OCR_{After\ Oligo.} \quad \textbf{(3)}$$

As suspected, the increased oxygen consumption by microglia challenged with *f*Aβ42 was not tied to increased ATP synthase respiration, indicating the oxygen buildup is indeed suggestive of ETC dysregulation (**Figure 2.4c**). Microglia that were pretreated with CD200 consumed significantly less oxygen than microglia undergoing *f*Aβ42 challenge. Together with TMRM staining and mitochondrial morphology, these data further suggest CD200 treatment protects microglia from *f*Aβ42-induced damage by directly supporting mitochondrial health.

To assess whether the increase in free NADH/NADPH seen in CD200-treated microglia is related to a glycolytic preference, we measured extracellular acidification rates (ECAR) of the

cells as they underwent ATP synthase inhibition via Oligomycin (**Figure 2.4d**). ECAR values were taken before Oligomycin injection and used to compare basal extracellular acidification. Microglia given CD200 or *f*Aβ42 alone did not experience any significant shifts in extracellular acidification compared to the untreated control. However, CD200-treated microglia undergoing *f*Aβ42 challenge did produce significantly lower ECAR levels compared to the untreated control (**Figure 2.4f**). To assess whether CD200 treatment causes a glycolytic shift in microglia, we inhibited glycolysis using 10 mM 2DG and quantified protein synthesis using an anti-puromycin antibody stain (Argüello et al., 2020). We used flow cytometry (Agilent Novocyte) to measure median fluorescence intensity (MFI) which was used to calculate percent protein synthesis that was detected despite glycolytic inhibition, normalized to untreated controls and compared against a negative harringtonine control for each condition (**Figure 2.4g**).

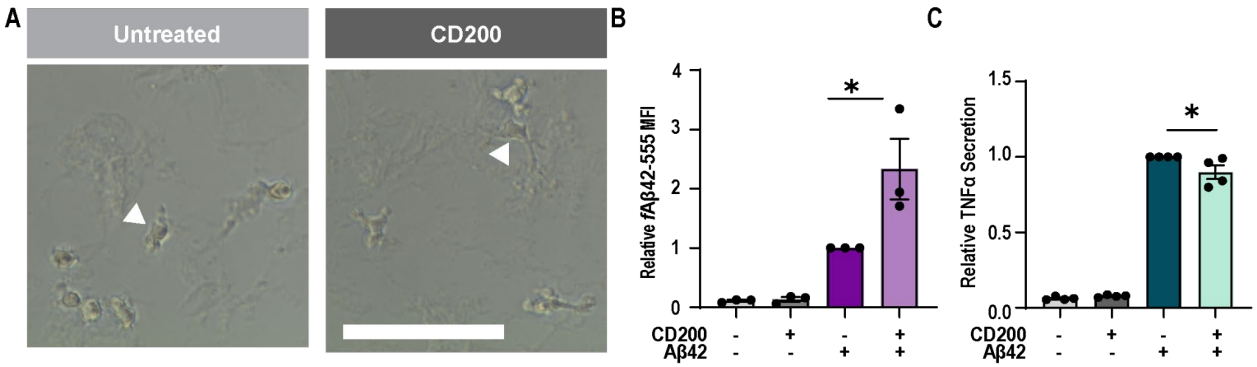


**Figure 2.5: CD200 treatment effect on inflammation and uptake in human cell lines**
(A) iPSC-derived microglia (iMGL) treated with CD200 for 72 hours. 20x, Sale bar = 100μm. (B) Flow cytometry quantification of iMGL given *f*Aβ42-555 for 24 hours after 72 hours of CD200 treatment. n=3, ****<0.05, Lognormal Welch's t-test. (C) TNFα secretion by human macrophage-like cells stimulated with *f*Aβ42, ****<0.05, Lognormal Welch's t-test, n=4.

### CD200 dampened inflammation in human cell lines

To assess the effect of CD200 on inflammation in a human system *in vitro*, we first cultured induced pluripotent stem cell (iPSC) with a StemDiff Hematopoietic kit (STEMCELL, 05310) for 14 days to produce hematopoietic stem cells (HPCs) before differentiating them to iMGL using a

protocol adapted from McQuade et al., 2021 (McQuade and Blurton-Jones, 2022). iMGLs were cultured for 36-37 days to reach maturity, then given 62.5 µg/mL CD200 for 72 hours. Bright field images captured with an EVOs light microscope at 20x indicate CD200-treated microglia may produce further reaching cellular projections, like the effects seen in BV2 microglia. After 72 hours of CD200 treatment, iMGLs were challenged with 2 µg/mL *f*Aβ42-555 and assessed via flow cytometry. The MFI of each condition was collected and normalized to untreated cells given *f*Aβ42. Like their BV2 counterparts, iMGLs also exhibited enhanced uptake of *f*Aβ42-555 after CD200 treatment. To assess the effects of CD200 treatment on human macrophage-like cells, we differentiated THP1 monocytes with 25 nM PMA for 24 hours. Cells were then given 62.5 µg/mL of CD200 for 72 hours, followed by stimulation with 2 µg/mL *f*Aβ42. After 24 hours, we collected the cell supernatants and measured TNFα secretion using a standard human TNFα ELISA kit (**Table A3**). Together, these data suggest the protective effects of CD200 against *f*Aβ42 are conserved across mouse and human immune cell lines.

### 2.4 Discussion

Neuroinflammation is quickly becoming a more relevant target in Alzheimer treatments (Harry and Kraft, 2008; Chakrabarty et al., 2010; Alzheimer's Disease Anti-inflammatory Prevention Trial Research Group, 2013; Burda and Sofroniew, 2014; Bettcher et al., 2019; Cavaliere et al., 2020; Biscetti et al., 2023; Dubois et al., 2023; Dutta et al., 2023; Forloni, 2023; Chen et al., 2024). However, general anti-inflammatories have so far been ineffective. Randomized trials performed across six US clinics concluded that naproxen or celecoxib, two types of NSAIDs, were ineffective in preventing disease onset in patients with a family history of AD. Similarly, a phase 2 trial of subcutaneous Etanercept, an anti-TNFα blocker, failed to improve the cognition of mild AD patients. A Phase 2 clinical trial concluded that Neflamapimod, an anti-inflammatory therapeutic targeting the p38α pathway, was able to decrease CSF biomarkers of synaptic dysfunction but did not improve episodic memory in patients with mild AD (Prins et al., 2021). Interestingly, CD200 has been shown to suppress p38 signaling in a mouse

staphylococcal infection model (Zhu et al., 2019). The results of these trials suggest a combination approach that can target neuroinflammation more specifically would be a more effective therapeutic for AD. Masitinib, an oral tyrosine kinase inhibitor, was used to target mast cells as a way of combating neuroinflammation in AD in a Phase 2 clinical trial (49, [NCTT00976118]). Treatment was associated with slower cognitive decline in AD, with an acceptable tolerance profile. A Phase 2 trial investigating NE3107 – an oral, anti-inflammatory and insulin-sensitizing molecule – found an association between NE3107 treatment and clinician-rated improvements in cerebral blood flow and functional connectivity within the brain, making it a successful therapeutic that can address multiple disease hallmarks (Haroon et al., 2024).

The CD200:CD200R signaling axis is the most well-characterized pathway for the CD200 ligand. However, Isec1 and Isec2 have also been named as ligands that can interact with CD200R1 in the gut and in the peripheral nervous system (124,125). While various clinical trials have investigated CD200-based therapies in the CNS, CD200 as a therapeutic target for AD remains largely understudied. 23ME-00610 is an antagonistic antibody for CD200R1 that was studied in patients with advanced solid malignancies (Kummar et al., 2025, NCT05199272). Phase 1 concluded 23ME-00610 inhibition of CD200R1 signaling successfully reversed CD200-mediated immune detection of tumors bearing neuroendocrine markers. CD200 Activation Receptor Ligand (CD200AR-L) was studied in two separate clinical trials, with one trial investigating the effects of CD200AR-L on recurrent glioblastoma and the other on recurrent high-grade glioma (HGG) in children and young adults. While the latter is still ongoing, a phase 1 trial of the former showed a positive immunological effect of CD200AR-L against recurrent glioblastoma (Neil et al., 2021, NCT04642937, NCT06305910). An active clinical trial that was last updated in 2025 is currently investigating dose effects of a CD200R1 antagonist for the treatment of metastatic solid malignancies.

Despite interest in CD200-mediated cell signaling, CD200-based therapies for dementia are largely understudied. Previous work established the benefits of tethering soluble CD200 to

biomaterials (Kim et al., 2014a; Chen et al., 2017). Particularly, CD200-coated particles encouraged uptake by bone-marrow derived macrophages (BMDMs) and dampened TNFα signaling. The role of CD200R was confirmed via siRNA knockdown in mouse BMDMs. These data served as a basis for expanding CD200-based therapeutics into microglia, the resident macrophage of the brain. Unlike other glial cells in the CNS, microglia are of myeloid origin – meaning they are the only glial cells that are also a specialized type of macrophage (Herz et al., 2017). Canonically, CD200 has been classified as a "don't eat me" signal that is present on many cell types (Barclay et al., 2002; Cui et al., 2007; Snelgrove et al., 2008; Walker et al., 2009; Cox et al., 2012; Hatherley et al., 2013; Varnum et al., 2015; Zhu et al., 2019; Kassiteridi et al., 2021; Nip et al., 2023; Pfeifer et al., 2023). However, studies in macrophages have shown CD200 can enhance phagocytosis when introduced with a foreign particle (Kim et al., 2014a; Chen et al., 2017). When combined with inflammatory conditions or mechanical force, M2-like macrophages have also been shown to secrete CD200R-positive extracellular vesicles (EVs) that contain mitochondria (mitoEVs) (van der Vlist et al., 2022; Li et al., 2026).

Injuries and diseases introduced throughout a patient's lifetime contribute to a state of chronic neuroinflammation which impacts AD prognosis (Levine et al., 2023; Ayerra et al., 2025). By using a soluble form of CD200, we are able to manipulate microglia without relying on other cells – namely neurons which naturally express this ligand. We show that CD200 treatment can be used to dampen inflammatory signaling in both mouse and human cell lines challenged with LPS and IFNγ or with Aβ42, when applied prior to stimulation. As such, microglia replacement therapies that allow LANDO/LAP polarization prior to pathogenic exposure could be a valuable AD treatment strategy. Extrapolation into an *in vivo* system would allow temporal monitoring of neuroinflammation in AD animals given CD200-treated microglia through PET scans, the standard for measuring chronic neuroinflammation (Liu et al., 2015; Chen and Zhang, 2022).

Activated microglia undergo phenotypic changes that allow them to perform functions like packing extracellular Aβ42 into plaques by aggregating around Aβ42 fibrils and using chemical

signals like MCP-1 to promote microgliosis in response to Aβ42 recognition (Hinojosa et al., 2011). Once localized to diffuse Aβ42, receptors like Trem2 enable microglia to form a multicellular wall around the Aβ42 to isolate the debris and further contribute to compacting fibrils into plaques (Wang et al., 2016a). We show a dampening effect on MCP-1 secretion by CD200-treated microglia indicative of reduced recruitment signaling. Morphological analyses of these cells show resting phenotypes accompanied by moderate decreases in Trem2 expression, suggesting that CD200 treatment could prevent microglial aggregation and subsequent Trem2-mediated Aβ42 compaction (**Figure S2**). This theory is supported by confocal images of Aβ42 colocalized with live cells which show larger, diffuse Aβ42 aggregates compared to CD200-treated microglia which contained smaller, punctate Aβ42 that were able to more successfully colocalize with lysosomes when assessed together with LysoTracker Green-DND. Together, these data suggest CD200 treatment drives microglia towards a state with readily available LC3 and free NADH/NADPH. As a result, cells are able to break down debris more effectively, without disturbing mitochondrial function. Enhanced uptake may also be attributed to smaller Aβ42 fibrils surrounding cells that cannot contribute to their aggregation due to downregulated mechanisms such as Trem2-mediated compaction (Wang et al., 2016b). As such, we recommend the overexpression and silencing of the Trem2 gene to provide insight into how uptake is affected by the cell's decreased ability to compact nearby fibrils into dense plaques.

Along with receptors like Trem2, activated microglia also use mechanisms like ASC specks to compact Aβ fibrils into plaques (Stutz et al., 2013; Venegas et al., 2017a). Apoptosis associated speck-like protein containing a caspase recruitment domain (ASC) is an adaptor protein required for the inflammasome activation of caspase-1 (Stutz et al., 2013; Ballotto et al., 2026). Following inflammasome activation in activated microglia, ASC assembles into a large protein complex called an ASC speck. ASC specks bind rapidly to Aβ and increase the formation of Aβ aggregates, thus acting as an inflammation-driven cross-seed for Aβ pathology (Venegas et al., 2017). Blood plasma from AD patients over the course of 3 years contained elevated TNFα

and decreased Aβ compared to healthy patients (Iulita et al., 2019). As Aβ aggregates cannot cross the blood brain barrier (BBB), decreased Aβ monomers in blood plasma could indicate impaired debris breakdown or clearance and deposition into insoluble plaques. While this study did not investigate ASC speck formation, we suspect the anti-inflammatory properties of CD200 treatment likely impact ASC speck formation to further discourage plaque formation outside of the cell, prior to phagocytosis and clearance. ASC specks can be detected via flow cytometry using anti-ASC antibodies (Basiorka et al., 2018; Wittmann et al., 2021; Sánchez et al., 2024). To strengthen these claims, we propose future studies that investigate ASC speck formation in models that lack Trem2 and MCP-1 expression.

Phase contrast and electron microscopy of CD200-treated microglia reveal increased vesicular structures clustered around lysosomes. Initial quantification of LC3 gene expression suggests significant upregulation of LC3 in CD200-treated microglia. Notably, we observed increased LC3 expression and vesicle formation even without exposure to *f*Aβ42. Western blotting of LC3 protein expression did not yield a similar increase in LC3I and LC3II, which could be attributed to protein turnover during LANDO/LAP as well as regular autophagic turnover as the cell maintains homeostasis (Martinez, 2020). We recommend future studies using a time course with labeled LC3 and inhibition of canonical autophagy to track LC3 levels and movement through the LANDO/LAP pathway to further confirm the effects of CD200 on mediating cell surveillance and debris engulfment.

In LANDO/LAP, an endosome is formed when a localized oxidative burst occurs (Martinez, 2020; Grijmans et al., 2022). FLIM quantification indicated an increase of unbound NADH/NADPH in cells treated with CD200, independent of *f*Aβ42 exposure. This suggests LANDO/LAP is activated solely by CD200 treatment and not as a response to pathogenic conditions. TMRM staining showed no difference in mitochondrial membrane potential (MMP) between untreated microglia and cells given CD200 alone, indicating the increased NADH/NADPH is not associated with decreased MMP. Seahorse assays indicate increased oxygen consumption in cells

challenged with *f*Aβ42 despite no significant difference in oxygen consumed by ATP synthase, indicative of ETC dysregulation. Microglia undergoing *f*Aβ42-induced mitochondrial damage have been known to initially consume more oxygen to compensate for reduced ETC efficiency (Baik et al., 2019; Liu et al., 2023). This effect is not seen in CD200-treated microglia, suggesting CD200 treatment can protect microglia from *f*Aβ42-induced ETC dysregulation. ECAR readings by Seahorse detected no observable difference in extracellular acidification by cells given CD200 alone or *f*Aβ42 alone. However, once ATP synthase was inhibited with oligomycin, cells that were challenged with *f*Aβ42 were able to more quickly increase extracellular acidification, suggesting they may be more ready to transition to a glycolytically dependent state. Indeed, when challenged with 2DG, cells given *f*Aβ42 experienced protein synthesis collapse comparable to the negative harringtonine controls. This effect was not seen in untreated controls or in cells given CD200 alone. Together, these data suggest CD200 treatment alone upregulates free NADH/NADPH to enable LC3-mediated endocytosis rather than driving the cell towards glycolysis. Combined with morphological analysis showing increased cell projections, we propose CD200 treatment drives microglia towards an energy-efficient state of cell surveillance that is quickly able to phagocytose debris without engaging inflammation.

CD200:CD200R signaling is known to dampen inflammation by downregulating Ras proteins through accelerated GTP-hydrolysis. Although this work did not investigate GTP metabolism, we believe quantification of GTP metabolics could also provide a valuable snapshot into the CD200-mediated clearance pathway (Mihrshahi et al., 2009a; Scheffzek and Shivalingaiah, 2019; Zhang et al., 2023; Santana et al., 2025; Teruya et al., 2026). We show that beyond dampening inflammatory signaling and enhancing uptake, CD200 treatment of microglia also plays a role in protecting mitochondrial integrity. Microglia have been known to secrete vesicles that contain functional mitochondria, and mitochondrial transfer has been shown to produce beneficial effects *in vivo* (van der Vlist et al., 2022; Liang et al., 2026). While extracellular vesicles containing functional mitochondria can play a neuroprotective role, EVs containing debris

act as an additional cross-seed for the disease. Thus, we recommend studying the effects of CD200 treatment on EV production and mitochondrial transfer using methods like flow cytometry and ImageStream to visualize the internal components of extracellular vesicles secreted by CD200-treated microglia.

**Supplemental**

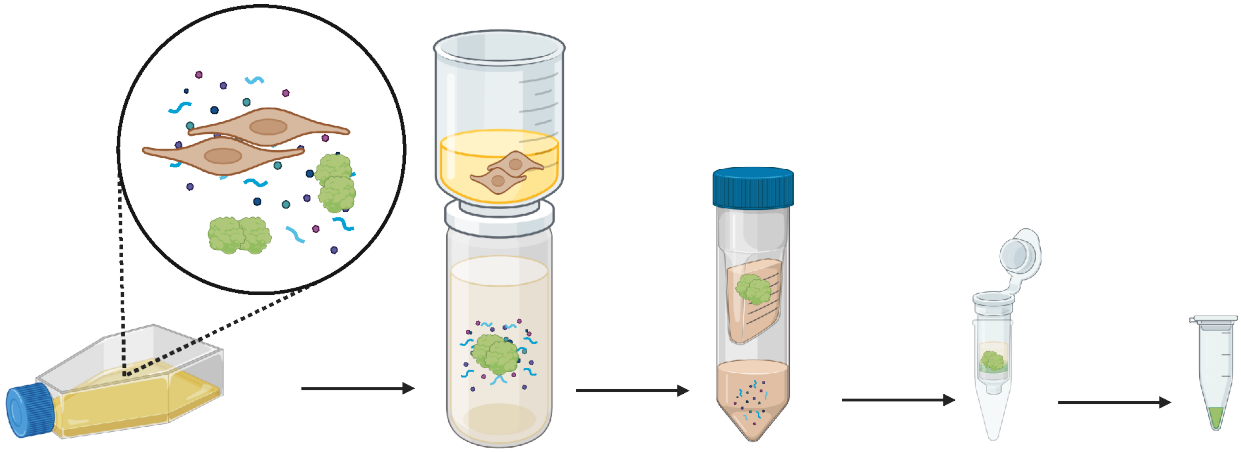

**Figure S1: CD200 production protocol**

CHO cells engineered to produce the CD200 extracellular domain by a previous study were grown in T182 flasks in serum-free expression systems protein expression media. One liter of spent cell media on average yields between 5-6mg/mL of protein. Adapted from Kim et al., 2014 (Kim et al., 2014).

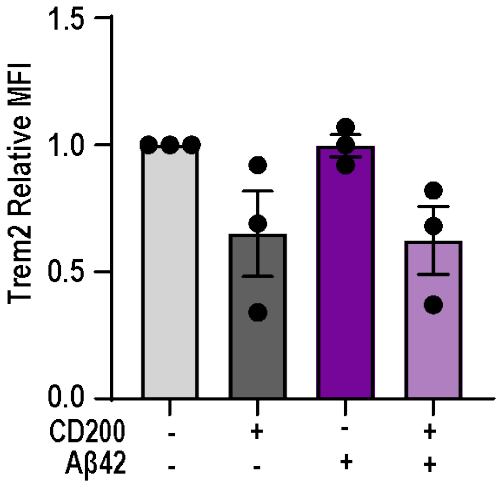


**Figure S2: Trem2 expression is measured by flow cytometry.**

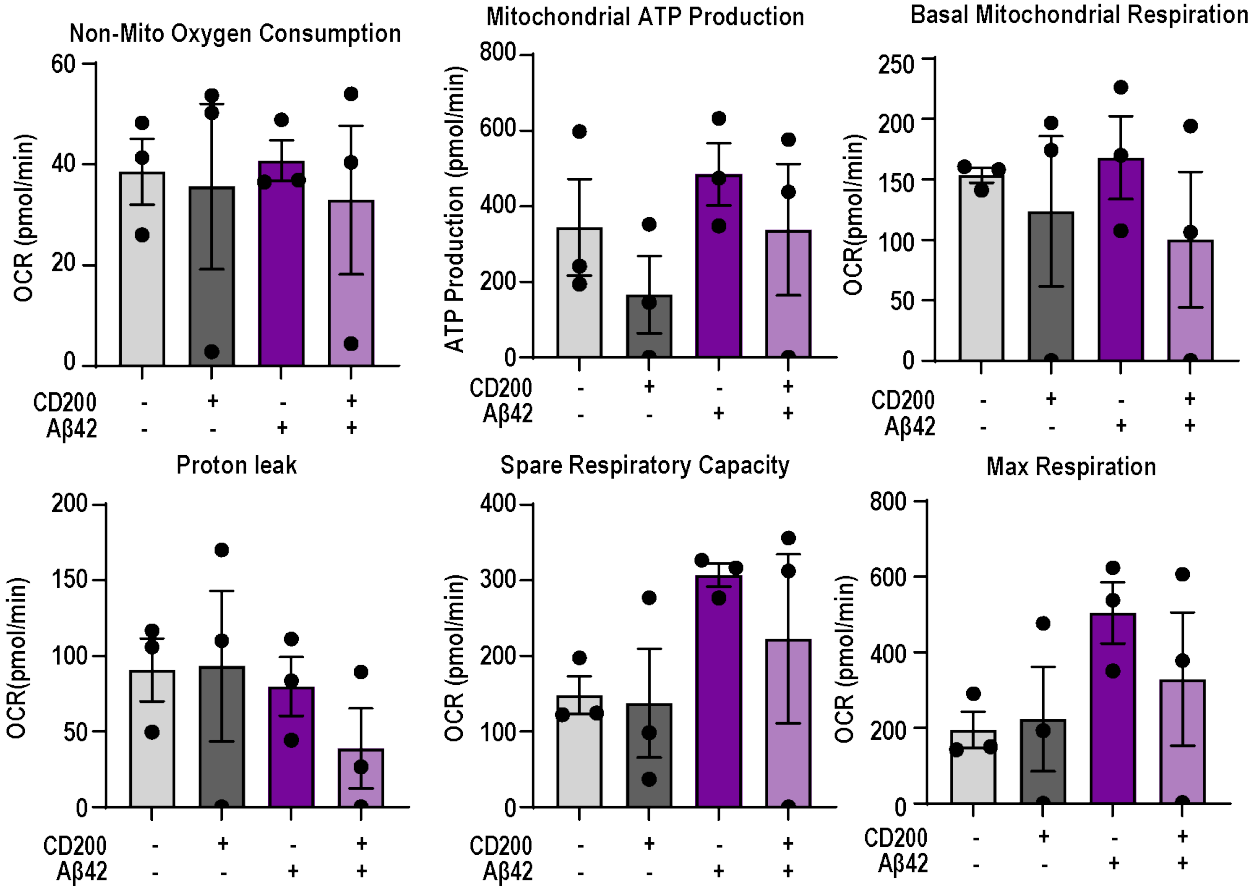


**Figure S3: Additional Mito Stress Assay Quantifications.**

**Table A1: Materials required for CD200 protein production**

| Item | Vendor | Cat. No |
|---|---|---|
| ESF protein expression media | Expression Systems | 98-001 |
| FBS | Fisher Scientific | A5256801 |
| PenStrep | Fisher Scientific | 15140163 |
| 0.22 µm PES membrane Vacuum filter | VWR | 10040-464 |
| 10k Amicon concentrator column | Fisher Scientific | UFC901024 |
| 40mg cut-off his-trap | Cytivia | 28-4013-53 |
| Zeba Desalting Column | Fisher Scientific | PI89882 |
| Sterile spin filter 0.2um | Fisher Scientific | UFC40GV0S |
| Pierce uBCA protein assay kit | Fisher Scientific | 23225 |

**Table A2: Materials required for BV2, iMGL, and THP1 cell culture**

| Item | Vendor | Cat. No |
|---|---|---|
| DMEM | Fisher Scientific | 11995081 |
| FBS | Fisher Scientific | A5256801 |
| PenStrep | Fisher Scientific | 15140163 |
| 0.22 µm PES membrane Vacuum filter | VWR | 10040-464 |
| RPMI | Fisher Scientific | 12633012 |
| β-meracaptoethanol | Millipore Sigma | M6250 |
| PMA | Sigma-Aldrich | P8139-1MG |
| Stem Cell HPC and MGL differentiation kits | STEM CELL | 05310<br>100-1215<br>100-0276 |

**Table A3: Primers, antibodies, and ELISA kits**

| **Primers** | **Forward** | **Reverse** |
|---|---|---|
| *Il6 (mouse)* | TACCACTTCACAAGTCGGAGGC | CTGCAAGTGCATCATCGTTGTTC |
| *Il1-β (mouse)* | TGGACCTTCCAGGATGAGGACA | GTTCATCTCGGAGCCTGTAGTG |
| *Mcp1 (mouse)* | TAAAAACCTGGATCGGAACCAAA | GCATTAGCTTCAGATTTACGGGT |
| *Lc3a* | CTGCCTGTCCTGGATAAGACCA | CTGGTTGACCAGCAGGAAGAAG |
| **Antibodies** | **Vendor** | **Cat. No** |
| LC3A | Cell Signaling | 12741T |
| pSQSTM1 / phospho-p62 | ThermoFisher | PA5-78267 |
| SQSTM1 / p62 | Cell Signaling | 88588T |
| Beclin-1 | Cell Signaling | 3495T |
| **ELISA kit** | **Vendor** | **Cat. No** |
| IL-6 (mouse) | Biolegend | 431301 |
| IL1-β (mouse) | Biolegend | 432601 |
| MCP1 (mouse) | Biolegend | 432701 |
| TNFα (human) | Biolegend | 430201 |

## References


Agilent Technologies. Agilent Seahorse Wave Software. Available from: https://www.agilent.com

Ai Y, Luo R, Yang D, Ma J, Yu Y, Lu H. 2022. Fluorescence lifetime imaging of NAD(P)H upon oxidative stress in Kluyveromyces marxianus. Front Bioeng Biotechnol 10:998800.

Ali A, Balakrishnan S, Xiang J, Bae H, Tsujishita M, Abulimiti A, Nemeth B, Barkoulas M, Alavian KN. Mitochondrial polarization and redox homeostasis couple glycolysis-to-OXPHOS metabolic rewiring to lifespan extension in C. elegans. MicroPublication Biol 2025:10.17912/micropub.biology.001858.

Alzheimer's Disease Anti-inflammatory Prevention Trial Research Group. 2013. Results of a follow-up study to the randomized Alzheimer's Disease Anti-inflammatory Prevention Trial (ADAPT). Alzheimers Dement J Alzheimers Assoc 9:714–723.

Anon. MEASUREMENTS OF SUBNANOSECOND FLUORESCENCE LIFETIMES WITH A CROSS-CORRELATION PHASE FLUOROMETER* - Spencer - 1969 - Annals of the New York Academy of Sciences - Wiley Online Library. Available from: https://nyaspubs.onlinelibrary.wiley.com/doi/10.1111/j.1749-6632.1969.tb56231.x

Argüello RJ, Combes AJ, Char R, Gigan J-P, Baaziz AI, Bousiquot E, Camosseto V, Samad B, Tsui J, Yan P, Boissonneau S, Figarella-Branger D, Gatti E, Tabouret E, Krummel MF, Pierre P. 2020. SCENITH: A Flow Cytometry-Based Method to Functionally Profile Energy Metabolism with Single-Cell Resolution. Cell Metab 32:1063-1075.e7.

Ayerra L, Shumilov K, Ni A, Aymerich MS, Friess SH, Celorrio M. 2025. Chronic traumatic brain injury induces neurodegeneration, neuroinflammation, and cognitive deficits in a T cell-dependent manner. Brain Res 1850:149446.

Bagyinszky E, Youn YC, An SSA, Kim S. 2014. The genetics of Alzheimer's disease. Clin Interv Aging 9:535–551.

Baik SH, Kang S, Lee W, Choi H, Chung S, Kim J-I, Mook-Jung I. 2019. A Breakdown in Metabolic Reprogramming Causes Microglia Dysfunction in Alzheimer's Disease. Cell Metab 30:493-507.e6.

Ballotto L, Baratta T, Winterberg H, Dusanter C, Sambin S, Corvol JC, Iovino L, Bubacco L, Corti O, Greggio E, Novello S. 2026. Nuclear ASC speck formation in microglia is associated with inflammasome priming and is exacerbated in LRRK2-G2019S Parkinson's disease. Neurobiol Dis 218:107237.

Barca C, Foray C, Hermann S, Herrlinger U, Remory I, Laoui D, Schäfers M, Grauer OM, Zinnhardt B, Jacobs AH. 2021. The Colony Stimulating Factor-1 Receptor (CSF-1R)-Mediated Regulation of Microglia/Macrophages as a Target for Neurological Disorders (Glioma, Stroke). Front Immunol 12:787307.

Barclay AN, Wright GJ, Brooke G, Brown MH. 2002. CD200 and membrane protein interactions in the control of myeloid cells. Trends Immunol 23:285–290.

Basiorka AA, McGraw KL, Abbas-Aghababazadeh F, McLemore AF, Vincelette ND, Ward GA, Eksioglu EA, Sallman DA, Ali NA, Padron E, Pinilla-Ibarz J, Komrokji R, Masala E, Santini V, Kosmider O, Fontenay M, Fenaux P, Sokol L, Wei S, Fridley B, List AF. 2018. Assessment of ASC specks as a putative biomarker of pyroptosis in myelodysplastic syndromes: an observational cohort study. Lancet Haematol 5:e393–e402.

Bernier L-P, York EM, Kamyabi A, Choi HB, Weilinger NL, MacVicar BA. 2020. Microglial metabolic flexibility supports immune surveillance of the brain parenchyma. Nat Commun 11:1559.

Bettcher BM, Neuhaus J, Wynn MJ, Elahi FM, Casaletto KB, Saloner R, Fitch R, Karydas A, Kramer JH. 2019. Increases in a Pro-inflammatory Chemokine, MCP-1, Are Related to Decreases in Memory Over Time. Front Aging Neurosci 11:25.

Bharadwaj PR, Dubey AK, Masters CL, Martins RN, Macreadie IG. 2009. Aβ aggregation and possible implications in Alzheimer's disease pathogenesis. J Cell Mol Med 13:412–421.

Bhatia S, Rawal R, Sharma P, Singh T, Singh M, Singh V. 2022. Mitochondrial Dysfunction in Alzheimer's Disease: Opportunities for Drug Development. Curr Neuropharmacol 20:675–692.

Biscetti L, Cresta E, Cupini LM, Calabresi P, Sarchielli P. 2023. The putative role of neuroinflammation in the complex pathophysiology of migraine: From bench to bedside. Neurobiol Dis 180:106072.

Bjørkøy G, Lamark T, Brech A, Outzen H, Perander M, Overvatn A, Stenmark H, Johansen T. 2005. p62/SQSTM1 forms protein aggregates degraded by autophagy and has a protective effect on huntingtin-induced cell death. J Cell Biol 171:603–614.

Brewer GJ, Herrera RA, Philipp S, Sosna J, Reyes-Ruiz JM, Glabe CG. 2020. Age-Related Intraneuronal Aggregation of Amyloid-β in Endosomes, Mitochondria, Autophagosomes, and Lysosomes. J Alzheimers Dis JAD 73:229–246.

Brioschi S, d'Errico P, Amann LS, Janova H, Wojcik SM, Meyer-Luehmann M, Rajendran L, Wieghofer P, Paolicelli RC, Biber K. 2020. Detection of Synaptic Proteins in Microglia by Flow Cytometry. Front Mol Neurosci 13:149.

Burda JE, Sofroniew MV. 2014. Reactive gliosis and the multicellular response to CNS damage and disease. Neuron 81:229–248.

Burm SM, Zuiderwijk-Sick EA, Jong AEJ 't, Putten C van der, Veth J, Kondova I, Bajramovic JJ. 2015. Inflammasome-Induced IL-1β Secretion in Microglia Is Characterized by Delayed Kinetics and Is Only Partially Dependent on Inflammatory Caspases. J Neurosci 35:678–687.

Cavaliere C, Tramontano L, Fiorenza D, Alfano V, Aiello M, Salvatore M. 2020. Gliosis and Neurodegenerative Diseases: The Role of PET and MR Imaging. Front Cell Neurosci [Internet] 14. Available from: https://www.frontiersin.org/articles/10.3389/fncel.2020.00075

Chakrabarty P, Jansen-West K, Beccard A, Ceballos-Diaz C, Levites Y, Verbeeck C, Zubair AC, Dickson D, Golde TE, Das P. 2010. Massive gliosis induced by interleukin-6 suppresses Aβ deposition in vivo: evidence against inflammation as a driving force for amyloid deposition. FASEB J 24:548–559.

Chen EY, Chu S-H, Gov L, Kim YK, Lodoen MB, Tenner AJ, Liu WF. 2017. CD200 modulates macrophage cytokine secretion and phagocytosis in response to poly(lactic-co-glycolic acid) microparticles and films. J Mater Chem B 5:1574–1584.

Chen H, Zeng Y, Wang D, Li Y, Xing J, Zeng Y, Liu Z, Zhou X, Fan H. 2024. Neuroinflammation of Microglial Regulation in Alzheimer's Disease: Therapeutic Approaches. Molecules 29:1478.

Chen X-X, Tao T, Liu X-Z, Wu W, Wang J-W, Yue T-T, Li X-J, Zhou Y, Gao S, Sheng B, Peng Z, Xu H-J, Ding P-F, Wu L-Y, Zhang D-D, Lu Y, Hang C-H, Li W. 2023. P38-DAPK1 axis regulated LC3-associated phagocytosis (LAP) of microglia in an in vitro subarachnoid hemorrhage model. Cell Commun Signal CCS 21:175.

Chen Z, Zhong D, Li G. 2019. The role of microglia in viral encephalitis: a review. J Neuroinflammation 16:76.

Chen Z-Y, Zhang Y. 2022. Animal models of Alzheimer's disease: Applications, evaluation, and perspectives. Zool Res 43:1026–1040.

Choi I, Zhang Y, Seegobin SP, Pruvost M, Wang Q, Purtell K, Zhang B, Yue Z. 2020. Microglia clear neuron-released α-synuclein via selective autophagy and prevent neurodegeneration. Nat Commun 11:1386.

Chow VW, Mattson MP, Wong PC, Gleichmann M. 2010. An Overview of APP Processing Enzymes and Products. Neuromolecular Med 12:1–12.

Cornell J, Salinas S, Huang H-Y, Zhou M. 2021. Microglia regulation of synaptic plasticity and learning and memory. Neural Regen Res 17:705–716.

Cox FF, Carney D, Miller A-M, Lynch MA. 2012. CD200 fusion protein decreases microglial activation in the hippocampus of aged rats. Brain Behav Immun 26:789–796.

Cui W, Cuartas E, Ke J, Zhang Q, Einarsson HB, Sedgwick JD, Li J, Vignery A. 2007. CD200 and its receptor, CD200R, modulate bone mass via the differentiation of osteoclasts. Proc Natl Acad Sci 104:14436–14441.

Dubois B, López-Arrieta J, Lipschitz S, Doskas T, Spiru L, Moroz S, Venger O, Vermersch P, Moussy A, Mansfield CD, Hermine O, Tsolaki M, AB09004 Study Group Investigators. 2023. Masitinib for mild-to-moderate Alzheimer's disease: results from a randomized, placebo-controlled, phase 3, clinical trial. Alzheimers Res Ther 15:39.

Dutta D, Jana M, Paidi RK, Majumder M, Raha S, Dasarathy S, Pahan K. 2023. Tau fibrils induce glial inflammation and neuropathology via TLR2 in Alzheimer's disease–related mouse models. J Clin Invest 133:e161987.

Elberg G, Liraz-Zaltsman S, Reichert F, Matozaki T, Tal M, Rotshenker S. 2019. Deletion of SIRPα (signal regulatory protein-α) promotes phagocytic clearance of myelin debris in Wallerian degeneration, axon regeneration, and recovery from nerve injury. J Neuroinflammation 16.

Elmore MRP, Hohsfield LA, Kramár EA, Soreq L, Lee RJ, Pham ST, Najafi AR, Spangenberg EE, Wood MA, West BL, Green KN. 2018. Replacement of microglia in the aged brain reverses cognitive, synaptic, and neuronal deficits in mice. Available from: https://onlinelibrary.wiley.com/doi/10.1111/acel.12832

Forloni G. 2023. Alpha Synuclein: Neurodegeneration and Inflammation. Int J Mol Sci 24:5914.

Fraser DA, Pisalyaput K, Tenner AJ. 2010. C1q enhances microglial clearance of apoptotic neurons and neuronal blebs, and modulates subsequent inflammatory cytokine production. J Neurochem 112:733–743.

Glick D, Barth S, Macleod KF. 2010. Autophagy: cellular and molecular mechanisms. J Pathol 221:3–12.

Gorczynski RM, Chen Z, Yu K, Hu J. 2001. CD200 immunoadhesin suppresses collagen-induced arthritis in mice. Clin Immunol Orlando Fla 101:328–334.

Graham NS, Sharp DJ. 2019. Understanding neurodegeneration after traumatic brain injury: from mechanisms to clinical trials in dementia. J Neurol Neurosurg Psychiatry 90:1221–1233.

GraphPad Software. GraphPad Prism. Available from: https://www.graphpad.com

Grijmans BJM, van der Kooij SB, Varela M, Meijer AH. 2022. LAPped in Proof: LC3-Associated Phagocytosis and the Arms Race Against Bacterial Pathogens. Front Cell Infect Microbiol [Internet] 11. Available from: https://www.frontiersin.org/journals/cellular-and-infection-microbiology/articles/10.3389/fcimb.2021.809121/full

Haghmorad D, Rahimmi A, Pazoki A, Namazi F, Rahmani MR, Amini AA. 2025. Modulation of the CD200/CD200R Axis by IFN-β Treatment in a Mouse Model of Experimental Autoimmune Encephalomyelitis. Iran J Immunol 22:131–141.

Hansen DV, Hanson JE, Sheng M. 2018. Microglia in Alzheimer's disease. J Cell Biol 217:459–472.

Haroon J, Jordan K, Mahdavi K, Rindner E, Becerra S, Surya JR, Zielinski M, Venkatraman V, Goodenowe D, Hofmeister K, Zhang J, Ahlem C, Reading C, Palumbo J, Pourat B, Kuhn T, Jordan S. 2024. A phase 2, open-label study of anti-inflammatory NE3107 in patients with dementias. Medicine (Baltimore) 103:e39027.

Harry GJ, Kraft AD. 2008. Neuroinflammation and Microglia: Considerations and approaches for neurotoxicity assessment. Expert Opin Drug Metab Toxicol 4:1265–1277.

Hatherley D, Lea S, Johnson S, Barclay A. 2013. Structures of CD200/CD200 Receptor Family and Implications for Topology, Regulation, and Evolution. Struct Lond Engl 1993 21.

Heckmann BL, Teubner BJW, Tummers B, Boada-Romero E, Harris L, Yang M, Guy CS, Zakharenko SS, Green DR. 2020. LC3-Associated Endocytosis Facilitates β-Amyloid Clearance and Mitigates Neurodegeneration in Murine Alzheimer's Disease. Cell 183:1733–1734.

Hernangómez M, Carrillo-Salinas FJ, Mecha M, Correa F, Mestre L, Loría F, Feliú A, Docagne F, Guaza C. 2014. Brain Innate Immunity in the Regulation of Neuroinflammation: Therapeutic Strategies by Modulating CD200-CD200R Interaction Involve the Cannabinoid System. Curr Pharm Des 20:4707–4722.

Herz J, Filiano AJ, Wiltbank AT, Yogev N, Kipnis J. 2017. Myeloid cells and their relationship with the central nervous system. Immunity 46:943–956.

Hinojosa AE, Garcia-Bueno B, Leza JC, Madrigal JLM. 2011. CCL2/MCP-1 modulation of microglial activation and proliferation. J Neuroinflammation 8:77.

Horie S, Robbie SJ, Liu J, Wu W-K, Ali RR, Bainbridge JW, Nicholson LB, Mochizuki M, Dick AD, Copland DA. 2013. CD200R signaling inhibits pro-angiogenic gene expression by macrophages and suppresses choroidal neovascularization. Sci Rep 3:3072.

Hughes C, Choi ML, Yi J-H, Kim S-C, Drews A, George-Hyslop PSt, Bryant C, Gandhi S, Cho K, Klenerman D. 2020. Beta amyloid aggregates induce sensitised TLR4 signalling causing long-term potentiation deficit and rat neuronal cell death. Commun Biol 3:79.

Hur J-Y. 2022. γ-Secretase in Alzheimer's disease. Exp Mol Med 54:433–446.

Ishiura S, Asai M, Hattori C, Hotoda N, Szabo B, Sasagawa N, Tanuma S. 2013. APP α-Secretase, a Novel Target for Alzheimer Drug Therapy. In: Madame Curie Bioscience Database [Internet]. Landes Bioscience. Available from: https://www.ncbi.nlm.nih.gov/books/NBK6595/

Iulita MF, Ganesh A, Pentz R, Flores Aguilar L, Gubert P, Ducatenzeiler A, Christie S, Wilcock GK, Cuello AC. 2019. Identification and Preliminary Validation of a Plasma Profile Associated with Cognitive Decline in Dementia and At-Risk Individuals: A Retrospective Cohort Analysis. J Alzheimer's Dis 67:327–341.

Jack CR, Andrews JS, Beach TG, Buracchio T, Dunn B, Graf A, Hansson O, Ho C, Jagust W, McDade E, Molinuevo JL, Okonkwo OC, Pani L, Rafii MS, Scheltens P, Siemers E, Snyder HM, Sperling R, Teunissen CE, Carrillo MC. 2024. Revised criteria for diagnosis and staging of Alzheimer's disease: Alzheimer's Association Workgroup. Available from: https://alz-journals.onlinelibrary.wiley.com/doi/10.1002/alz.13859

Kabeya Y, Mizushima N, Ueno T, Yamamoto A, Kirisako T, Noda T, Kominami E, Ohsumi Y, Yoshimori T. 2000. LC3, a mammalian homologue of yeast Apg8p, is localized in autophagosome membranes after processing. EMBO J 19:5720–5728.

Kamal A, Almenar-Queralt A, LeBlanc JF, Roberts EA, Goldstein LS. 2001. Kinesin-mediated axonal transport of a membrane compartment containing beta-secretase and presenilin-1 requires APP. Nature 414:643–648.

Kaneko N, Kurata M, Yamamoto T, Morikawa S, Masumoto J. 2019. The role of interleukin-1 in general pathology. Inflamm Regen 39:12.

Kanki T, Wang K, Cao Y, Baba M, Klionsky DJ. 2009. Atg32 Is a Mitochondrial Protein that Confers Selectivity during Mitophagy. Dev Cell 17:98–109.

Kassiteridi C, Cole JE, Griseri T, Falck-Hansen M, Goddard ME, Seneviratne AN, Green PA, Park I, Shami AG, Pattarabanjird T, Upadhye A, Taylor AM, Handa A, Channon KM, Lutgens E, McNamara CA, Williams RO, Monaco C. 2021. CD200 Limits Monopoiesis and Monocyte Recruitment in Atherosclerosis. Circ Res 129:280–295.

Kim YK, Que R, Wang S-W, Liu WF. 2014a. Modification of biomaterials with a self-protein inhibits the macrophage response. Adv Healthc Mater 3:989–994.

Kim YK, Que R, Wang S-W, Liu WF. 2014b. Modification of Biomaterials with a Self-Protein Inhibits the Macrophage Response. Adv Healthc Mater 3:989–994.

Lee J-W, Mizuno K, Watanabe H, Lee I-H, Tsumita T, Hida K, Yawaka Y, Kitagawa Y, Hasebe A, Iimura T, Kong SW. 2024. Enhanced phagocytosis associated with multinucleated microglia via Pyk2 inhibition in an acute β-amyloid infusion model. J Neuroinflammation 21:196.

Lehrman EK, Wilton DK, Litvina EY, Welsh CA, Chang ST, Frouin A, Walker AJ, Heller MD, Umemori H, Chen C, Stevens B. 2018. CD47 Protects Synapses from Excess Microglia-Mediated Pruning during Development. Neuron 100:120-134.e6.

Levine KS, Leonard HL, Blauwendraat C, Iwaki H, Johnson N, Bandres-Ciga S, Ferrucci L, Faghri F, Singleton AB, Nalls MA. 2023. Virus exposure and neurodegenerative disease risk across national biobanks. Neuron 111:1086-1093.e2.

Li Y, Yan Z, Dai Y, Cai H, Chen Y, Chen Y, Jin R, Sun W, Wang H. 2026. Mechanical Force Promotes Mitochondrial Transfer From Macrophages to BMSCs to Enhance Bone Formation. Cell Prolif 59:e70121.

Liang C, Zhou Y, Zhuang K, Wang S, Zhong L, Can D, Lei A, Li H, Zhang J, Leng L. 2026. Microglial mitochondria transfer to astrocytes via GPNMB-enriched extracellular vesicles alleviates cognitive deficits in tauopathy mice. Nat Neurosci 29:1573–1584.

Liu B, Le KX, Park M-A, Wang S, Belanger AP, Dubey S, Frost JL, Holton P, Reiser V, Jones PA, Trigg W, Carli MFD, Lemere CA. 2015. In Vivo Detection of Age- and Disease-Related Increases in Neuroinflammation by 18F-GE180 TSPO MicroPET Imaging in Wild-Type and Alzheimer's Transgenic Mice. J Neurosci 35:15716–15730.

Liu S, Yang C, Zhang N, Xiang L, Li F, Qi L, Xu X. 2026. AXL prevents amyloid-β-induced microglial ferroptosis by sustaining SLC2A3-mediated mitochondrial respiration. Pharmacol Res 228:108203.

Liu X, Jiang N, Zhou W. 2023. Various Energetic Metabolism of Microglia in Response to Different Stimulations. Molecules 28:4501.

Lyra e Silva NM, Gonçalves RA, Pascoal TA, Lima-Filho RAS, Resende E de PF, Vieira ELM, Teixeira AL, de Souza LC, Peny JA, Fortuna JTS, Furigo IC, Hashiguchi D, Miya-Coreixas VS, Clarke JR, Abisambra JF, Longo BM, Donato J, Fraser PE, Rosa-Neto P, Caramelli P, Ferreira ST, De Felice FG. 2021. Pro-inflammatory interleukin-6 signaling links cognitive impairments and peripheral metabolic alterations in Alzheimer's disease. Transl Psychiatry 11:251.

Marshall KE, Vadukul DM, Staras K, Serpell LC. 2020. Misfolded amyloid-β-42 impairs the endosomal–lysosomal pathway. Cell Mol Life Sci 77:5031–5043.

Martinez J. 2020. Detection of LC3-Associated Phagocytosis (LAP). Curr Protoc Cell Biol 87:e104.

Mattson MP, Keller JN, Begley JG. 1998. Evidence for synaptic apoptosis. Exp Neurol 153:35–48.

McQuade A, Blurton-Jones M. 2022. Human Induced Pluripotent Stem Cell-Derived Microglia (hiPSC-Microglia). In: Nagy A, Turksen K, editors. Induced Pluripotent Stem (iPS) Cells: Methods and Protocols. New York, NY: Springer US. p 473–482. Available from: https://doi.org/10.1007/7651_2021_429

Mecca AP, O'Dell RS, Sharp ES, Banks ER, Bartlett HH, Zhao W, Lipior S, Diepenbrock NG, Chen M-K, Naganawa M, Toyonaga T, Nabulsi NB, Vander Wyk BC, Arnsten AFT, Huang Y, Carson RE, van Dyck CH. 2022. Synaptic density and cognitive performance in Alzheimer's disease: A PET imaging study with [11C]UCB-J. Alzheimers Dement 18:2527–2536.

Mihrshahi R, Barclay AN, Brown MH. 2009a. Essential roles for Dok2 and RasGAP in CD200 receptor-mediated regulation of human myeloid cells. J Immunol 183:4879–4886.

Mihrshahi R, Barclay AN, Brown MH. 2009b. Essential roles for Dok2 and RasGAP in CD200 receptor-mediated regulation of human myeloid cells. J Immunol 183:4879–4886.

Millet A, Ledo JH, Tavazoie SF. 2024. An exhausted-like microglial population accumulates in aged and APOE4 genotype Alzheimer's brains. Immunity 57:153-170.e6.

Morgan JT, Barger N, Amaral DG, Schumann CM. 2014. Stereological Study of Amygdala Glial Populations in Adolescents and Adults with Autism Spectrum Disorder. PLOS ONE 9:e110356.

Müller L, Di Benedetto S. 2025. Neuroimmune crosstalk in chronic neuroinflammation: microglial interactions and immune modulation. Front Cell Neurosci [Internet] 19. Available from: https://www.frontiersin.org/journals/cellular-neuroscience/articles/10.3389/fncel.2025.1575022/full

Neumann H, Kotter MR, Franklin RJM. 2009. Debris clearance by microglia: an essential link between degeneration and regeneration. Brain 132:288–295.

Nicholls DG. 2004. Mitochondrial membrane potential and aging. Aging Cell 3:35–40.

Nip C, Wang L, Liu C. 2023. CD200/CD200R: Bidirectional Role in Cancer Progression and Immunotherapy. Biomedicines 11:3326.

Nolfi-Donegan D, Braganza A, Shiva S. 2020. Mitochondrial electron transport chain: Oxidative phosphorylation, oxidant production, and methods of measurement. Redox Biol 37:101674.

Pankiv S, Clausen TH, Lamark T, Brech A, Bruun J-A, Outzen H, Øvervatn A, Bjørkøy G, Johansen T. 2007. p62/SQSTM1 Binds Directly to Atg8/LC3 to Facilitate Degradation of Ubiquitinated Protein Aggregates by Autophagy*. J Biol Chem 282:24131–24145.

Parajuli B, Sonobe Y, Horiuchi H, Takeuchi H, Mizuno T, Suzumura A. 2013. Oligomeric amyloid β induces IL-1β processing via production of ROS: implication in Alzheimer's disease. Cell Death Dis 4:e975–e975.

Patel JR, Brewer GJ. 2008. Age-related changes to tumor necrosis factor receptors affect neuron survival in the presence of beta-amyloid. J Neurosci Res 86:2303–2313.

Peña-Martinez C, Rickman AD, Heckmann BL. Beyond autophagy: LC3-associated phagocytosis and endocytosis. Sci Adv 8:eabn1702.

Pfeifer CW, Walsh JT, Santeford A, Lin JB, Beatty WL, Terao R, Liu YA, Hase K, Ruzycki PA, Apte RS. 2023. Dysregulated CD200-CD200R signaling in early diabetes modulates microglia-mediated retinopathy. Proc Natl Acad Sci 120:e2308214120.

Piette F, Belmin J, Vincent H, Schmidt N, Pariel S, Verny M, Marquis C, Mely J, Hugonot-Diener L, Kinet J-P, Dubreuil P, Moussy A, Hermine O. 2011. Masitinib as an adjunct therapy for mild-to-moderate Alzheimer's disease: a randomised, placebo-controlled phase 2 trial. Alzheimers Res Ther 3:16.

Prins ND, Harrison JE, Chu H-M, Blackburn K, Alam JJ, Scheltens P, Arnold, Coskinas, Gonzales, Joseph, Khan, McConnehey, Paricio, Taylor, Rowell Z, Groom, Summers, White, Thein, Bolouri, Schwartz, Vasquez, Asher, Ball, Munthali, Kabir, Langford, Komuravelli, Lynch, MacSweeney, Pearson, Faulkner, Miller, Underwood, Prins, Dautzenberg, Norden V, Pazdera, Bar, Dvacka, Valis, Votypkova, Areovimata, Justesen, Schmidt, for the REVERSE-SD Study Investigators. 2021. A phase 2 double-blind placebo-controlled 24-week treatment clinical study of the p38 alpha kinase inhibitor neflamapimod in mild Alzheimer's disease. Alzheimers Res Ther 13:106.

Pszczołowska M, Walczak K, Miśków W, Mroziak M, Chojdak-Łukasiewicz J, Leszek J. 2024. Mitochondrial disorders leading to Alzheimer's disease—perspectives of diagnosis and treatment. GeroScience 46:2977–2988.

Quiles JM, Najor RH, Gonzalez E, Jeung M, Liang W, Burbach SM, Zumaya EA, Diao RY, Lampert MA, Gustafsson ÅB. 2023. Deciphering Functional Roles and Interplay

Between Beclin1 and Beclin2 in Autophagosome Formation and Mitophagy. Sci Signal 16:eabo4457.

Remnitz AD, Hadad R, Keane RW, Dietrich WD, de Rivero Vaccari JP. 2025. Comparison of Methods of Detecting IL-1β in the Blood of Alzheimer's Disease Subjects. Int J Mol Sci 26:831.

Safaiyan S, Frosch M, Bickel T, Monaco G, Dvir R, Madry C, Bosch LFP, Kierdorf K, Innocenti M, Priller J, Prinz M, Lämmermann T. 2026. The Arp2/3 complex controls the development of homeostatic microglia. EMBO Rep 27:1696–1719.

Sagar MdAK, Ouellette JN, Cheng KP, Williams JC, Watters JJ, Eliceiri KW. 2020. Microglia activation visualization via fluorescence lifetime imaging microscopy of intrinsically fluorescent metabolic cofactors. Neurophotonics 7:035003.

Saimi D, Reymond L, Aziz T, Shen X, Luo Z, Pi S, Liu Y, Fu S, Ding S, Meng A, Chen L, Jiang H, Chen Z. 2025. Imaging mitochondrial membrane potential via concentration-dependent fluorescence lifetime changes. Nat Commun 16:11088.

Sánchez KE, Jiang S, Palencia Desai S, Thompson J, Hobson S, Rosenberg GA, Bhaskar K. 2024. Protocol to measure apoptosis-associated speck-like protein containing a CARD specks in human cerebrospinal fluid via imaging flow cytometry. STAR Protoc 5:102916.

Sanchez-Sanchez JL, Giudici KV, Guyonnet S, Delrieu J, Li Y, Bateman RJ, Parini A, Vellas B, de Souto Barreto P, Vellas B, Guyonnet S, Carrié I, Brigitte L, Faisant C, Lala F, Delrieu J, Villars H, Combrouze E, Badufle C, Zueras A, Andrieu S, Cantet C, Morin C, Van Kan GA, Dupuy C, Rolland Y, Caillaud C, Ousset P-J, Lala F, Willis S, Belleville S, Gilbert B, Fontaine F, Dartigues J-F, Marcet I, Delva F, Foubert A, Cerda S, Marie-Noëlle-Cuffi, Costes C, Rouaud O, Manckoundia P, Quipourt V, Marilier S, Franon E, Bories L, Pader M-L, Basset M-F, Lapoujade B, Faure V, Tong MLY, Malick-Loiseau C, Cazaban-Campistron E, Desclaux F, Blatge C, Dantoine T, Laubarie-Mouret C, Saulnier I, Clément J-P, Picat M-A, Bernard-Bourzeix L, Willebois S, Désormais I, Cardinaud N, Bonnefoy M, Livet P, Rebaudet P, Gédéon C, Burdet C, Terracol F, Pesce A, Roth S, Chaillou S, Louchart S, Sudres K, Lebrun N, Barro-Belaygues N, Touchon J, Bennys K, Gabelle A, Romano A, Touati L, Marelli C, Pays C, Robert P, Le Duff F, Gervais C, Gonfrier S, Gasnier Y, Bordes S, Begorre D, Carpuat C, Khales K, Lefebvre J-F, El Idrissi SM, Skolil P, Salles J-P, Dufouil C, et al. 2022. Plasma MCP-1 and changes on cognitive function in community-dwelling older adults. Alzheimers Res Ther 14:5.

Santana R, McWhirt J, Brewer G. 2025. Treatment of age-related decreases in GTP levels restores endocytosis and autophagy. GeroScience 48.

Scaduto RC, Grotyohann LW. 1999. Measurement of mitochondrial membrane potential using fluorescent rhodamine derivatives. Biophys J 76:469–477.

Schafer DP, Lehrman EK, Kautzman AG, Koyama R, Mardinly AR, Yamasaki R, Ransohoff RM, Greenberg ME, Barres BA, Stevens B. 2012. Microglia Sculpt Postnatal Neural Circuits in an Activity and Complement-Dependent Manner. Neuron 74:691–705.

Scheffzek K, Shivalingaiah G. 2019. Ras-Specific GTPase-Activating Proteins—Structures, Mechanisms, and Interactions. Cold Spring Harb Perspect Med 9:a031500.

Shen S-Y, Liang L-F, Shi T-L, Shen Z-Q, Yin S-Y, Zhang J-R, Li W, Mi W-L, Wang Y-Q, Zhang Y-Q, Yu J. 2025. Microglia-Derived Interleukin-6 Triggers Astrocyte Apoptosis in the Hippocampus and Mediates Depression-Like Behavior. Adv Sci 12:e2412556.

Snelgrove RJ, Goulding J, Didierlaurent AM, Lyonga D, Vekaria S, Edwards L, Gwyer E, Sedgwick JD, Barclay AN, Hussell T. 2008. A critical function for CD200 in lung immune homeostasis and the severity of influenza infection. Nat Immunol 9:1074–1083.

Soteros BM, Sia GM. 2022. Complement and microglia dependent synapse elimination in brain development. WIREs Mech Dis 14:e1545.

Stringari C, Edwards RA, Pate KT, Waterman ML, Donovan PJ, Gratton E. 2012. Metabolic trajectory of cellular differentiation in small intestine by Phasor Fluorescence Lifetime Microscopy of NADH. Sci Rep 2:568.

Stutz A, Horvath GL, Monks BG, Latz E. 2013. ASC Speck Formation as a Readout for Inflammasome Activation. In: De Nardo CM, Latz E, editors. The Inflammasome: Methods and Protocols. Totowa, NJ: Humana Press. p 91–101. Available from: https://doi.org/10.1007/978-1-62703-523-1_8

Teruya R, Ueda K, Taketomi T, Yamamoto T, Yamashita N, Konno H, Tsuruta F. 2026. Mycophenolate mofetil reduces the branching of microglial processes. Mol Brain 19:12.

Vainchtein ID, Molofsky AV. 2020. Astrocytes and microglia: in sickness and in health. Trends Neurosci 43:144–154.

Varnum MM, Kiyota T, Ingraham KL, Ikezu S, Ikezu T. 2015. The anti-inflammatory glycoprotein, CD200, restores neurogenesis and enhances amyloid phagocytosis in a mouse model of Alzheimer's disease. Neurobiol Aging 36:2995–3007.

Venegas C, Kumar S, Franklin BS, Dierkes T, Brinkschulte R, Tejera D, Vieira-Saecker A, Schwartz S, Santarelli F, Kummer MP, Griep A, Gelpi E, Beilharz M, Riedel D, Golenbock DT, Geyer M, Walter J, Latz E, Heneka MT. 2017a. Microglia-derived ASC specks cross-seed amyloid-β in Alzheimer's disease. Nature 552:355–361.

Venegas C, Kumar S, Franklin BS, Dierkes T, Brinkschulte R, Tejera D, Vieira-Saecker A, Schwartz S, Santarelli F, Kummer MP, Griep A, Gelpi E, Beilharz M, Riedel D, Golenbock DT, Geyer M, Walter J, Latz E, Heneka MT. 2017b. Microglia-derived ASC specks cross-seed amyloid-β in Alzheimer's disease. Nature 552:355–361.

van der Vlist M, Raoof R, Willemen HLDM, Prado J, Versteeg S, Martin Gil C, Vos M, Lokhorst RE, Pasterkamp RJ, Kojima T, Karasuyama H, Khoury-Hanold W, Meyaard L, Eijkelkamp N. 2022. Macrophages transfer mitochondria to sensory neurons to resolve inflammatory pain. Neuron 110:613-626.e9.

Walker DG, Dalsing-Hernandez JE, Campbell NA, Lue L-F. 2009. Decreased expression of CD200 and CD200 receptor in Alzheimer's disease: A potential mechanism leading to chronic inflammation. Exp Neurol 215:5–19.

Wang Y, Ulland TK, Ulrich JD, Song W, Tzaferis JA, Hole JT, Yuan P, Mahan TE, Shi Y, Gilfillan S, Cella M, Grutzendler J, DeMattos RB, Cirrito JR, Holtzman DM, Colonna M. 2016a. TREM2-mediated early microglial response limits diffusion and toxicity of amyloid plaques. J Exp Med 213:667–675.

Wang Y, Ulland TK, Ulrich JD, Song W, Tzaferis JA, Hole JT, Yuan P, Mahan TE, Shi Y, Gilfillan S, Cella M, Grutzendler J, DeMattos RB, Cirrito JR, Holtzman DM, Colonna M. 2016b. TREM2-mediated early microglial response limits diffusion and toxicity of amyloid plaques. J Exp Med 213:667–675.

Wen L, Bi D, Shen Y. 2024. Complement-mediated synapse loss in Alzheimer's disease: mechanisms and involvement of risk factors. Trends Neurosci 47:135–149.

Wittmann N, Behrendt A-K, Mishra N, Bossaller L, Meyer-Bahlburg A. 2021. Instructions for Flow Cytometric Detection of ASC Specks as a Readout of Inflammasome Activation in Human Blood. Cells 10:2880.

Wong S-W, Sil P, Martinez J. 2018. Rubicon: LC3-associated phagocytosis and beyond. FEBS J 285:1379–1388.

Zacher AC, Hohaus K, Felmy F, Pätz-Warncke C. Developmental profile of microglia distribution in nuclei of the superior olivary complex. Available from: https://onlinelibrary.wiley.com/doi/10.1002/cne.25547

Zahedi A, On V, Phandthong R, Chaili A, Remark G, Bhanu B, Talbot P. 2018. Deep Analysis of Mitochondria and Cell Health Using Machine Learning. Sci Rep 8:16354.

Zhang X-J, Han X-W, Jiang Y-H, Wang Y-L, He X-L, Liu D-H, Huang J, Liu H-H, Ye T-C, Li S-J, Li Z-R, Dong X-M, Wu H-Y, Long W-J, Ni S-H, Lu L, Yang Z-Q. 2023. Impact of inflammation and anti-inflammatory modalities on diabetic cardiomyopathy healing: From fundamental research to therapy. Int Immunopharmacol 123:110747.

Zhou T, Li Y, Li X, Zeng F, Rao Y, He Y, Wang Y, Liu M, Li D, Xu Z, Zhou X, Du S, Niu F, Peng J, Mei X, Ji S-J, Shu Y, Lu W, Guo F, Wu T, Yuan T-F, Mao Y, Peng B. 2022. Microglial debris is cleared by astrocytes via C4b-facilitated phagocytosis and degraded via RUBICON-dependent noncanonical autophagy in mice. Nat Commun 13:6233.

Zhou X, Ji B, Seki C, Nagai Y, Minamimoto T, Fujinaga M, Zhang M-R, Saito T, Saido TC, Suhara T, Kimura Y, Higuchi M. 2021. PET imaging of colony-stimulating factor 1 receptor: A head-to-head comparison of a novel radioligand, 11C-GW2580, and 11C-CPPC, in mouse models of acute and chronic neuroinflammation and a rhesus monkey. J Cereb Blood Flow Metab 41:2410–2422.

Zhu B, Yu Y, Liu X, Han Q, Kang Y, Shi L. 2019. CD200 Modulates S. aureus-Induced Innate Immune Responses Through Suppressing p38 Signaling. Int J Mol Sci 20:659.

## Chapter 3: CD200 effect on mitochondria transfer in mouse microglia


### Abstract

Mitochondrial dysfunction is recognized as a key hallmark of AD and is observed in neurons as well as microglia. Microglia have been observed donating mitochondria to astrocytes using extracellular vesicles and debris to other microglia using tunneling nanotubes (TNTs). Using confocal microscopy and immunostaining, we were able to detect signs of mitochondrial transfer and observed an effect of CD200 on CD200R-positive EVs and on TNTs between adjacent microglia. However, whether these phenomena independently correlate with increased mitochondrial transfer is still unclear.


### 3.1 Introduction

Alzheimer's Disease (AD) is a neurodegenerative disorder that affects over 7 million Americans. As the most prevalent form of dementia, AD is most prominently caused by age and is positively associated with life events that lead to chronic neuroinflammation such as brain injury or infectious disease (Graham and Sharp, 2019; Levine et al., 2023). Disease hallmarks include AD neuropathologic changes (ADNPC), amyloid-beta (Aβ) plaques and phosphorylated tau (pTau) protein tangles that lead to neurodegenerative damage. Astroglia (astrocytes) and microglia are roaming immune cells that use chemical and mechanical cues to detect injurious stimuli and break down debris (Müller and Di Benedetto, 2025; Müller et al., 2025). Astrocytes regulate neurotransmitter balance, water and ion exchange, neurogenesis, immune defense, regulation of blood flow, and energy metabolism (Vainchtein and Molofsky, 2020; Theparambil et al., 2024). Microglia are crucial to synaptic pruning during development and are required in the adult brain for clearance of apoptotic cells and other cellular byproducts (Mattson et al., 1998; Fraser et al., 2010; Brioschi et al., 2020; Cornell et al., 2021). When these mechanisms are impaired either through overload or energy deprivation in AD, debris buildup and neuroinflammation work in tandem to further exacerbate the disease (Santana et al., 2025).

As a roaming immune cell, microglia need to be able to take up and pass debris and resources along to other cells in the CNS while avoiding healthy cells and immune responses. Recent studies have highlighted extracellular vesicles (EVs) as a way for macrophages to transfer mitochondria under inflammatory conditions or mechanical force (van der Vlist et al., 2022; Liang et al., 2026; Li et al., 2026). Notably, EVs transferred from peripheral macrophages to neurons contained CD200R on their surface. Microglia have been shown to use both EVs and tunneling nanotubes (TNTs) to mediate clearance of AD-related debris like Tau and alpha-synuclein (α-syn) proteins (Chakrabarty et al., 2010; Scheiblich et al., 2024; Liang et al., 2026). Additionally, mitochondrial transport is impaired in AD (Bhatia et al., 2022).

Previous work revealed increased vesicle formation and rescued mitochondria network formation in CD200-treated microglia. As microglia also express CD200R, we sought to investigate whether similar mitochondrial transfer mechanisms would be employed in CD200-treated cells challenged by Aβ. This work focuses on isolating and characterizing extracellular vesicles in the 200nm-1.0μm range as well as on analyzing preliminary imaging results that suggests CD200 promotes TNT formation and mitochondrial movement between cells.

### 3.2 Materials and Methods

#### Fibrillar Amyloid-beta preparation

Fibrillar Amyloid-beta was prepared from unlabeled Aβ42 and Aβ42-555 monomers (AnaSpec, #AS-60480-01). Lyophilized Aβ42 powder was resuspended in sterile milliQ water to a concentration of 4mg/mL and kept at -80°C until one week prior to use. Resuspended Aβ42 was thawed on ice and diluted to 2mg/mL in 1% $NH_4OH$. Aβ42 monomers were incubated at 37°C for 7 days in the dark to allow aggregate formation, *f*Aβ42 and *f*Aβ42-555.

**General BV2 cell culture**

Unless otherwise stated, BV2 microglia *(generously donated by the Tenner lab)* were seeded at $0.5x10^5$ cells per well 24-well at a final density of $2.63x10^4$ cells/$cm^2$. Cells were cultured in DMEM supplemented with 10% fbs and 1% Penstrep for 24 hours after seeding to recover, followed by 48 hours of CD200 treatment using 10 µg/mL soluble CD200 generated in an engineered cell line previously described by Kim et al., 2014 (Kim et al., 2014). Unless otherwise stated, cells were then co-stimulated with 10 µg/mL soluble CD200 and 2 µg/mL *f*Aβ42 for an additional 24 hours.

**BV2 cell culture for EV analysis**

After 48 hours of 10µg/mL CD200 treatment, cells were stained with 1 µM MitoTracker Red CMXRos (ThermoFisher Scientific, #M7512) for 30 minutes in serum free media. The dye was removed and cells were washed twice with cell culture media supplemented with 10% FBS, then given 10 µg/mL CD200 and 2 µg/mL *f*Aβ42 for an additional 24 hours. Cell supernatant was collected and centrifuged to isolate extracellular vesicles.

**BV2 cell culture for mitochondrial transfer analysis**

BV2 microglia were lifted with 0.05% Trypsin and adjusted to $1.0x10^6$ cells/mL. Approximately $1.0x10^6$ cells were stained with CellTracker Green (100 nM) or Mitotracker Red (100 nM) for 30 minutes in serum-free DMEM. Cells were then quenched with an equal volume of cell culture media (supplemented with 10% FBS), pelleted and washed with cell culture media to remove excess dye, and seeded at a 1:1 ratio of red to green cells in an 8-chamber glass slide at a final concentration of $1.0x10^3$ cells per chamber. Cells were cultured with 10 µg/mL CD200 for 48 hours prior to co-stimulation with *f*Aβ42 for an additional 24 hours. Cells were imaged live using a 63x oil LSM-980 microscope at 63x oil, 37°C, 5.0% $CO_2$ to visualize co-localization of

CellTracker Green and Mitotracker Red respectively. Bright field images of live microglia were obtained using an LSM-980 microscope (63x oil, 37°C, 5.0%$CO_2$).

**BV2 cell culture for cell projection analysis**

BV2 microglia were seeded at 1.0x$10^3$ cells per well in an 8-chamber glass coverslide (Cellvis, #C8SB-1.5H). Cells were treated with CD200 and *f*Aβ42 as previously described, then imaged live using an LSM-980 microscope (63x oil, 37°C, 5.0% $CO_2$).

**EV isolation**

BV2 microglia were cultured with CD200 and challenged with *f*Aβ42 as previously described. After 24 hours of CD200 and *f*Aβ42 co-stimulation, we collected supernatant and used differential centrifugation to separate cell debris from extracellular vesicles (1000 xg, 4°C, 10min; 6000 xg, 4°C, 10min). The remaining supernatant was stained with 1:1000 CD200R-FITC antibody overnight at 4°C in the dark (16-20h). Stained supernatant was pelleted (1.5h, 4°C, 21,300 xg) and resuspended in 1% BSA for flow cytometry analysis.

**3.3 Results**

**CD200 treatment enhances cell projections and EV-like structures**

CD200 treatment has been well-established as an anti-inflammatory molecule implicated in AD (Walker et al., 2009; Varnum et al., 2015). Resting microglia have functional similarities with M2-polarized microglia and express a receptor profile skewed towards M2 polarization (Cherry et al., 2014). Additionally, microglia have been known to employ EVs and TNTs to both clear debris and transfer mitochondria, making the effect of CD200 on these two functions highly valuable – primarily as EVs are capable of crossing the blood brain barrier (Aires et al., 2020; Scheiblich et al., 2024; Lerussi et al., 2025; Liang et al., 2026). To assess the effect of CD200 on cell projection and EV generation, we captured images of live microglia using an LSM-980 microscope and

revealed enhanced ramified structures resembling tunneling nanotubes (TNTs) and vesicular budding events in CD200-treated cells (**Figure 3.1**).

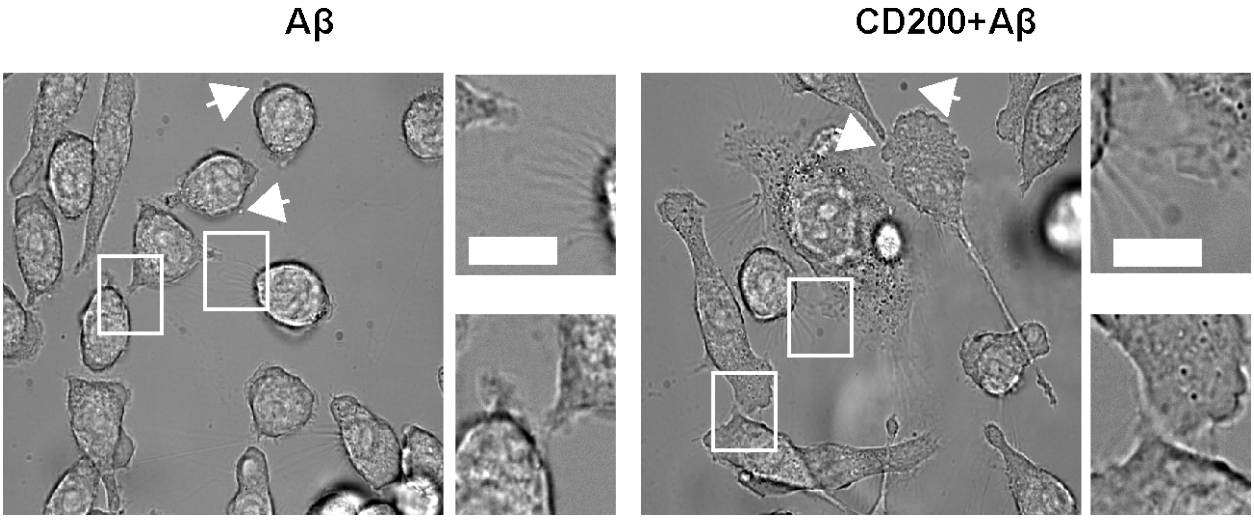


**Figure 3.1: CD200 treatment affected cell projections and vesicular structures**
BV2 microglia treated with CD200 prior to *f*Aβ42 challenge feature robust cell projections and vesicular structures. Scale bar = 10μm.

**CD200 treatment enhances mitochondrial transfer**

Macrophages are known to export functional mitochondria to surrounding cells as a means of support (van der Vlist et al., 2022; Li et al., 2026). More importantly, microglia have been shown to also transfer mitochondria to fellow immune cells (Liang et al., 2026). To assess whether the enhanced TNT and EV features observed under phase contrast microscopy could be related to mitochondria transfer, we stained BV2 microglia with CellTracker Green or Mitotracker Red CMXRos and cultured these two fluorescently labeled populations together at a 1:1 ratio for 48 hours with CD200 (**Figure 3.2a**).

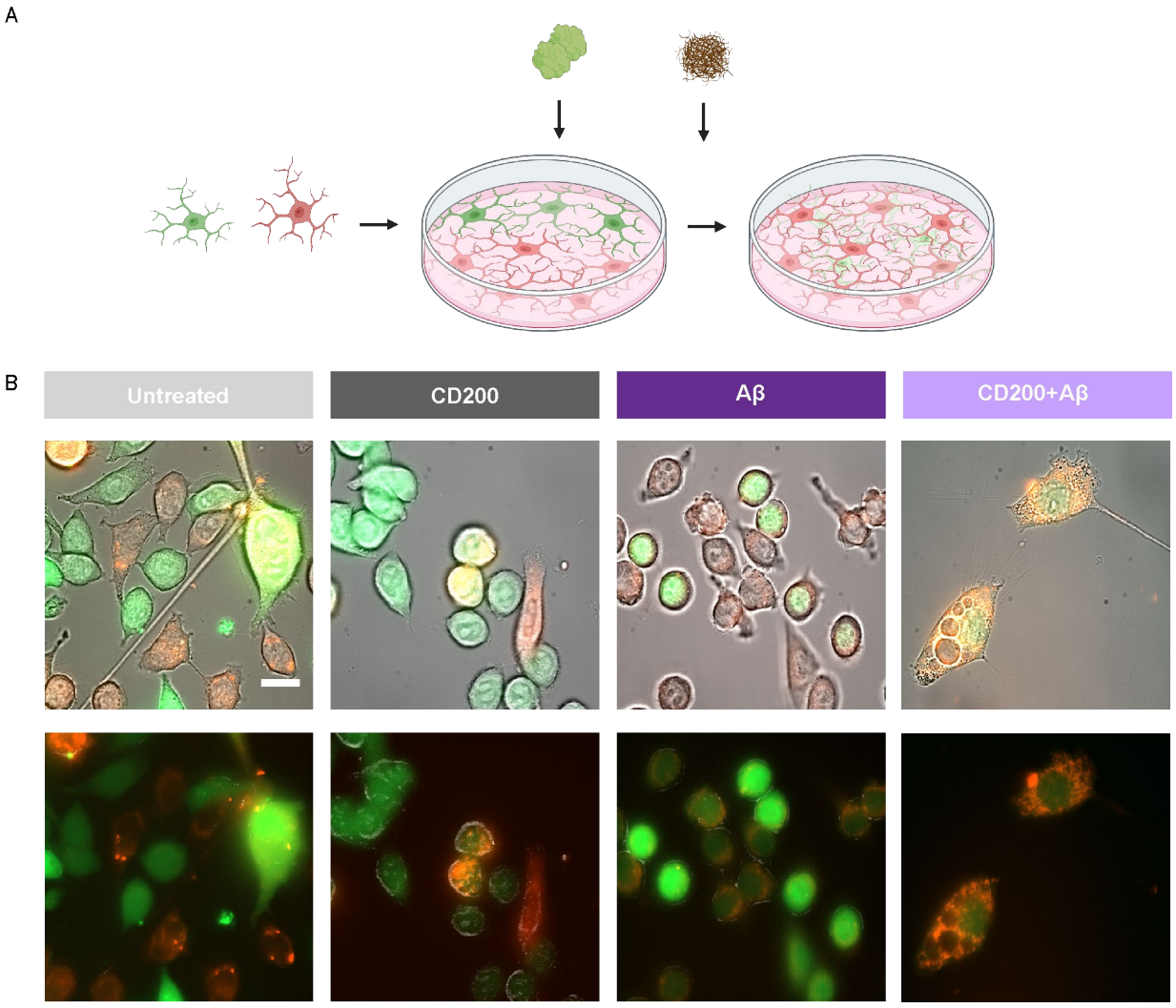


**Figure 3.2: Mitochondrial transfer in BV2 Microglia**

(A) Microglia labeled with CellTracker Green or MitoTracker Red were treated with CD200 and challenged with *f*Aβ42. Scale bar = 20μm. (B) Live cells were imaged at 63x oil using an LSM-980 microscope.

Following 24 hours of *f*Aβ42 challenge, cells were imaged live using an LSM-980 microscope (63x oil, 37°C, 5.0% $CO_2$). Untreated microglia largely maintained a heterogeneous fluorescence profile despite the presence of what seems to be TNT and EV-like structures (**Figure 3.2b**). Microglia given CD200 alone experienced colocalization of red and green signals indicative of mitochondria colocalization into cells initially labeled with CellTracker Green alone. Interestingly, mitochondria in cells challenged with amyloid-beta alone seem to localize on the periphery of the

cell as opposed to diffuse colocalization seen in cells treated with CD200 alone. This effect could be due to increased energetic demand at the cell surface where phagosomes are more likely to form (Ramond et al., 2019). Microglia treated with CD200 prior to *f*Aβ42 challenge featured characteristic vesicle-like structures surrounded by mitochondria, possibly indicating increased mitochondrial volume around CD200-induced phagosomes.

**CD200 treatment enhances CD200R+ mitoEV production**

To investigate whether CD200 treatment affects cell communication through EV secretion, we collected condition media from cells treated with CD200 prior to amyloid-beta challenge. Mitotracker was added after 48 hours of CD200 treatment for 30 minutes in serum-free DMEM while cells were still adherent. The dye was washed out with cell culture media twice and CD200 and *f*Aβ42 were added for an additional 24 hours. Condition media was collected and cell debris were removed via differential centrifugation. EVs were pelleted and labeled with FITC-CD200R overnight at 4°C in the dark. Once the dye was washed out via centrifugation, cells were resuspended in 1% BSA for flow cytometry. Despite visualization of EV-like structures containing MitoTracker signals in microglia treated with CD200 alone, EVs with CD200R and MitoTracker could not be consistently detected using flow cytometry (BioLegend, #123910) (**Figure 3.3**). This could be attributed to a loss of larger EVs during the differential centrifugation step used to prepare flow cytometry samples. To capture larger microvesicles, an optimized centrifugation protocol and EV detection antibodies is required. As expected, *f*Aβ42 challenge induced EV secretion measurable by flow cytometry. Microglia given both CD200 and *f*Aβ42 experienced an overall increase in the number of EV-like events compared to the untreated controls. This nonsignificant increase could be due to loss of EVs during differential centrifugation or to background noise from particles that are not EVs. A counterstain designed to label EVs rather than just cell membrane components would be a beneficial addition to this protocol. Additionally, the use of reporter cell

lines that negate complications related to dye optimization could be a valuable tool for future mitochondrial transfer studies.

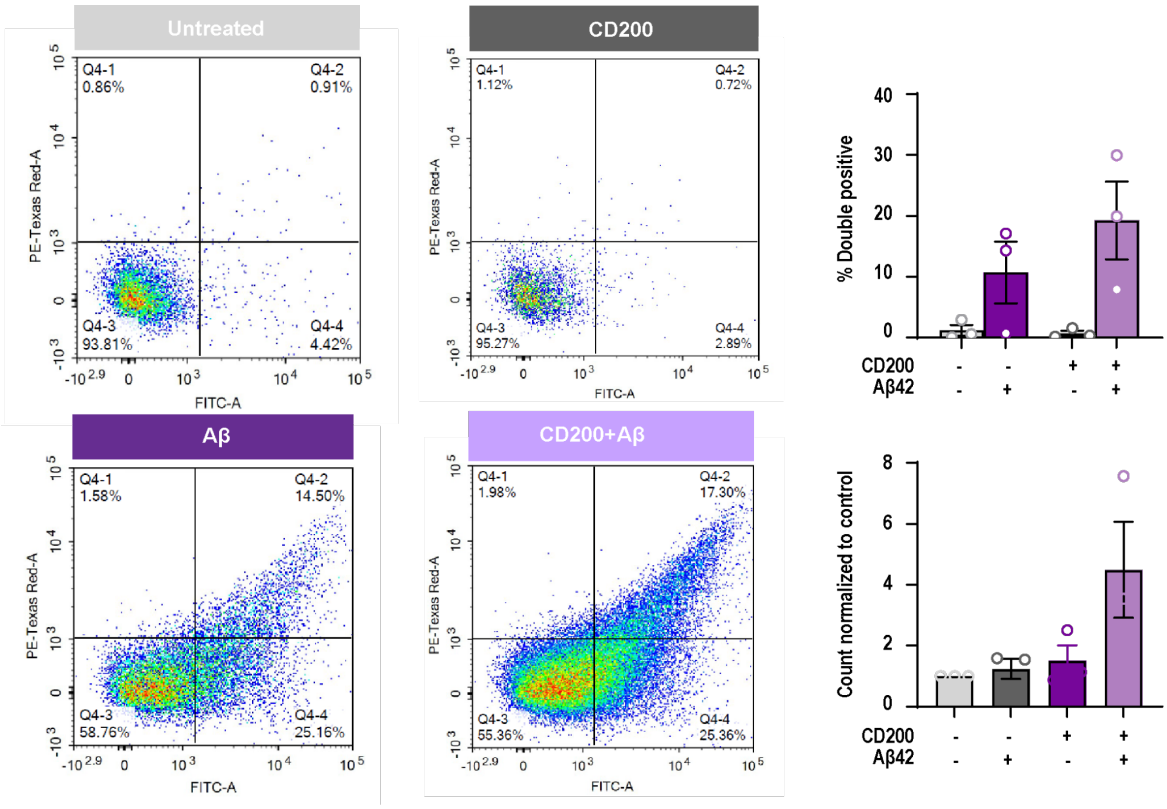


**Figure 3.3: Possible MitoEV production in CD200-treated Microglia**
Preliminary flow cytometry results of EVs labeled with CD200R-FITC and MitoTracker Red.

**CD200 treatment increases mitochondria-dense cell projections**

Mitochondria move around the cell to meet energetic demand (Ramond et al., 2019). CD200 treatment visibly increases cell projections that are able to reach longer distances. As such, we hypothesize that these projections can also be modes of mitochondrial transfer within and between cells. We used 100 nM MitoTracker Red CMXRos combined with Airyscan imaging on an LSM-980 to reveal mitochondrial structures inside of these cell projections. CD200-treated microglia seem to produce more mitochondria-containing projections – although amyloid-beta challenge alone also produced cell projections with mitochondrial signal inside (**Figure 3.4**).

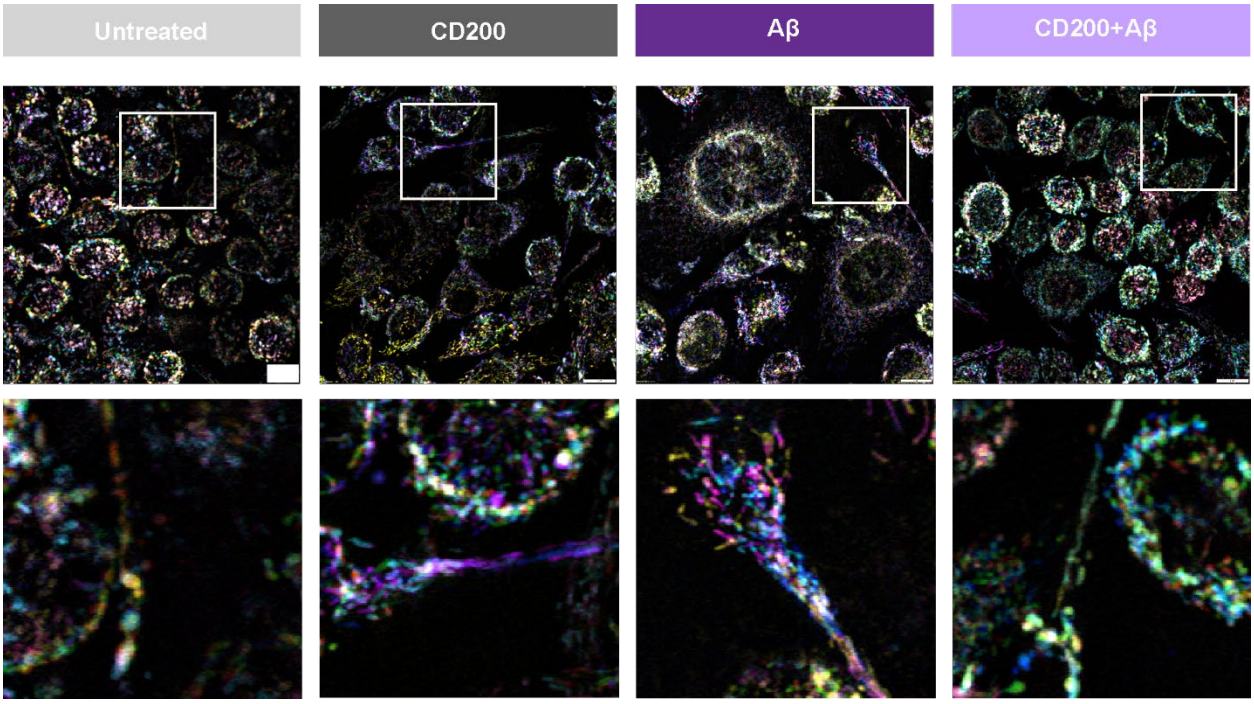


**Figure 3.4: Microglia feature mitochondria-dense projections**

Cells stained with 100nM mitotracker, imaged using Airyscan microscopy, and pseudo-colored to reflect z-stack reveal enhanced production of mitochondria-containing cell projections in microglia treated with CD200 alone. Cell projections were also seen in microglia challenged with amyloid-beta independent of CD200 treatment prior to exposure. Scale bar = 10μm.

### 3.4 Discussion

Preliminary data suggests CD200-treated microglia can engage mitochondrial transfer between cells, although whether this is primarily accomplished through TNTs or EVs remains unclear. We show qualitatively that CD200 treatment can enhance both TNT and EV formation in microglia under *f*Aβ42 challenge. However, additional biological replicates are required to accurately quantify either phenomenon in a representative manner. While current data indicate increased mitoEV export, the size range is enriched for 200 μm, which is more closely related to exosomes that are released under inflammatory conditions. To assess whether microvesicles containing mitochondria are exported by CD200-treated cells, a differential centrifugation protocol that is relevant to this cell type and can target large extracellular vesicles is still needed.

Mitochondrial imaging revealed positive mitochondrial signals in cell projections, possibly due to cells funneling resources to pockets away from the cell body to facilitate degradation of

toxic debris in lysosomal synapses (Jacquet et al., 2024). The presence of these projections even without *f*Aβ42 challenge suggests CD200 can cause cells to remodel into a “ready” state before the cells are stimulated. To assess whether mitochondria are being sent to these cellular pockets to power lysosome function, it would be important to assess whether lysosomal activity and ATP synthesis are correlated with mitochondria-dense areas away from the cell body. Not only would metabolic assays be useful for this analysis, techniques that allow the visualization of ATP around or near organelles connected by these cell projections would also be valuable.

## Chapter 4: Summary of Findings

### 4.1 Summary of Findings

**Table 4.1: Summary of finding**

| Chapter | Main finding |
|---|---|
| 1 | Neuroinflammation and debris clearance have been studied extensively in AD brains |
| 2.1 | CD200 dampens inflammation and enhances debris uptake |
| 2.2 | CD200 enhances debris clearance through LC3-associated phagocytosis and protects microglia from *f*Aβ42-induced damage |
| 3 | CD200 supports microglial function by facilitating mitochondrial transfer |
| 4 | Summary and Future Steps |

In summary, this work establishes soluble CD200 as an effective therapeutic against two major AD hallmarks *in vitro*: neuroinflammation and impaired debris clearance. Chapter 1 connects the chemical microenvironment of the CNS to AD prognosis using information gathered from published literature. Chapter 2 provides original work detailing the effects of CD200 on two hallmarks mentioned in chapter 1, while chapter 3 seeks to explore the additional mechanisms behind the therapeutic effects of CD200 – namely mitochondrial transfer. Finally, chapter 4 serves as a summary and proposes long-term future work.

### 4.2 Future steps

This work serves as an early characterization of soluble CD200 in the context of AD therapeutics. We show that CD200 has the potential to dampen and prevent harmful AD hallmarks that have been shown to contribute to memory loss and cognitive decline. Even though pretreatment with CD200 is a promising avenue, the need to use it prophylactically requires some engineering considerations as applying it directly into the brain may not yield similarly therapeutic effects. Similar to how Car-T cells are trained outside of the patient's body to target cancer cells, the CD200 mechanisms present in microglia can be leveraged to support

the patient's native immune system. To get from bench to bedside however, there are still many questions that need to be answered. One major limitation of this study was the absence of CD200R knockdown experiments to confirm the role of CD200R in the signaling axis responsible for the therapeutic effects of soluble CD200 in microglia. An immediate next step would be to either produce a CD200R knockdown or knockout cell line using lentiviral or CRISPR strategies, or to obtain cells from a CD200R knockout animal. If these studies cannot be repeated in CD200R KO cells, it will further support the hypothesis that the engagement of CD200 to CD200R is required for non-canonical autophagic regulation in microglia. Once the signaling axis has been confirmed, manipulating microglia to stealthily target amyloid-beta without triggering an inflammatory response should be the next engineering target.

**References**


Aires ID, Ribeiro-Rodrigues T, Boia R, Catarino S, Girão H, Ambrósio AF, Santiago AR. 2020. Exosomes derived from microglia exposed to elevated pressure amplify the neuroinflammatory response in retinal cells. Glia 68:2705–2724.

Anon. 2022. 2022 Alzheimer's disease facts and figures. Alzheimers Dement J Alzheimers Assoc 18:700–789.

Bhatia S, Rawal R, Sharma P, Singh T, Singh M, Singh V. 2022. Mitochondrial Dysfunction in Alzheimer's Disease: Opportunities for Drug Development. Curr Neuropharmacol 20:675–692.

Brioschi S, d'Errico P, Amann LS, Janova H, Wojcik SM, Meyer-Luehmann M, Rajendran L, Wieghofer P, Paolicelli RC, Biber K. 2020. Detection of Synaptic Proteins in Microglia by Flow Cytometry. Front Mol Neurosci 13:149.

Chakrabarty P, Jansen-West K, Beccard A, Ceballos-Diaz C, Levites Y, Verbeeck C, Zubair AC, Dickson D, Golde TE, Das P. 2010. Massive gliosis induced by interleukin-6 suppresses Aβ deposition in vivo: evidence against inflammation as a driving force for amyloid deposition. FASEB J 24:548–559.

Cherry JD, Olschowka JA, O'Banion MK. 2014. Are "Resting" Microglia More "M2"? Front Immunol 5:594.

Cornell J, Salinas S, Huang H-Y, Zhou M. 2021. Microglia regulation of synaptic plasticity and learning and memory. Neural Regen Res 17:705–716.

Elward K, Gasque P. 2003. "Eat me" and "don't eat me" signals govern the innate immune response and tissue repair in the CNS: emphasis on the critical role of the complement system. Mol Immunol 40:85–94.

Fraser DA, Pisalyaput K, Tenner AJ. 2010. C1q enhances microglial clearance of apoptotic neurons and neuronal blebs, and modulates subsequent inflammatory cytokine production. J Neurochem 112:733–743.

Graham NS, Sharp DJ. 2019. Understanding neurodegeneration after traumatic brain injury: from mechanisms to clinical trials in dementia. J Neurol Neurosurg Psychiatry 90:1221–1233.

Jacquet RG, González Ibáñez F, Picard K, Funes L, Khakpour M, Gouras GK, Tremblay M-È, Maxfield FR, Solé-Domènech S. 2024. Microglia degrade Alzheimer's amyloid-beta deposits extracellularly via digestive exophagy. Cell Rep 43:115052.

Kim YK, Que R, Wang S-W, Liu WF. 2014. Modification of Biomaterials with a Self-Protein Inhibits the Macrophage Response. Adv Healthc Mater 3:989–994.

Lerussi G, Villagrasa-Araya V, Moltó-Abad M, del Toro M, Pintos-Morell G, Seras-Franzoso J, Abasolo I. 2025. Extracellular Vesicles as Tools for Crossing the Blood–Brain Barrier to Treat Lysosomal Storage Diseases. Life 15:70.

Levine KS, Leonard HL, Blauwendraat C, Iwaki H, Johnson N, Bandres-Ciga S, Ferrucci L, Faghri F, Singleton AB, Nalls MA. 2023. Virus exposure and neurodegenerative disease risk across national biobanks. Neuron 111:1086-1093.e2.

Li Y, Yan Z, Dai Y, Cai H, Chen Y, Chen Y, Jin R, Sun W, Wang H. 2026. Mechanical Force Promotes Mitochondrial Transfer From Macrophages to BMSCs to Enhance Bone Formation. Cell Prolif 59:e70121.

Liang C, Zhou Y, Zhuang K, Wang S, Zhong L, Can D, Lei A, Li H, Zhang J, Leng L. 2026. Microglial mitochondria transfer to astrocytes via GPNMB-enriched extracellular vesicles alleviates cognitive deficits in tauopathy mice. Nat Neurosci 29:1573–1584.

Mattson MP, Keller JN, Begley JG. 1998. Evidence for synaptic apoptosis. Exp Neurol 153:35–48.

Müller L, Di Benedetto S. 2025. Neuroimmune crosstalk in chronic neuroinflammation: microglial interactions and immune modulation. Front Cell Neurosci [Internet] 19. Available from: https://www.frontiersin.org/journals/cellular-neuroscience/articles/10.3389/fncel.2025.1575022/full

Müller L, Di Benedetto S, Müller V. 2025. The dual nature of neuroinflammation in networked brain. Front Immunol [Internet] 16. Available from: https://www.frontiersin.org/journals/immunology/articles/10.3389/fimmu.2025.1659947/full

Ramond E, Jamet A, Coureuil M, Charbit A. 2019. Pivotal Role of Mitochondria in Macrophage Response to Bacterial Pathogens. Front Immunol [Internet] 10. Available from: https://www.frontiersin.org/journals/immunology/articles/10.3389/fimmu.2019.02461/full

Santana R, McWhirt J, Brewer G. 2025. Treatment of age-related decreases in GTP levels restores endocytosis and autophagy. GeroScience 48.

Scheiblich H, Eikens F, Wischhof L, Opitz S, Jüngling K, Cserép C, Schmidt SV, Lambertz J, Bellande T, Pósfai B, Geck C, Spitzer J, Odainic A, Castro-Gomez S, Schwartz S, Boussaad I, Krüger R, Glaab E, Di Monte DA, Bano D, Dénes Á, Latz E, Melki R, Pape H-C, Heneka MT. 2024. Microglia rescue neurons from aggregate-induced neuronal dysfunction and death through tunneling nanotubes. Neuron 112:3106-3125.e8.

Theparambil SM, Begum G, Rose CR. 2024. pH regulating mechanisms of astrocytes: A critical component in physiology and disease of the brain. Cell Calcium 120:102882.

Vainchtein ID, Molofsky AV. 2020. Astrocytes and microglia: in sickness and in health. Trends Neurosci 43:144–154.

Varnum MM, Kiyota T, Ingraham KL, Ikezu S, Ikezu T. 2015. The anti-inflammatory glycoprotein, CD200, restores neurogenesis and enhances amyloid phagocytosis in a mouse model of Alzheimer's disease. Neurobiol Aging 36:2995–3007.

van der Vlist M, Raoof R, Willemen HLDM, Prado J, Versteeg S, Martin Gil C, Vos M, Lokhorst RE, Pasterkamp RJ, Kojima T, Karasuyama H, Khoury-Hanold W, Meyaard L, Eijkelkamp N. 2022. Macrophages transfer mitochondria to sensory neurons to resolve inflammatory pain. Neuron 110:613-626.e9.

Walker DG, Dalsing-Hernandez JE, Campbell NA, Lue L-F. 2009. Decreased expression of CD200 and CD200 receptor in Alzheimer's disease: A potential mechanism leading to chronic inflammation. Exp Neurol 215:5–19.

# Appendix

## Abbreviations

| | |
|---|---|
| **1% media** | ESF CHO cell media with 1% FBS |
| **0% media** | ESF CHO cell media with no FBS |
| **cDMEM** | Complete DMEM cell culture medium |
| **cRPMI** | Complete RPMI cell culture medium |
| **FBS** | Heat inactivated fetal bovine serum |
| **D10** | cDMEM supplemented with MCSF |
| **MCSF** | Macrophage Colony Stimulating Factor |

## CD200 Production Protocol

| Day 1 | Day 2 | Day 3-5 | Day 6-8 | Day 9 |
|---|---|---|---|---|
| Thaw mCD200 or hCD200 in 1% media | Refresh 1% media | Monitor cells and change media as needed | Expand to ten (or up to 15) T182 flasks | Refresh 1% media |
| **Day 10-12** | **Day 13** | **Day 14** | **Day 15** | **Day 16** |
| Monitor cells and change media as needed | Change to 0% | Collection #1 Thaw #1 | Collection #2 Clean Filter | Collection #3 Condensation 1 (#1 and #3) Thaw #2 |
| **Day 17** | **Day 18** | **Day 19** | **Day 20** | **Day 21** |
| Collection #4 Condensation 2 (#2 and #4) | Collection #5 Condensation 3 (#5) | Purification Concentration assay | Seed Functional Assay | Mouse CD200 Functional Assay |
| **Day 22** | **Day 23** | | | |
| Human CD200 Functional Assay | ELISA assays | | | |

1. Make ESF media for CHO cell culture[1]:
    a. 1% media: 5mL penStrept + 5mL FBS + 490mL ESF media (Expression Systems #98-001)
    b. 0% media: 5mL penStrept + 495mL ESF media

[1] sterile filter all components together in sterile filter bottle and store at 4°C

2. Thaw cd200-CHO-Avitag-His32 cells:
    a. Add cells from bullet to 5mL 1% serum media and pellet to remove DMSO (300 rcf for 5 minutes)
    b. Resuspend in 2mL 1% serum media
    c. Add 9mL 1% media to two tissue culture plates.
    d. Add 1mL cell suspension into each plate
    e. Change to fresh 1% media after 24 hours
    f. Refresh media as needed until cells reach 90% confluency[2]
3. Expansion
    a. Aspirate media and wash 3x with sterile PBS
    b. Lift cells with 3 mL CellStripper (Fisher Scientific, #MT25056CI)
    c. Fill a 15mL conical tube with 3mL 1% media
    d. Add 3mL 1% media to each cell plate to gently collect cells from both plates into one tube.
    e. Pellet cells at 300 rcf for 5 minutes
    f. Fill ten T182 flasks with 19mL 1% media
    g. Resuspend cells in 10mL 1% media. Thoroughly mix cells by inverting the tube 2-3 times. Add 1mL cell suspension to each flask. Shake flasks in circular motion to encourage even cell deposition.
    h. Change media every other day as needed until cells reach 90% confluency
4. Change to 0% media
    a. At 90% confluency, aspirate 1% media and replace with 20mL 0% media[3]
    b. Let cells rest for 24 hours

[2] Exceeding 90% confluency will result in cell aggregation and lower protein yield
[3] Cells will aggregate in the absence of serum over time, will recover with re-addition of serum

c. Collect supernatant into four 50mL conical tubes and centrifuge at 300 rcf for 5 minutes to remove cell debris.
d. Decant supernatant into a 250mL 0.22 PES µm vacuum filter and filter to remove dead cells
e. Collect media for five consecutive days, refilling flasks with 20mL 0% media after each collection

5. Storage: store supernatant at -80°C (up to 1 week, no more than 2 weeks) and thaw overnight at 4°C for condensation.
6. Clean TFF system (TFF LabScale millipore)
    a. One day before first condensation, wash the chamber with 500mL 0.1N NaOH
        i. Make 1L of 0.1N NaOH with 900mL milliQ water and 100mL 1N NaOH[4]
        ii. Pour 500mL 0.1NaOH into the TFF chamber and make sure “ret in” and “ret out” ports are connected.
        iii. Turn on the TFF pump and set stir speed to high (pressure gauge should show very low to zero fluctuation in pressure without a filter cassette attached)
        iv. Cycle cleaning solution through the TFF system for 1 hour to dislodge debris that may have accumulated in the chamber or tubing. Spot clean with q-tips and serological pipettes as needed.
        v. Turn pump off, disconnect tube from “ret in” port and redirect to waste container.
        vi. Fully deplete the NaOH from the system and attach filter cassette
        vii. Reattach the tube to the “ret in” port and run the remaining 500mL 0.1NaOH through the filter cassette.

[4] MilliQ filters out particles that can clog the filter cassette. Do not use tap water or unfiltered DI water.

viii. Before the chamber is fully depleted, add 500mL milliQ water and drain system[5]

ix. Store the freshly cleaned filter cassette at 4°C overnight.

x. Disconnect ret in and connect to waste container

7. Condensation

a. Attach filter cassette to TFF system and run 300mL of milliQ water through the cassette

b. Combine 2 bottles of thawed cell supernatant and use a 500mL 0.22 μm PES vacuum filter to remove any debris aggregates that may have formed during the thawing period.

c. Before the chamber fully empties, pour in 300mL of thawed supernatant at a time[6]

d. Once the protein solution in the chamber is almost empty tube from “ret in” and attach to empty syringe[7]

e. Disconnect tube from “pump outlet” port and set to a 50mL collection tube

f. Use syringe to push condensate still in the filter or tubing back towards the “pump outlet” port into the collection tube

g. Disconnect tube from the “pump inlet / feed in” port and set to collection tube

h. Turn on the pump and stir bar to drain the chamber directly into the collection tube. A successful collection should look dark yellow in color with a yield of about 10-25mL.

i. Repeat condensation steps for remaining collections and store at -80°C

[5] Disconnect cassette before the system empties and starts pumping air into the filter cassette membrane.
[6] Make sure the top pressure gauge does not exceed 10 psi and bottom gauge does not exceed 40 psi. Keep protein not currently being filtered at 4°C or on ice.
[7] Filter cassette sends condensed protein back into the chamber.

8. Purification
    a. Fill a beaker with water and set on ice
    b. Place protein condensates into the beaker to thaw in cold water
    c. Once thawed, pellet protein condensates at 300 rcf for 5 minutes.
    d. Prepare two 10k Amicon condenser columns and add 15mL of condensate to each column
    e. Centrifuge at 4000 rcf for 10 minutes at 4°C
    f. Discard flow-through into a waste tube (keep on ice or frozen until protein concentration is measured)
    g. Add condensate to the column and spin down as many times as needed until the 10-50mL of combined condensate is further compressed into 2mL.[8]
    h. Collect 2mL protein condensate and transfer into a 2mL tube, vortex thoroughly
    i. Prepare a Cytivia his-trap column[9]
        i. Set fixed rotor centrifuge to 4°C
        ii. Remove seal tab and spin column down to remove buffer, 100 rcf for 30 seconds
        iii. Wash with 600uL binding buffer (20mM imidazole in phosphate buffer)
        iv. Add condensate to nickel column 600uL at a time and spin for 30 seconds at 100 rcf (may increase time as needed but not speed)
        v. Wash with 600uL wash buffer and transfer column to a fresh tube
        vi. Add 400 uL elution buffer and incubate for 1 minute at room temperature to allow maximal permeation of the buffer into the resin.
        vii. Elute at 100 rcf for 2 minutes at 4°C
    j. Desalt

[8] Dislodge aggregates at the bottom of the column membrane between spins to prevent clogging
[9] Columns should always be stored upright to prevent resin damage

i. Remove imidazole with a Zeba desalting column:

1. Spin down column to remove buffer (1500 rcf, 2 minutes)
2. Transfer column to fresh collection tube
3. Add full volume of protein (about 400uL) to desalting column and incubate at room temperature for 1 minute
4. Desalt at 1500 rcf for 2 minutes

k. Sterile filter

i. Add full volume of desalted protein to 0.22um sterile spin filter

ii. Centrifuge at 16,000 rcf for 5 minutes at 4°C.

iii. Aliquot 25uL for concentration assay and the rest into 50uL for later use

9. Concentration assay (Pierce™ BCA Protein Assay Kit, #23225)

a. Thaw aliquot on ice

b. Make working reagent (50A:1B): 100uL B + 4900uL A

c. Add 200uL to each well in 96-well low binding plate

d. Prepare diluted samples:

i. 2.5 uL sample + 22.5 uL milliQ water

ii. 5 uL sample + 20uL milliQ water

iii. 12.5 uL sample + 12.5 milliQ water

e. Add 10uL samples or standards to appropriate well

f. Incubate at 37°C for 30 minutes in the dark.

g. Allow plate to cool to room temp for 5 minutes

h. Read at 570 nm and average across dilutions to calculate protein concentration

10. Functional assay (BMDMs)

a. Harvest mouse bone marrow and isolate bone marrow stem cells

b. Allow cells to differentiate for 6 days in D10 media

c. Seed $2.0x10^4$ cells per well into 12 wells in a 96-well plate

d. Allow adherence overnight
e. Refresh media with 0ug,2ug,or 5ug of cd200 in 100uL D10, incubate at 37°C for four hours
f. Make 2x M1 mastermix (6ng/mL IFN-y and 2ng/mL LPS) and add 100uL to appropriate wells
g. Incubate at 37°C overnight (16 hours), collect supernatant and assess with mouse TNFα ELISA kit (BioLegend 430901)

11. Functional assay (BV2)
    a. Seed $2.0x10^4$ BV2 per well into 12 wells in a 96-well plate and allow adherence overnight in cDMEM.
    b. Refresh media with 0ug, 2ug, or 5ug of cd200 in 100uL DMEM, incubate at 37°C for two hours
    c. Make 2x M1 mastermix (0.2ug/mL LPS) and add 100uL to appropriate wells for a final concentration of 0.1ug/mL LPS
    d. Incubate at 37°C overnight, collect supernatant and assess with mouse IL-6 ELISA kit (BioLegend)
12. Functional assay (THP1)
    a. Seed $2.0x10^4$ THP1 per well into 12 wells in a 96-well plate with 25nM PMA and allow adherence overnight in cRPMI.
    b. Refresh media with 0ug, 12.5ug, or 25ug of cd200 in 100uL DMEM, incubate at 37°C for two hours
    c. Make 2x M1 mastermix (6ng/mL hIFN-y and 2ng/mL LPS) and add 100uL to appropriate wells for a final concentration of 0.1ug/mL LPS
    d. Incubate at 37°C overnight, collect supernatant and assess with human TNFα ELISA kit (BioLegend).

## Seahorse Protocol

| Day 1 | Day 2-4 | Day 5 | Day 6 |
|---|---|---|---|
| Seed BV2 microglia | CD200 treatment | Transfer to cells to Seahorse cell culture plate<br>CD200 treatment<br>Add *f*Aβ<br>Hydrate Seahorse sensors and prepare Seahorse cell culture media | Run Mito Stress Seahorse assay |

1. 2. Thaw BV2 in cDMEM
    a. Thaw 1 cell bullet into 5mL of cDMEM
    b. Pellet cells (300 rcf, 5 min)
    c. Remove media and resuspend cells in 1mL cDMEM
    d. Prepare a tissue culture plate with 9 mL cDMEM and add cell suspension
    e. Allow cells to recover for 24 hours, change media as needed until 70-90% confluency.

## Day 1

2. Seed $0.1x10^6$ cells into two tissue culture plates
    a. Remove media and wash cells with *cold* 1x PBS twice
    b. Add 3mL of 0.05% Trypsin to cell plate and incubate at 37°C for 3-5 minutes
    c. While cells incubate prepare:
        i. 6mL warm cDMEM
        ii. Cell counting chip
        iii. 10uL Trypan blue
    d. Neutralize trypsin by adding 3mL cDMEM directly to plate
    e. Use a p1000 pipette to lift cells by gently pipetting in a circular motion
    f. Transfer lifted cells to 15mL tube containing 6mL cDMEM
    g. Pellet cells at 300 rcf for 5 minutes and remove supernatant

h. Resuspend pellet in 5mL cDMEM

i. Calculate cell density and use **Equation A1** to calculate the volume containing $1.0x10^6$ cells

$$Volume\ in\ mL\ = \frac{1 \times 10^6}{cell\ density} \quad \textbf{(A1)}$$

j. Prepare two 15mL tubes with 10mL cDMEM in each tube

k. Remove volume calculated from step 11 from each tube and replace with equal volume of cell suspension

l. Invert 3-4 times gently to mix and dispense 100mL cells into a standard tissue culture petri dish with 10mL CDMEM

m. Allow cells to recover overnight

**Day 2-4**

1. Treat one plate with 10ug/mL CD200. Refresh media daily.

**Day 5**

3. Transfer cells to Seahorse cell culture plate and stimulate with *f*Aβ42
    a. Lift cells with 0.05% Trypsin and adjust to $0.2x10^6$ cells/mL of 10ug/mL CD200-supplemented media
    b. Seed 100uL cell suspension into appropriate wells of Seahorse cell culture plate for a final concentration of $0.02x10^6$ cells per well[10]
    c. Add 1uL of 100x *f*Aβ42 (0.2mg/mL) to appropriate wells
    d. Culture cells for additional 24 hours
4. Prepare fresh seahorse media (XF DMEM) and hydrate sensors
    a. Combine the following: 47.5mL XF DMEM, 1mL sodium pyruvate, 1mL L-glutamate, 0.5mL glucose
    b. Warm media in 37°C bath

[10] Avoid seeding cells in any of the outer wells to prevent variation in data from wicking effect

c. Soak sensors in 200uL of calibration buffer.

d. Incubate at 37°C overnight without $CO_2$

e. pH media until it reaches 7.4 *exactly*

f. Sterile filter and wrap in foil to protect from light. Store at 4°C overnight

### Day 6

1. Warm media to 37°C in the dark
2. Aliquot XF DMEM into two tubes with 3mL in each, and a third tube with 4mL of XF DMEM. wrap in foil and incubate in 37°C
3. Thaw drug aliquots briefly in 37°C
4. Wash cells once with 100uL XF DMEM per well, then refill wells with warm XF DMEM.
5. Incubate Seahorse cell culture plate at 37°C without $CO_2$ for 1 hour[11]
6. While vortexing conical tubes from step 2, add[12]:
    a. 3uL oligomycin to 3mL XF DMEM
    b. 2.7uL BAM15 to 3mL XF DMEM
    c. 1uL antimycin and 1uL rotenone to 4mL XF DMEM
7. Vortex thoroughly, incubate at 37°C for 10 minutes
8. Dispense 22uL of **a** into port A, 25uL of **b** into port B, and 28uL of **c** into port C
9. Load sensors into Seahorse analyzer and run calibration[13]
10. Discard buffer plate when prompted
11. Load cell plate and run assay
12. Save cell lysates in a sealable v-bottom 96-well plate in -20°C for up to one week

[11] Do not exceed 1 hour in incubation before assay

[12] Test speed of vortex on open tube containing equal volume of water to determine optimal speed to thoroughly dissolve drugs in media without spillage

[13] This step should include a brief 10-15 minute incubation to warm up the sensors followed by a 30 minute calibration. Be aware of this when starting your cell plate incubation without $CO_2$

## Mitochondria Transfer Protocol

| Day 1 | Day 2-4 | Day 5 | Day 6 |
|---|---|---|---|
| Seed BV2 microglia | CD200 treatment | CD200 treatment<br>Add *f*Aβ | Image |

1. Thaw BV2 in cDMEM
    a. Thaw 1 cell bullet into 5mL of cDMEM
    b. Pellet cells (300 rcf, 5 min)
    c. Remove media and resuspend cells in 1mL cDMEM
    d. Prepare a tissue culture plate with 9 mL cDMEM and add cell suspension
    e. Allow cells to recover for 24 hours, change media as needed until 70-90% confluency.

### Day 1

2. Label cells with MitoTracker Red and CellTracker Green
    a. Remove media and wash cells with *cold* 1x PBS twice
    b. Add 3mL of 0.05% Trypsin to cell plate and incubate at 37°C for 3-5 minutes
    c. While cells incubate prepare:
        i. 6mL warm cDMEM
        ii. Cell counting chip
        iii. 10uL Trypan blue
    d. Neutralize trypsin by adding 3mL cDMEM directly to plate
    e. Use a p1000 pipette to lift cells by gently pipetting in a circular motion
    f. Transfer lifted cells to 15mL tube containing 6mL cDMEM
    g. Pellet cells at 300 rcf for 5 minutes and remove supernatant
    h. Resuspend pellet in 5mL cDMEM
    i. Transfer $1.0x10^6$ cells into two 15mL conical tube and pellet (300 rcf, 5min)

j. Resuspend in 1mL of (1:1000) Cell Tracker Green or MitoTracker Red in serum free DMEM
k. Incubate in the dark for 30 minutes at 37°C
l. Pellet cells and wash with cDMEM twice
m. Seed 100uL of CellTracker cells on the top left corner of the 8-chamber glass slide and 100uL of the MitoTracker cells on the bottom right corner
n. Use a pipette tip to make sure the two cell populations merge in the middle
o. Change and collect media daily as needed
p. Add *f*Aβ42 after 48 hours and incubate for 24 hours
q. Image cells live at 37°C, 5% $CO_2$ using bright field, green and red fluorescence at 63x oil.